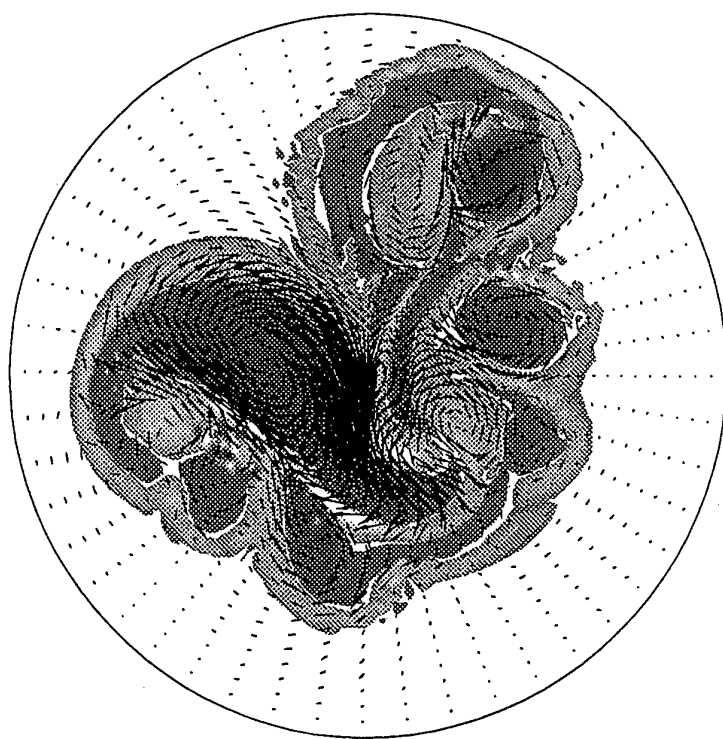


EUROMECH Colloquium 396
with ERCOFTAC and TAO Workshops

VORTICAL STRUCTURES IN
ROTATING AND STRATIFIED FLUIDS



DTIC QUALITY INSPECTED 4

CORTONA JUNE 22nd-25th 1999

DISTRIBUTION STATEMENT A
Approved for Public Release
Distribution Unlimited

19991004 151

SPONSORS:

- Università di Roma “La Sapienza”,
- Technical University of Eindhoven,
- European Science Fundation TAO,
- European Research Office (U.S. Army),
- European Office of Aerospace Research and Development,
- Office of Naval Research International Field Office,
- ERCOFTAC,
- EUROMECH,
- EUROMECH305 “Vorticity Dynamics”.

PROVISIONAL PROGRAM FOR EUROMECH 396

Day 0, June 21st, Pre-registration

18:00-20:00 Pre-registration & welcome party

Day 1, June 22nd, ERCOFTAC Workshop/EUROMECH Colloquium

8:30-9:20 Registration
9:20-9:30 Opening Remarks
9:30-9:50 Caillol & Zeitlin
9:50-10:10 Clercx & Nielsen
10:10-10:30 Ern & Wesfreid
10:30-11:00 Coffee break
11:00-11:20 Galmiche, Hunt, Thual & Bonneton
11:20-11:40 Gyr
11:40-12:00 Nielsen, Coutsias & Clercx
12:00-12:15 Short break
12:15-12:35 Pedrizzetti & Vassilicos
12:35-12:55 Rubinstein
12:55-14:30 Lunch break
14:30-15:10 Invited Lecture C. Cambon
15:10-15:30 Chillà, Simand & Pinton
15:30-15:50 Coffee/Tea break
15:50-16:10 Delfos & Poppe
16:10-16:30 Piantini & Pedrizzetti

Day 2, June 23rd, EUROMECH Colloquium

9:00-9:40 **Invited Lecture J. Fernando**
9:40-10:00 Boubnov
10:00-10:20 Bush & Woods
10:20-10:50 **Coffee break**
10:50-11:10 Leweke & Meunier
11:10-11:30 Swaters
11:30-11:50 Grayannik, Borth & Olbers
11:50-12:00 **Short break**
12:00-12:20 Beckers, Verzicco, Clercx & van Heijst
12:20-12:40 Bonnier, Eiff & Bonneton
12:40-14:30 **Lunch break**
14:30-15:10 **Invited Lecture D. Etling**
15:10-15:30 Afanasyev & Peltier
15:30-15:50 Billant & Chomaz
15:50-16:20 **Coffee/Tea break**
16:20-16:40 Flór
16:40-17:00 van de Konijnenberg, Naulin, Stenum & Rasmussen
17:00-17:20 Fincham

20:00 **Conference Banquet**

Day 3, June 24th, EUROMECH Colloquium

9:00-9:40 Invited Lecture P. Orlandi
9:40-10:00 Sorensen & Jorgensen
10:00-10:20 Tillmark & Alfredsson
10:20-10:50 Coffee break
10:50-11:10 Hoffmann & Busse
11:10-11:30 Le Dizès
11:30-11:50 Eiff
11:50-12:00 Short break
12:00-12:20 Richardson, Bower & Zenk
12:00-12:40 Zhvania, Zhvania, Lominadze, Nanobashvili, Tsakadze, Chagelishvili & Yan'kov
12:40-14:25 Lunch break
14:25-15:10 Poster Exhibit
15:10-15:30 Cenedese C.
15:30-15:50 Tychensky & Carton
15:50-16:20 Coffee/Tea break
16:20-16:40 Ungarish
16:40-17:00 Zavala-Sansón & van Heijst

Poster Exhibit

14:25-14:30 Bottausci, Petitjeans, Wesfreid, Maurel & Manneville
14:30-14:35 Flór & Eames
14:35-14:40 Petitjeans, Bottausci, Wesfreid, Maurel & Manneville
14:40-14:45 Pagneux & Maurel
14:45-14:50 van Noordenburg & Hoeijmakers
14:50-14:55 Manneville, Tanter, Sandrin, Maurel & Pagneux
14:55-15:00 Pasmanter & Capel
15:00-15:05 Chagelishvili, Chanishvili, Lominadze & Tevzadze
15:05-15:10 Vranjes

Day 4, June 25th, TAO Workshop/EUROMECH Colloquium

9:00-9:40 **Invited Lecture G. Carnevale**
9:40-10:00 Meleshko
10:00-10:20 Krasnoploskaya & Melesko
10:20-10:50 **Coffee break**
10:50-11:10 Capel & Pasmanter
11:10-11:30 Pavia, Ochoa & Sheinbaum
11:30-11:50 **Short break**
11:50-12:10 Espa & Querzoli
12:00-12:20 Mancini, Espa & Cenedese
12:30-14:30 **Lunch break**
14:30-14:50 Bouruet-Aubertot & Linden
14:50-15:10 Trieling, Wesenbeeck & van Heijst
15:10-15:30 Zhvania, Zhvania, Lominadze, Nanobashvili, Tsakadze & Petviashvili
15:30-16:00 **Coffee/Tea break**
16:00-16:20 Jovanović
16:20-16:40 Bouche & Sallusti
16:40-16:50 Closing remarks

P. Caillo & V. Zeitlin

Kinetic Equations and Stationary Energy Spectra in Stratified Turbulence
in Flows with and without Mean Potential Vorticity

Weak stratified turbulence is considered in the dynamical framework of the Euler - Boussinesq equations. For flows with zero mean potential vorticity a kinetic equation for the mean spectral energy density is obtained under hypothesis of Gaussian statistics with zero correlation length for weakly nonlinear internal gravity waves. Exact stationary scaling solutions of this equation are found for almost vertically propagating waves. The resulting spectra are anisotropic in vertical and horizontal wave numbers.

For flows with small but non-zero mean potential vorticity, under the same statistical hypothesis applied to the wave part of the flow, it is shown that the vortex part and the wave part decouple. The vortex part obeys a so-called limiting dynamics equation exhibiting vertical collapse and layering which contaminates the wave-part spectra. Relation of these results to the in situ measurements is discussed.

Vortex statistics for decaying 2D turbulence in containers with periodic and with no-slip boundaries

H.J.H. Clercx¹ and A.H. Nielsen²

¹Eindhoven University of Technology,

Department of Physics, Fluid Dynamics Laboratory,

P.O. Box 513, 5600 MB Eindhoven, The Netherlands

²Association EURATOM-Risø National Laboratory, OFD-128 Risø,
DK-4000 Roskilde, Denmark

Numerical studies of decaying two-dimensional (2D) turbulence, based on simulations of the Navier-Stokes equations for incompressible flows on a square domain with periodic boundary conditions, have revealed the emergence of coherent vortex structures. This process, already known for a few decades, is commonly referred to as self-organization of the flow. Additionally, several studies of 2D turbulence have recently been carried out in several laboratories in order to understand the self-organization of the flow (i.e. the presence of an inverse energy cascade) and also passive tracer transport in both forced and decaying 2D turbulence. By employing periodic boundary conditions it is implicitly assumed that boundaries have no significant effect either on the decay process itself or on passive tracer transport. Many quasi-2D flows are nevertheless constrained by rigid boundaries, which is particularly relevant for many geophysical flows. For that reason we have carried out two sets of numerical simulations of decaying 2D turbulence with periodic (2D Fourier pseudo-spectral code) and with no-slip (2D Chebyshev pseudo-spectral code) boundary conditions, respectively. Simulations have been performed for $Re=5.000$ and 10.000 with an initial distribution of 100 nearly equal-sized vortices with slightly different absolute vortex amplitudes. Half of the vortices have positive circulation, and the remaining vortices have negative circulation. The vortices are placed on a regular lattice with a random displacement of the vortex centers equal to approximately 10% of the lattice parameter. The angular momentum of the initial flow field is thus approximately equal to zero for the no-slip case. This kind of initial condition (chess-board pattern) enables comparison with experimental results on vortex statistics and tracer transport. We discuss the properties of decaying 2D turbulence in terms of ensemble averaged values of the vortex density, vortex radius, nearest neighbour distance and vortex amplitude. Additionally, the time evolution of energy, enstrophy, and average scale of the coherent structures for both sets of simulations (with periodic and with no-slip boundary conditions) are compared. It appears that these properties depend strongly on the type of boundary conditions in the numerical experiment.

Instabilities in time-periodic flows induced by curvature and rotation effects

Patricia Ern and J. Eduardo Wesfreid

Laboratoire Physique et Mécanique des Milieux Hétérogènes, UMR CNRS 7636
Ecole Supérieure de Physique et Chimie Industrielles
10, rue Vauquelin, 75231 Paris cedex 05, France
e-mail: ern@pmmh.espci.fr

We consider oscillatory flows between two concentric co-rotating cylinders at the angular velocity $\Omega(t) = \Omega_m + \Omega_0 \cos \omega t$ as a prototype to investigate the competing effects of centrifugal and Coriolis forces on the flow stability. We first study by flow visualization the effect of the mean rotation Ω_m on the instability threshold of the centrifugal destabilization induced by the temporal modulation. For several forcing frequencies, we show that increasing the mean rotation first destabilizes and then restabilizes the flow.

We also performed velocity field measurements in the rotating frame of the cylinders with an ultrasound Doppler apparatus. The global axial root-mean-square value $W_{rms}(t)$ of the axial velocity W is used to analyze the evolution of the instability over a time period. We observed that the instability appears and disappears several times during a flow period, even at large Taylor numbers (the Taylor number T_a is proportional to the modulation amplitude Ω_0). The effect of the mean rotation on the $W_{rms}(t)$ time evolution is illustrated in Figure 1. The peaks correspond to time periods where instability is present in the flow. For $Ro = 0.015$ and $T_a = 280$, we observe a stabilizing effect of the mean rotation during the second half period with the disappearance of the W_{rms} peaks. Moreover, we observe that the rotation number shifts the temporal regions of flow instability. For instance, the first peak when $Ro = 0$ at $t \approx 0.1$ shifts towards $t \approx 0$ for $Ro \approx 0.1$ and then towards $t \approx 0.95$ for larger Ro . Note also the growth of a second peak that shifts from $t \approx 0.5$ (for $Ro = 0.015$) to $t \approx 0.65$ (for $Ro = 0.2$). For larger Ro , the peak tends to disappear and the flow is stable ($Ro \approx 0.3$).

The experimental observations of the transient flow behavior and earlier theoretical studies on the validity of the quasi-steady stability analysis induced us to analyze the linear stability of the basic flow with this approach. Our goal is to understand the pulsed behavior of the instability and recover the times of growth and damping of the instability. We establish an analytical solution of the basic flow, valid for a finite gap and we determine numerically the linear instability threshold at different time. The quasi-steady linear stability analysis has been compared to experimental velocity measurements. The good

agreement obtained in this configuration is valid until intermediate frequencies. Results obtained concern the prediction of the instability threshold, the flow destabilization and restabilization when the mean rotation is increased, the prediction of the particular times of appearance and disappearance of the instability for several Taylor numbers and the effect of the mean rotation on these times. We also analyze the dynamical similarity of our system (same stability equations) at some particular times to well-documented systems (like counter-rotating Taylor-Couette, Dean or Rayleigh-Bénard flows). This provides an interpretation of the flow stability and instability at some particular times, as observed experimentally and numerically when the rotation number is varied. Also we point out that the quasi-steady stability analysis has to be performed taking into account the finite gap, as for instance the restabilization of the flow when increasing the rotation number can not be recovered using the classical small gap approximation for cylinders flows ($\delta \rightarrow 0$).

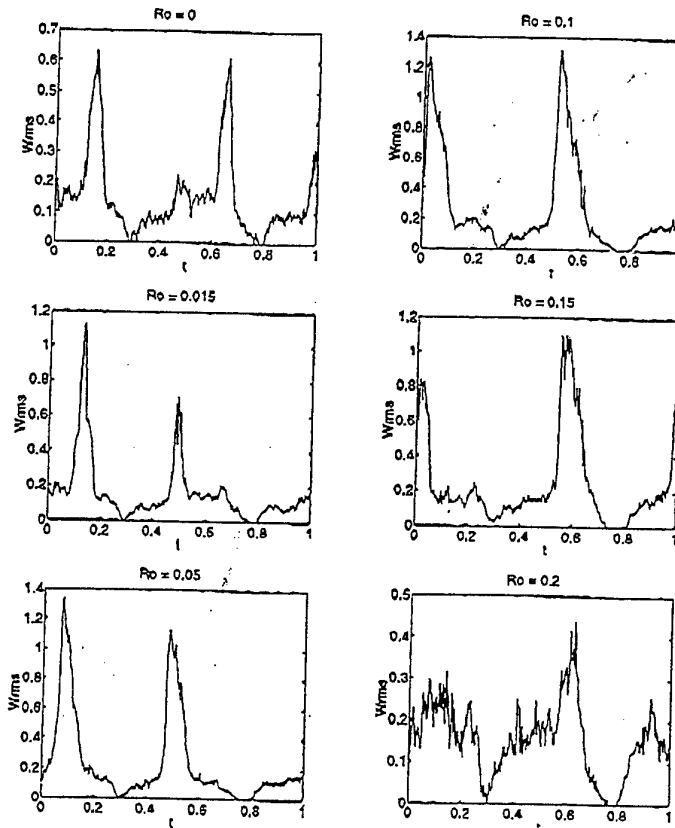


Figure 1: Examples of behavior of $W_{rms}(t)$ over a period for different rotation number and for $T_a = 280$ and $\gamma = 1$ ($\delta = 0.112$). Unity of W_{rms} is mm/s. The beginning of the period corresponds to cylinders at rest.

Turbulence-mean flow interaction in a stratified fluid

Abstract

Martin Galmiche¹, Julian Hunt², Olivier Thual¹
and Philippe Bonneton³

¹Institut de Mécanique des Fluides de Toulouse

Allée du Pr. Camille Soula, 31400 Toulouse, France

²Department of Applied Mathematics and Theoretical Physics
University of Cambridge, Silver Street, Cambridge CB39EW UK

³Département de Géologie et d'Océanographie
URA CNRS 197 Université Bordeaux 1, 33405 Talence, France

February 26, 1999

The question of vertical variability in stratified turbulent flows has already been addressed by many authors. There are a lot of evidences for the presence of shear and density layers in stratified atmospheres and oceans and this raises many questions on momentum and mass transports in geophysical fluids. In short papers, Phillips (1971) and later Posmentier (1976) had conjectured that turbulence in strongly stratified fluids may be "unstable" in the sense that the presence of a stable stratification in a turbulent flow may lead to a "negative eddy viscosity and diffusivity" effect and thus explain the amplification of any perturbation in the mean shear and density profiles. However, a physical interpretation for this mechanism has never been clearly exposed.

To answer this question, we have performed direct numerical simulations of freely decaying stratified turbulence with an initial perturbation of the horizontal mean flow $U(z) \sim \cos z$ (Galmiche, Thual & Bonneton, 1999a). Direct numerical simulation is here a powerful tool to investigate the behaviour of turbulence-mean flow interaction at the very beginning of the decay. The important property of such flows is that the vertical mean shear and thus the Richardson number $(N/\partial_z U)^2$ (where N is the Brunt-Väisälä frequency) are functions of the altitude. We found that for a sufficiently intense stratification, the horizontal mean flow was indeed accelerated on a time scale of order N^{-1} instead of transferring its energy to smaller vortical

structures as is usually the case in non-stratified turbulent shear flows. In these simulations, the mean flow was thus subject to the effect of an eddy viscosity which was found to reach negative values.

To better describe this phenomenon at the very beginning of the decay, Rapid Distortion Theory was used (Galmiche & Hunt, 1999b) to compute turbulent momentum fluxes while linear processes are dominant. This calculation allowed us to show that the restoring buoyancy forces acting on fluid particles induced the onset of counter-gradient turbulent fluxes and the mean flow was found to evolve following equation:

$$\partial_t U(t) = \nu_e(t) \partial_{zz} U(z, t) ,$$

with the time-dependant eddy viscosity

$$\nu_e = u'_0{}^2 [(2/5)t - (2/15)N^2 t^3] + O(t^5) ,$$

where u'_0 is the root mean square velocity of the initial turbulent fluctuations. This shows that for $Nt > \sqrt{3}$, the mean flow is subject to the effect of a negative eddy viscosity and is then accelerated. This short-time behaviour was in good agreement with the simulations performed by Galmiche, Thual & Bonneton (1999a) at the beginning of turbulence decay, and provides us with a good description of the mechanism proposed by Phillips (1972) and Posmentier (1977).

References

- [1] Galmiche, M., Thual, O., Bonneton, P. 1999a. Shear and density layers in stably-stratified turbulence. Part I: direct numerical simulation. Submitted to *J. Fluid Mech.*
- [2] Galmiche, M., Hunt, J.C.R. 1999b. Shear and density layers in stably-stratified turbulence. Part II: linear processes. Submitted to *J. Fluid Mech.*
- [3] Phillips, O.M. 1972. Turbulence in a strongly stratified fluid-is it unstable ? *Deep-sea Res.* 19, 79-81.
- [4] Posmentier, E.S. 1977. The generation of salinity finestructure by vertical diffusion. *J. Phys. Ocean.* 7, 298-300.

Interaction of Two Taylor Vortex Systems

Albert Gyr, Inst. of Hydromechanics, ETHZ, Switzerland

Extended Abstract

Some basic mechanisms in turbulence are related to the interaction of areas of concentrated vorticity. Therefore it makes sense to investigate the interaction of well defined vortices. One possibility is to study the interference of vortex rings. This interaction has been treated numerically as well as experimentally for all kinds of relative geometrical positions of their axes before the interference. The interaction is violent and highly transient. This behavior impaired the experimental investigations, because neither the initial nor the boundary conditions of the experiment could be held constant enough to achieve reproducible results.

In order to study the interaction of vortex rings under more repeatable and more stationary conditions the interaction of vortices occurring due to Taylor instabilities in Couette flows between two rotating cylinders separated by a small gap were investigated.

In this arrangement the axes of the vortex rings are parallel, however by turning the axis the method can be used to study vortex rings under all kind of geometrical positions to each other.

In the present study the results of the most simplest interaction are described.

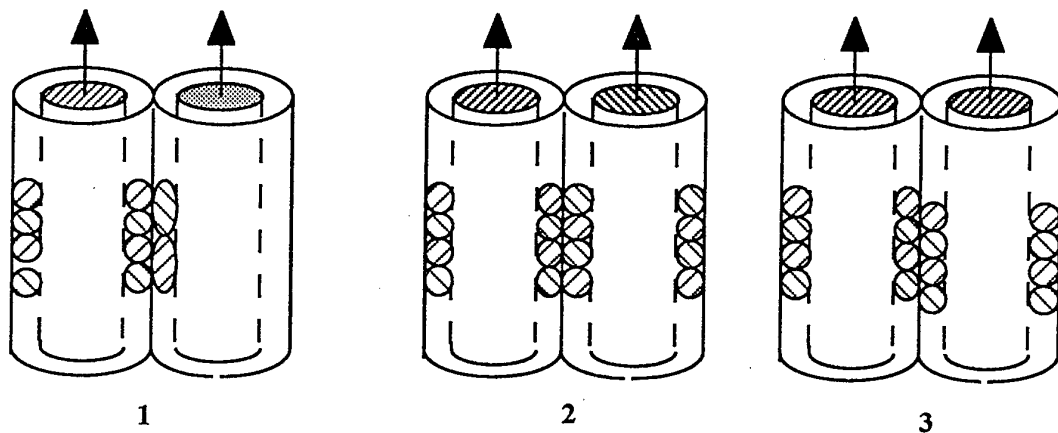
The conditions were:

1. The rings are produced in one column only and it was investigated which kind of flow the vorticity released through the gap is inducing in the column at rest. The Couette flow has a constant vorticity in the axial direction of the cylinders and the circumferential vorticity of the Taylor vortices. These two vorticities produce a very weak symmetric flow in the second cell similar to the Taylor vortices in the first one. These disturbances die out very rapidly along their path, such that the flow in the primary cells impacts with fluid at rest in the second column. However when the flow in the primary cell becomes turbulent, a slight mixing can be observed on the entire second column. The interesting result is that the radial scale of the Taylor vortices in the second cell is twice as large as the natural one in the primary cell. Therefore the vortices developing in the second cell are elliptical in cross section with the main axis twice the natural scale which corresponds to the gap width of the cells. (Figure 1)

2. The Couette flows are counterrotating, so that no additional shear is produced in the common gap. At high rotation rates (0.5 s/turn) in both cells the flow is transitional with a strong wave mode. These waves traverse the common gap so that no phase disturbance occurs between the modes in the two cells. As in the first case the scale of the Taylor vortices perpendicular to the flow direction is twice the natural scale, but after the fluid has completed one revolution the natural scale is recovered. At lower rotational speed the two cells contain a symmetric system of Taylor vortices turning in opposite directions. (Figure 2)

3. The Couette flows in both columns have a rotation of the same sign, therefore a singularity in the shear occurs at the free interface in the gap. Again, after the fluid has completed one revolution the natural mode is recovered, but the centers of the vortices in one column are staggered with respect to those in the other. (Figure 3)

Details of these flows with parametrized rotational velocities will be discussed. The mechanisms leading to different modes will be explained based on vorticity interaction.



Figures. 1. One cylinder only is rotating 2. The cylinders are counterrotating 3. The cylinders are rotating in the same direction

Forced and decaying 2D turbulence in circular containers

A.H. Nielsen¹, E.A. Coutsias² and H.J.H. Clercx³

¹Association EURATOM-Risø National Laboratory, OFD-128 Risø, DK-4000 Roskilde

²Mathematics and Statistics, University of New Mexico, Albuquerque, NM 87131, USA

³Eindhoven University of Technology, Department of Technical Physics,
Fluid Dynamics Laboratory, P.O. Box 513, 5600 MB Eindhoven, The Netherlands

Two-dimensional turbulence in unbounded or double periodic domains, in Navier-Stokes fluids and plasmas has been investigated intensively during the last decades by means of numerical simulations. The presence of an inertial range in the energy spectrum of these flows has been well documented. As two-dimensional flows exhibit an inverse cascade in the energy, coherent structures comparable with the size of the periodic domain will eventually emerge. Thus, the presence of boundaries and especially the conditions imposed on these will play a significant role in the evolution of the turbulence and the coherent structures, see e.g. [?, ?].

In this contribution we present numerical investigations of both forced and decaying flows in circular geometries. The model equations are the Navier-Stokes equations, which are solved using a pseudo spectral method based on a Chebyshev-Fourier expansion of the solutions. We investigate two different types of boundary conditions: first, the condition of free-slip boundaries with no vorticity generation at the wall. Secondly, a no-slip condition where, due to the strong boundary layers, small scale structures are injected into the interior of the flow, whenever vortices interact with the wall. These small scale structures will thus feed the turbulence. The Reynolds number, based on the radius of our domain and the rms of the velocity field, accessible for our code is in the range 2.000 – 5.000.

For the decaying turbulence we use random initial conditions. From a double periodic squared box we initialize a random vorticity field with a specific length scale in Fourier space. This field, expressed in a series of Fourier modes, is then spectrally interpolated onto our domain. We observe that the flow, by vortex merging, organises into large coherent structure(s) regardless of the boundary conditions. Also we observe a relative spinup of the flow as the normalised angular momentum increases with time. For the no-slip boundary condition strong boundary layers are observed, these layers are not present using the free-slip boundary condition.

For the forced turbulence we have added a forcing term to the Navier-Stokes equations, with a profile that is nearly identical to the initial condition described above. This investigation has just been started and only preliminary results are available at the moment. Our aim is to study the semi steady state of the flow field and due to the periodic nature of the azimuthal coordinate the energy spectrum can thus be compared with results obtained in doubly periodic domains.

References

- [1] S. Li, D. Montgomery and W.B. Jones, JPL (1996) vol. 56, part 3 pp. 615-639.
- [2] H.J.H. Clercx, S.R. Maassen and G.J.F. van Heijst, Phys. Fluids (1999) vol. 11 pp. 611-626.

Transfer between scales in an evolving vortex spiral

Gianni Pedrizzetti

Dipartimento Ingegneria Civile, Universit=E0 di Trieste, Italy.

J. C. Vassilicos

Department of Applied Mathematics and Theoretical Physics, University of =
Cambridge, UK.

Vortex spirals may appear naturally in turbulent flows as a result of =
vortex-sheet instability, filamentation, or advection by a local =
differential rotation. For this reason spirals may shed light on some =
properties of small-scale turbulence as well as large scale vortex =
dynamics (Vassilicos and Brasseur 1996). Since the seminal work of =
Lundgren (1982) where vortex spirals have been introduced in connection =
to turbulence structure, several works have been presented in literature =
about the energy spectrum associated to spirals of vorticity and of =
passive scalar (Gilbert 1988; Flohr and Vassilicos 1997) and their =
dynamics (Bernoff and Lingevitch 1994; Bassom and Gilbert 1998). These =
work have shown the connection between the singular, or quasi singular, =
geometry of a spiral with the flow dynamics, namely accelerated =
dissipation and power-law spectrum.

The property of transfer between different scales of motion in evolving =
spirals is studied here, and a general mathematical framework is =
developed to describe the transfer between scales inside compact =
structures. It represents an alternative view, for vortex structures, to =
the analysis of transfer in general homogeneous and isotropic turbulence =
(Brasseur and Wei 1994).

This new approach is firstly applied to the case of an axisymmetric =
advection which generates spirals of passive scalars and also represents =
the leading order (large time) approximation for Lundgren's vortex =
spiral. Secondly, it is generalised and applied to non-axisymmetric =
velocity fields in order to analyse higher order non-axisymmetric =
dynamics of rolling-up spiral vortex sheets.=20

It is shown that scale interactions are essentially local in spirals of =
passive scalar created by an axisymmetric advection and also, =
asymptotically in time, in the non-axisymmetric self-advection of a =
Lundgren's spiral vortex sheet. A physical interpretation of the results =
is given, which can be summarised by saying that locality of scale =
interactions is caused by the uniformity of shear at a given scale and =
is therefore increasingly natural at small length-scales. Local =
interactions are shown to arise naturally in axisymmetric advection but =
to be uncommon in non-axisymmetric advection.

Bassom, A.P. & Gilbert, A.D. 1998 The spiral wind-up of vorticity in an =
inviscid planar vortex. *J. Fluid Mech.* 371, 109-140.=20

Bernoff, A.J. & Lingevitch, J.F. 1994 Rapid relaxation of an =
axisymmetric vortex. *Phys. Fluids* 6, 3717-3723.=20

Flohr, P. & Vassilicos, J.C. 1997 Accelerated scalar dissipation in a =
vortex. *J. Fluid Mech.* 348, 295-317.=20

Gilbert, A.D. 1988 Spiral structures and spectra in two-dimensional =
turbulence. *J. Fluid Mech.* 193, 475-497.=20

Lundgren, T.S. 1982 Strained spiral vortex model for turbulence fine =
scale structure. *Phys. Fluids* 25 (12), 2193-2203.=20

Vassilicos, J.C. & Brasseur, J.G. 1996 Self-similar flow structure in =
low Reynolds number isotropic and decaying turbulence. *Phys. Rev. E* 54 =
(1), 467-485.=20

Brasseur, J.G. & Wei, C.H. 1994 Interscale dynamics and local isotropy =
in high Reynolds number turbulence within triadic interactions. *Phys. =
Fluids* 6 (2), 842-870.=20

ANISOTROPIC INERTIAL AND DISSIPATION RANGE DYNAMICS IN ROTATING TURBULENCE

Robert Rubinstein

*Institute for Computer Applications in Science and Engineering
ICASE, MS-403*

6 North Dryden Street

NASA Langley Research Center

*Hampton, VA 23681
USA*

e-mail: bobr@icase.edu

In rotating turbulence, heuristic arguments concerning the turbulent time scale suggest that the inertial range energy spectrum scales as k^{-2} . The existence in rotating turbulence of *inertial wave modes*

$$\mathbf{u}(\mathbf{x}, t) = \mathbf{U} \exp i\{\mathbf{k} \cdot \mathbf{x} - \omega(\mathbf{k})t\} \quad (1)$$

where the dispersion relation is

$$\omega(\mathbf{k}) = \pm \Omega \frac{k_z}{k} \quad (2)$$

suggests the application of the *weak turbulence* theory to rotating turbulence.

The present work applies weak turbulence theory to assess the validity and limitations of the simple scaling arguments which lead to the k^{-2} scaling law in the form

$$E(k) = C\sqrt{\varepsilon\Omega}k^{-2} \quad (3)$$

We also apply weak turbulence theory to explore the anisotropic properties of rotating turbulence which naturally lie beyond the reach of scaling arguments.

From the viewpoint of weak turbulence theory, two possibilities might invalidate the heuristic arguments which lead to Eq. (3): double resonances could alter the turbulent time scale, and four-wave interactions could dominate three-wave interactions leading to a modified inertial range energy balance.

The dispersion relation of the waves defines a resonance surface $h = 0$, where

$$h(\mathbf{k}, \mathbf{p}, \mathbf{q}) = \omega(\mathbf{k}) \pm \omega(\mathbf{p}) \pm \omega(\mathbf{q}) \quad (4)$$

If this surface is nonsingular, weak turbulence theory justifies taking the time-scale of rotating turbulence for scaling purposes to be the inverse rotation rate Ω^{-1} . Eq. (3) follows at once from this scaling by an inertial range energy balance.

This conclusion would be invalidated by singularities like double curves and multiple points which can modify the time scale; the most notable example is provided by nonlinear sound waves in two space dimensions in which the formal scaling law analogous to Eq. (3) does not occur. We find that although double resonances do exist in rotating turbulence, they are irrelevant to energy transfer and do not change the inertial range scaling law.

Four-wave interactions imply a $k^{-7/3}$ inertial range spectrum and a special three-dimensional inverse cascade. Although these interactions are generally dominated by three-wave processes, we identify some special problems, including rotating turbulence in a small-aspect ratio region with a large in-plane viscosity, in which depletion of three-wave interactions could lead to dominant four-wave processes. We show that four-wave processes may also be important in the dissipation range of turbulence under asymptotically large rotation rates such that $RoRe^{1/2} \ll 1$. The restriction of dissipation range interactions to nearly collinear triads is incompatible with three-wave interactions.

A spectral form like Eq. (3) only applies to energy averaged over spheres in wavevector space; it ignores the anisotropy of rotating turbulence. Previous investigations of inertial range energy transfer have focused on transfer through spheres in wavevector space. But it is known that in rotating turbulence, energy is also preferentially transferred toward the plane $k_z = 0$. We show how this *directional anisotropy* effect can be understood in terms of energy transfer through wavevector cones $k_z/k = \text{const}$. In isotropic turbulence, rotational symmetry implies zero net energy flux through such cones, but symmetry breaking by rotation permits it. We quantify this type of energy transfer in terms of anisotropic expressions for the correlation function of rotating turbulence.

Turbulence and vortex structures in rotating and stratified flows

Claude Cambon

Laboratoire de Mécanique des Fluides et d'Acoustique,
U.M.R n° 5509, Ecole Centrale de Lyon,
BP 163, 69131 Ecully Cedex, France

Abstract

The main part of the talk is devoted to a survey of experimental, theoretical, and numerical (DNS/LES) results about structuring effects and possible creation of organised vortices from three-dimensional (3D) turbulence in a rotating frame. Two aspects are successively addressed.

- Linear and nonlinear effects of the Coriolis force on homogeneous turbulence.
Wave-turbulence and developed turbulence.
- Additional role of confinement and of localised forcing. Recent DNS data.

Then, stability of two-dimensional (2D) organised vortices to 3D disturbances, in rotating frame, is briefly discussed in connection with the previous results. Competition of centrifugal and elliptical instabilities is touched upon.

Analogies and differences with the stably stratified and rotating stably stratified cases are discussed at the end, with particular emphasis placed on the following themes:

- Linear dynamics: role of the steady mode of the linear regime (vortex mode, quasi-geostrophic mode) in turbulent mixing and horizontal one-particle dispersion.
- Nonlinear structuring effects: collapse of vertical motion, rise of pancake structures.
- Wave turbulence in horizontally elongated boxes.

In conclusion, it is hoped to bring new elements to a timely debate in progress about some controversial aspects, namely: order of relevant resonant wave-interactions, influence of the aspect ratio of computational boxes, directions for future asymptotic analyses and high resolution DNS/LES.

STRUCTURES AND TURBULENCE IN THE CLOSED COROTATIVE
VON KÁRMÁN FLOW AT HIGH REYNOLDS NUMBER

F. CHILLÁ, C. SIMAND, J.F. PINTON

*Laboratoire de Physique, CNRS URA 1325,
École Normale Supérieure de Lyon, 69364 Lyon France*

The flow is produced in the gap between two coaxial disks rotating in the same direction. The working fluid are air or water, the flow is enclosed in a cylindrical vessel. In this situation one observes a large scale dynamics that is controlled by the disks rotation rates, superimposed to turbulent fluctuations (the integral Reynolds number of the flow is $Re > 5 \cdot 10^4$). For equal rotation rates, the vertical vorticity concentrates to build a strong stable axial vortex. The flow has a large core in solid body rotation. When the disks rotate at quite different rates the axial vortex is unstable. One observes intermittent sequences of formation and breakdown of a very strong and thin axial vortex. We use local hot-wire anemometry or laser doppler anemometry to study the velocity field characteristics as a function of the distance r to the rotation axis. We observe that the small scale velocity statistics is strongly affected from the large scale structure in a not trivial way. The power spectra display a power law behavior indicating the existence of a self similar region, but with slopes that change continuously with the distance to the axis of rotation. The energy transfer (i.e. third order structure functions) seems to be also strongly influenced by the large scale dynamics of the coherent structure, its characteristics depend on the distance to the coherent vortex and is quite different from that of homogeneous, isotropic turbulence.

The prediction of axi-symmetric vortex-breakdown behind a small-amplitude contraction in a straight tube.

René Delfos & Hans E.G. Poppe

J.M. Burgers centre, Delft University of Technology.

Laboratory for Aero- and Hydrodynamics, Rotterdamseweg 145, 2628 AL Delft, The Netherlands

We have done calculations on the axi-symmetric motion of a rotating column of fluid in a straight tube. Such flows are relevant for various purposes: Vortex break-down, the occurrence of a return flow region in the flow, has been subject of fundamental study over the last few decades, with still many questions being unanswered. We are applying a strongly swirling flow for the separation of oil droplets from water; in that case vortex break-down causes an axial backflow that is used in the apparatus.

The calculations presented here are basically meant to show that our method is able to reproduce literature results, such as the calculations done by Beran & Culick (1992) (B&C). They analysed the influence of Reynolds number Re and swirl ratio V on the flow structure.

The flow geometry is a straight pipe section with a length L of 15 radii R . To prevent the eventual recirculating bubble from creeping towards the inlet and thereby corrupting the inflow conditions, they were dynamically separated by a small-amplitude ($\alpha \cdot R$) and length $5 \cdot R$ Venturi nozzle. As a disadvantage, the slight adverse pressure gradient of the initial quasi-cylindrical flow just after the throat is expected to initiate break-down, and in fact to be a control parameter.

We solved the full Navier-Stokes equations under axi-symmetric restriction in a cylindrical coordinate system. Instead of the velocities (u, v, w) and pressure p , the circulation Γ , stream function Ψ and azimuthal vorticity η were calculated. On the inlet axial plug flow, was assumed, with a Burgers vortex for the tangential flow with core radius $R_C = \frac{1}{2} \cdot R$. The outer wall is a streamline with constant circulation. The latter condition is not equal to frictionless flow; because of diffusion, this condition is absorbing angular momentum from the flow. At high $Re = U_{\infty} \cdot R_C / v$, this effect is small, however.

First the equations were transformed to a rectangular grid. A finite difference scheme was set up for the three equations. In fact, the time dependent equations (Γ, η, Ψ) were solved, but we only consider stationary conditions. The calculations were done on the Cray J-90 of Delft University. After a short study on the influence of the resolution, fixed values were taken of 53 radial and 301 axial nodes.

We varied the parameters over the following range: The swirl ratio $V = (0 \dots 1.6)$, the Reynolds number $Re = (250, 500, 1000)$ and the contraction depth $\alpha = (0.025, 0.05, 0.1)$. We calculated two series of solutions.

In the first series, (I), the flow was started from a columnar flow in the whole domain. This method was used to obtain stationary solutions. Basically, two kinds of solutions exist. In the first set, Ψ is positive everywhere, and the flow is unidirectional. For $V > V^* = V^*(Re, \alpha)$, a break-down solution is found, which contains a closed recirculating region just behind the throat. For V just beyond V^* , the bubble is located on the axis. With increasing V and Re , entrainment occurs; the moving of the rear stagnation point towards the frontal one. Finally, the vortex structure evolves into a ring, nearly but not fully detaching from the axis. In those solutions, however, the axial gradients in Ψ are such steep, that one may wonder if the resolution of the numerical model is sufficient.

The dependence on α is relatively large. The value of V^* decreases with increasing α . It is probably the positive pressure gradient that easily destabilises the vortex core.

The second calculation series, (II), was used to study the influence of V . In contrast to series I, here the flow was started from a converged flow field at a near-by value of V . Convergence was much faster than in I. We calculated the minimum axial velocity on the symmetry axis (W_M) as a function of the swirl ratio, V . For $Re = 250$, $\alpha = 0.025$, there is a single-valued dependence between W_M and V , with a very steep decrease in the region where break-down occurs.

For $Re = 500$, $\alpha = 0.025$, a more complex behaviour was found. For $V > V^* = 1.510$, a sudden break-down occurs with a discontinuous change in W_M to a negative value. This is a so-called primary limit point. Further increasing V makes W_M increase, but stay negative. On the other hand, by decreasing V below V^* we still found break-down solutions, until below $V^{**} = 1.502$ the bubble disappeared with a discontinuous rise of W_M . Thus for $1.502 < V < 1.510$ we found a multi-valued solution, the choice of which one is actually present depends on the hysteresis of the system. It is expected that the range in V of multiple solutions grows further with increasing Re . The calculations at $Re = 1000$ are still running.

We also considered the axial position, Z_M , where W_M is found. We see that for $V < 1.4$, Z_M is fixed on the exit of the pipe, $Z = 15 R$. Then for $V > 1.42$, Z_M shifts fast to a position $Z = 7.5 \dots 5.8 R$ just after the place where the pipe has retained its original diameter ($Z = 5 D$). When break-down takes place, i.e. $V > V^*$, Z_M jumps to a position inside the diverging throat, downstream of the smallest diameter, creeping further against the flow with increasing V . For V sufficiently high, the bubble is expected to pass through the throat.

Conclusion.

We conclude that we have developed a numerical model with which we are able to calculate the occurrence and structure of an axi-symmetric vortex break-down region. We were able to obtain results very similar to those found by Beran & Culick (1992). In principle we are able to calculate transient flows as well. For $Re = 500$, we found a multi-valued solution for swirl-ratio $1.502 < V < 1.510$

Ref. Beran, P.S. and Culick, F.E.C. "The role of non-uniqueness in the development of vortex break-down in tubes" *J. Fluid Mech.* 242, 491-527

ABSTRACT

Three-dimensional interaction between a turbulent boundary layer and a bluff body

The interaction between a turbulent boundary layer and a rectangular cross-section tall bluff body placed vertically in the flow is studied experimentally at high Re numbers (10^4

$- 10^5$), with particular attention in the body near wake.

In an ideal two-dimensional configuration the wake is expected to show the periodic alternate

shedding. The present configuration is highly three-dimensional due to the variation of flow

velocity along the body height and due to the presence of the finite body top end which is inside

the boundary layer and the bottom-end where the body is attached to the wall.

In correspondence of the top free-end, the incoming flow separates at body leading edge and

interacts with the shedding from the body lateral sharp edges, making interference with regular

vortex shedding phenomena expected downstream. Furthermore the regular shedding characteristics (i.e. frequency) is modulated along the height because of the variation of the

incoming velocity and gives rise to additional three-dimensional phenomena

The aim of this research is to understand the main features of this kind of interaction and to

investigate how, in spite of the strong three-dimensionality, vorticity structures are shed from body

at certain characteristic frequencies and maintain their coherency along the height.

Experimental investigation on this problem has been performed in the boundary layer wind

tunnel of CRIACIV-DIC located in Prato. It is an open circuit wind tunnel with a testing section

of $2.4 \text{ m} \times 1.6 \text{ m}$ and velocities ranging from 2 m/s to 30 m/s . The bluff body with low aspect

ratio (4) was fully immersed in a boundary layer with free stream turbulence of some % and free-

stream velocity set at values between 2 m/s and 20 m/s . The resulting Reynolds number based on

body length in direction normal to flow varied from $1.2 \cdot 10^4$ to $1.2 \cdot 10^5$.

Visualisations has been performed with a smoke wire technique supported by light

sheets in

either stream-wise and span-wise directions. Even if the dynamics of phenomena evolution is very

complex, it is possible by means of visualisations to understand qualitatively the role of vorticity

structures in the near wake and to highlight their evolution. Vortex shedding has been detected in

the stream-wise direction showing an alternate formation of vortices in the turbulent wake and

their sometime sudden destruction due to some structure instabilities. Span-wise

oblique shedding

distorted by the interaction of structures with separated flow from body top free end and from

bottom constrain has been clearly detected by vertical visualisation. From the images it has been

possible to estimate the shedding frequencies, whose values has been confirmed by pressure

measurements.

Quantitative data have been carried out with pressure measurements on body surface, at high

frequency and at different Re, by means of a pressure system which let to acquire simultaneously

64 pressure taps. Pressure measurements have been performed arranging all taps

Mar 24 1999 13:30

c.piantini

Page 2

in various configurations in such a way to obtain a complete characterisation of the pressure field on body surface. Different values of flow velocity has been used to find the relation of shedding frequency with Re number value. Spectra of signals have been extracted from a Fourier analysis of pressure measurements up to 100 Hz, in addition to correlations and cross-correlations. It has been identified the evolution of shedding frequency at increasing Re number values and the frequency content in spectra at different quotes. Informations on the coherency of phenomena at various frequencies and in different directions have been extracted from the study of coherence function. Results of analysis are shown.

Vortex Structures in Rotating Convection

H.J.S. Fernando
Arizona State University,
Department of Mechanical & Aerospace Engineering
Tempe, AZ 85287-9809, USA

3D Hetons in Rotating Stratified Fluids

Boubnov B.M., Rhines P.B.

Institute of Atmospheric Physics RAS, 109017, Moscow, Russia
School of Oceanography, University of Washington, Seattle, WA 98195-7940, USA

Results of an experimental study of a vortical structures in a convection from a local source of buoyancy in rotating and linear stratified fluids are considered. There are two motivations for this study. One of them is a laboratory simulation of a deep convection in the ocean, the another is a study of a fundamental properties of a vortex dynamic.

A source of buoyancy is a disk with a diameter D , from which a uniform and constant flux of more dense fluid come to main fluid. This disk is placed in the centre of a large cylinder filled with a linear stratified salt fluid. All system are on a table which is rotated with a constant angular velocity. Experimental set up is usual for a "dense convection" (see for example Whitehead et.al. 1996, Narimousa 1998). The main dimensional parameters, which change in large ranges in experiments are: rotation frequency $f = 0.02-3.4$ rad/s, buoyancy frequency $N = 0.37-2.63$ rad/s and buoyancy flux $B = 0.01-30$ cm 2 s $^{-3}$. The main non-dimensional parameters are: $f/N = 0.016-4.59$ and Richardson number Ri , scaled by a local convection velocity.

Depend on the main non-dimensional parameters three different regimes of convection are study. For small f/N a well-known baroclinic vortices are existed (see for example Griffith & Linden, 1981, Hopfinger & van Heijst, 1993). For large f/N and large Ri a regime of convective vortices is existed. In this regime below the source a convective vortices are concentrated as a confined vortex structure. For f/N about 1 and small Richardson number a regime of 3D hetons is existed. In this regime a pair of vorices is spread out from a source. In this pair a cyclonic vortex is near the free surface, while a anticyclonic vortex is on the surface at some depth. With a time a cyclonic part of 3D heton is propagated to the free surface, while an anticyclonic part is concentrated below the surface. A regime diagram in $(f/N, Ri)$ were plotted, which includes as present study, as the results of all previous experiments. A boundary between regimes of baroclinic vortices and 3D hetons well defined by a conditions $Ro = \text{const}$.

A density and velocity structures of a different regimes are studied. Some parts of this hetons were experimentally studied by Whitehead et.al. (1996), Narimousa (1998), Helfrich & Batisti (1991). Numerical study of 3D heton mechanism were studied by Doronina et.al. (1999).

References

Doronina, T., Gryank, V., Olbert, D. & Warncke, T. 1999 A 3D heton mechanism of lateral spreading in localised convection in a rotating stratified fluid. *J.Fluid Mech.* (accepted).

Griffiths, R.W. & Linden P.F. 1981 The stability of vortices in a rotating, stratified fluid. *J.Fluid Mech.*, V.105, 283-316.

Helfrich, K.R. & Batisti T.M. 1991 Experiments on baroclinic vortex shedding from hydrothermal plumes. *J.Geophys. Res.* V.96, No. C7, 12,511-12,518.

Hopfinger E.J. & van Heijst G.J.F. 1993 Vortices in rotating fluids. *Ann.Rev. Fluid Mech.*, V.25, 241-289.

Narimousa, S. 1998 Turbulent convection into a linearly stratified fluid: generation of "subsurface anticyclones". *J.Fluid Mech.* V.354, 101-121.

Whitehead, J.A., Marshall, J. & Hufford, G.E. 1996 Localized convection in rotating stratified fluid. *J.Geophys. Res.*, V.101 (C11), 25,705-25,721.

Vortex generation by line plumes in a rotating stratified fluid

John W. M. Bush [†] & Andrew W. Woods [‡]

[†] Department of Mathematics, MIT, U.S.A.

[‡] Department of Mathematics, University of Bristol, U.K.

We present the results of an experimental investigation of the generation of coherent vortical structures by buoyant line plumes in rotating fluids. Both uniform and stratified ambients are considered. By combining the scalings describing turbulent plumes and geostrophically balanced vortices, we develop a simple model which predicts the scale of the coherent vortical structures in excellent accord with laboratory experiments.

We examine the motion induced by a constant buoyancy flux per unit length B , released for a finite time t_s , from a source of length L into a fluid rotating with angular speed $\Omega = f/2$. When the plume discharges into a uniformly stratified environment characterised by a constant Brunt-Vaisala frequency, $N > f$, the fluid rises to its level of neutral buoyancy unaffected by the system rotation before intruding as a gravity current. Rotation has a strong impact on the subsequent dynamics: shear develops across the spreading neutral cloud which eventually goes unstable, breaking into a chain of anticyclonic lenticular vortices. The number of vortices n emerging from the instability of the neutral cloud,

$$n = (0.65 \pm 0.1) \frac{L f^{1/2}}{t_s^{1/2} B^{1/3}} ,$$

is independent of the ambient stratification, which serves only to prescribe the intrusion height and aspect ratio of the resulting vortex structures. The experiments indicate that the Prandtl ratio characterising the geostrophic vortices is given by

$$P = \frac{Nh}{fR} = 0.47 \pm 0.12.$$

where h and R are, respectively, the half-height and radius of the vortices. The lenticular vortices may merge soon after formation, but are generally stable and persist until they are spun-down by viscous effects.

When the fluid is homogeneous, the plume fluid rises until it impinges on a free surface. The nature of the flow depends critically on the relative magnitudes of the layer depth H and the rotational lengthscale $L_f = B^{1/3}/f$. For $H > 10 L_f$, the ascent phase of the plume is influenced by the system rotation and the line plume breaks into a series of unstable anticyclonic columns of characteristic radius $(5.3 \pm 1.0) B^{1/3}/f$ which typically interact and lose their coherence before surfacing. When $H < 10 L_f$, the system rotation does not influence the plume ascent, but does control the spreading of the gravity current at the free surface. In a manner analogous to that observed in the stratified ambient, shear develops across the surface current, which eventually becomes unstable and generates a series of anticyclonic surface eddies with characteristic radius $(1.6 \pm 0.2) B^{1/3} t_s^{1/3}/f^{2/3}$. These surface eddies are significantly more stable than their columnar counterparts, but less so than the lenticular eddies arising in the uniformly stratified ambient.

The relevance of the study to the formation of coherent vortical structures by leads in the polar ocean and hydrothermal venting is discussed.

EUROMECH 396: "Vortical Structures in Rotating and Stratified Fluids"
June 22-25, 1999 - Cortona, Italy

EXPERIMENTAL STUDY OF THE INTERACTION OF TWO CO-ROTATING VORTICES

T. Leweke & P. Meunier

Institut de Recherche sur les Phénomènes Hors Equilibre
CNRS/Universités Aix-Marseille I & II, Marseille, France

Introduction - We present experimental results concerning the evolution of a flow consisting initially of two parallel vortices with circulations of the same sign, i.e. a co-rotating vortex pair. Such a pair rotates around the midpoint between the vortex centres at an initially constant rate; it is therefore useful for the study of elementary vortex interactions in a rotating frame of reference. Despite the intrinsic interest of this basic flow configuration on a fundamental level, as well as its relevance for some practical applications like aircraft wakes, very little data is available from precise laboratory experiments to date, which is one of the motivations for this study.

Experimental details - The vortex pairs are generated in a water tank at the sharpened parallel edges of two flat plates moved in a prescribed symmetric way by computer-controlled step motors. The vortices are typically separated by a distance of 2.5 cm. Visualisation is achieved using fluorescent dye. A vortex pair is characterised by several parameters: the circulation Γ of each vortex, the separation b between the vortex centres, and a characteristic core radius a . They were determined from flow field measurements using Digital Particle Image Velocimetry (DPIV). These measurements also showed that the initial velocity profiles of the vortices are very well represented by the one of a Lamb-Oseen vortex with a Gaussian vorticity distribution. The Reynolds number based on the initial circulation ($Re = \Gamma v$) was in the range between 1500 and 6000 in this study. More details on the experimental techniques can be found in Leweke & Williamson (1998).

Three-dimensional stability - For the case of a large separation distance, compared to the diameter of the vortex cores, the study of Jimenez (1975) has shown that, for the corotating pair, there is no equivalent to the well known Crow instability (Crow 1970), occurring in counter-rotating pairs. This is confirmed in our experimental study, where the pair is found to be stable with respect to three-dimensional long-wavelength perturbations. In addition, no evidence of a short-wave length three-dimensional instability, similar to the cooperative elliptic instability described in Leweke & Williamson (1998) for the counter-rotating pair could be observed experimentally so far. Both of these characteristic 3D vortex pair instabilities appear to be inhibited by the global rotation of the vortex system. In addition, the time available for a potential three-dimensional instability to develop is limited by another mechanism of essentially two-dimensional nature leading to a rapid change in the large-scale structure of the flow: the merging, or fusion, of the two initially separated vorticity distributions.

Vortex merging - Figure 1 shows an experimental observation of this process at a Reynolds number of about 5000. The flow is visualised in a plane perpendicular to the vortex axes, and time is expressed in units of the global turnover time of the initial pair. The merging begins with an elongation of the initially circular cores in a direction close, but not equal to the line joining the two centres. Pronounced tips appear at both ends of each dye patch, which rapidly develop into large-scale spiral arms on the outside, whereas the inner part bears a strong resemblance to the Chinese

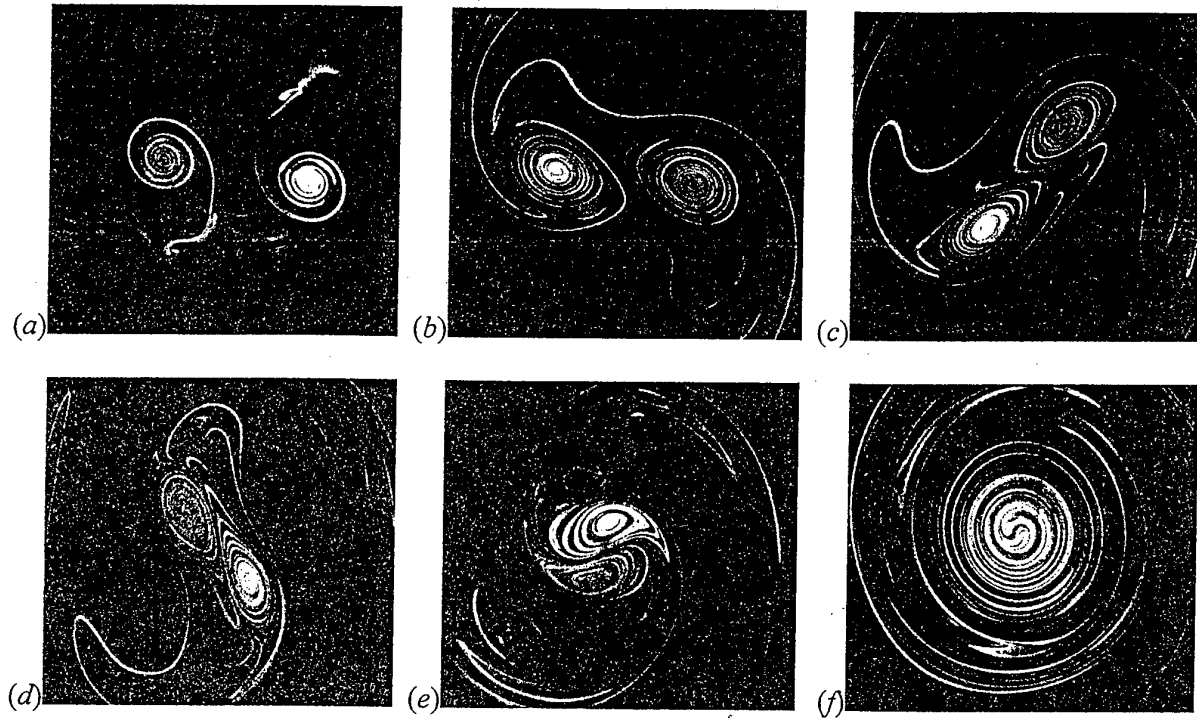


Figure 1 - Visualisation of the merging of two co-rotating vortices at $Re \approx 5000$.
 (a) $t^*=0$, (b) $t^*=0.5$, (c) $t^*=0.6$, (d) $t^*=0.7$, (e) $t^*=0.9$, (f) $t^*=t\pi/2\pi^2b^2$.

yin-yang symbol (fig. 1e). At very late times, the pair evolves into a single large vortex. Although the velocity and vorticity fields are smooth and axisymmetric at this stage, as shown from quantitative measurements using DPIV, one can still identify the different layers of dyed fluid originating in each of the two initial vortices. The distribution of the (almost) passive dye scalar exhibits a distinct radial scale not present in the velocity field. The characteristic time of the fusion process is given by the turnover time of the initial pair, which is a convective time, and which is several orders of magnitude smaller than the characteristic vorticity diffusion time b^2/v .

Although the interpretation of dye patterns has to be done with care, especially at later times, the experimentally observed flow features in figure 1 are in good qualitative agreement with numerical simulations shown by Melander *et al.* (1988), and with results from a contour dynamics study by Overman & Zabusky (1982), using patches of constant vorticity, at least in the initial stages of the core interaction.

The experimental study of co-rotating vortex pairs is currently still in progress. More quantitative results concerning the fusion process, its dependence on vortex separation and Reynolds number, as well as the influence of three-dimensional forced perturbations, will be presented at the meeting.

We acknowledge the financial support from the "Direction Générale de l'Armement" of the French Ministry of Defence, under contract no. ERS 97-1097.

References

- CROW, S. C. 1970 Stability theory for a pair of trailing vortices. *AIAA J.* **8**, 2172.
- JIMENEZ, J. 1975 Stability of a pair of co-rotating vortices. *Phys. Fluids* **18**, 1580.
- LEWEKE, T. & WILLIAMSON, C. H. K. 1988 Cooperative elliptic instability of a vortex pair. *J. Fluid Mech.* **360**, 85.
- MELANDER, M. V., ZABUSKY, N. J. & MCWILLIAMS, J. C. 1988 Symmetric vortex merger in two dimensions: causes and conditions. *J. Fluid Mech.* **195**, 303.
- OVERMAN, N. J. & ZABUSKY, N. J. 1982 Evolution and merger of isolated vortex structures. *Phys. Fluids* **25**, 1297.

Tentative Title: Dynamics of radiating cold domes on a sloping bottom

Authors: Gordon E. Swaters

Abstract:

Numerical simulations of benthic gravity-driven currents along continental shelves suggest they exhibit considerable time and spatial variability and tend to organize themselves into large scale bottom-intensified cold domes or eddies. Attempts to

derive simple relations governing the evolution of the spatial moments of the mass equation for baroclinic eddies have failed because it is not clear how to express the form or wave drag stresses associated with the excited (topographic) Rossby wave field in the surrounding fluid in terms of the eddy moments. We develop a simple model for the leading order time evolution of a cold dome configuration which initially nearly satisfies the Mory-Stern isolation constraint. As the topographic Rossby wave field in the surrounding fluid interacts with the cold dome, higher azimuthal modes are excited within the cold dome which develop into spiral-like filamentary structures on the eddy boundary. The trajectory followed by the position of the maximum height of the cold dome corresponds to sub-inertial along and cross slope oscillations superimposed on a mean along slope drift (well described by the Nof velocity). Nevertheless, the theory suggests that there are no oscillations (at least to second order) in the horizontal spatial moments of the eddy height, that is, the centre of mass of the eddy moves steadily in the along and down slope direction (i.e., "southwestward" relative to the topographic beta-plane). The theoretical analysis is in good agreement with a nonlinear numerical simulation which we present.

Von Kármán-like vortex streets on a two layer β -plane and baroclinic jet streams

Vladimir Gryank^{1,2}, Hartmut Borth¹ and Dirk Olbers¹

Abstract

We present an analytical theory of von Kármán-like vortex streets on a two-layer β -plane consisting of periodic arrangements of modified point vortices. The point vortex streets exist as quasi-stationary states and have essential new features if compared to their 2-dimensional counterparts. The generalized von Kármán vortex streets induce zonal mean flows which can be seen as a special class of baroclinic jet streams. The basic equations for our theory are the standard evolution equations of potential vorticity on a two-layer β -plane with flat bottom, rigid lid and no exterior vorticity sources and sinks. For equal layer thicknesses one gets

$$\frac{\partial q_k}{\partial t} + [\psi_k, q_k] + \beta \frac{\partial \psi_k}{\partial x} = 0 \quad k = 1, 2 \quad (1)$$

with the potential vorticity distribution q_k of the k -th layer defined by

$$q_k = \Delta \psi_k + (-1)^k F (\psi_1 - \psi_2) \quad k = 1, 2. \quad (2)$$

We denote by ψ_k the two stream functions, by $\Delta f = f_{xx} + f_{yy}$ and $[f, g] = f_x g_y - f_y g_x$ the Laplace and Jacobi operator, by $F = f_0^2 \rho_0 / g H \Delta \rho$ the coupling constant where ρ_0 is the reference density, $\Delta \rho$ the density difference between the layers, g the gravitational acceleration and H the thickness of each layer. The planetary vorticity f is linearly approximated by $f = f_0 + \beta y$.

We found different classes of periodic vortex streets as quasi-stationary solutions propagating with constant speed c to the east. The streets consist of two parallel symmetric or staggered rows (see e.g. Lamb (1932)) of equally spaced point vortices having in one row the vorticity strength κ and in the other $-\kappa$. The street width is given by b and the vortex separation in x -direction by a . The rows can be located in the same or in different layers. Each point vortex is a mixed barotropic-baroclinic dirac singularity of the modified vorticity fields $Q_k = q_k - (\beta/c) \psi_k$ (the one-layer β -plane case is analyzed by Gryank (1986)). For our investigations we introduced a new set of variables: A non-dimensional propagation speed $1/\xi^2$ with $\xi = b\sqrt{\beta/c}$, a non-dimensional street width $\sigma = b/L$ with $L = 1/\sqrt{2F}$ the Rossby radius, a non-dimensional vorticity strength $1/\mu$ where $\mu = c_L/v_L$ with the two reference speeds $c_L = L^2 \beta$ and $v_L = \kappa/4\pi L$ and finally the aspect ratio of a street $k = b/a$.

In terms of this new set of parameters we derived a nonlinear dispersion relation for generalized von Kármán point vortex streets. Using the non-dimensional distance function $r_m(k) = \sqrt{1 + (m/k)^2}$ for symmetric streets and $r_m(k) = \sqrt{1 + ((2m+1)/2k)^2}$

¹Alfred-Wegener-Institute for Polar- and Marine Research, Bremerhaven, Germany

²A.M. Obukhov Institute for Atmospheric Physics, Russian Academy of Sciences, Moscow, Russia

for staggered streets we can write this non-linear dispersion relation as

$$\mu = \frac{\xi^2}{\sigma^3} \sum_{m=-\infty}^{\infty} \frac{1}{r_m(k)} \left[\xi K_1[\xi r_m(k)] \pm \sqrt{\xi^2 + \sigma^2} K_1[\sqrt{\xi^2 + \sigma^2} r_m(k)] \right] \quad (3)$$

where $K_1[x]$ is the modified Bessel function of first order. The plus sign is taken for streets with both vortex rows in the same layer and the minus sign for streets with vortex rows in different layers. To each solution $\xi(\mu, \sigma, k)$ of this equation corresponds a vortex street existing as a quasi-stationary state on the two-layer β -plane.

These solutions have a series of interesting new properties. The two-layer β -plane von Kármán streets can only move to the east, unlike their classical 2D counterparts which can move either to the east or to the west. The structure of the point vortices composing the von Kármán street does depend on the propagation speed of the whole street and is therefore a dynamical property. For a fixed non-dimensional street width σ , a von Kármán vortex street will only be a quasi-stationary solution if the vorticity strength κ of the individual vortices is above a critical vorticity strength κ_{crit} . Or equivalently, for a fixed vorticity strength κ_{crit} , a vortex solution will only be a quasi-stationary solution if the street width σ does not exceed a critical value σ_{crit} . If for a given set of parameters von Kármán streets can exist as quasi-stationary states, there will always exist two different types of streets except in one critical case for $c = c_{crit}$, where there will exist only one street. There exists a fast type having for $\xi \rightarrow 0$ a corresponding limiting state on the f -plane and a slow type being a pure β -plane state with no corresponding limit on the f -plane. For vortex pairs (see Gryanik (1983) and Hogg and Stommel (1985)), i.e. the limit of dilute vortex streets with aspect ratios $k \ll 1$, and for two parallel vortex sheets, i.e. the limit of dense vortex streets with aspect ratios $k \gg 1$, we give first and second order expressions for the propagation speed c of fast ($\xi \ll \min\{1, \sigma\}$) and of slow ($\xi \gg \max\{1, \sigma\}$) solutions. The first correction terms of the asymptotical expansions for the propagation speeds c show that the β -effect changes the f -plane behaviour in a complex way.

We can use the above theory to describe the class of baroclinic jet streams on a two-layer β -plane which are induced by quasi-stationary vortex streets. We see that the shapes, i.e. the width and the tails, of the velocity mean profiles of such jets depend directly on the propagation speed and that for fixed vorticity strengths jet streams can only exist up to a maximum width.

References

- [1] Gryanik, V.M., 1986: Singular Geostrophic Vortices on the β -Plane as a Model for Synoptic Vortices. *Oceanology*, 26(2), 126–130
- [2] Gryanik, V.M., 1983: Dynamics of Singular Geostrophic Vortices in a Two-Layer Model of the Atmosphere (Ocean). *Izv. Atmos. Ocean Phys.*, 19(3), 171–179.
- [3] Hogg, N.G., and H.M. Stommel, 1985: The Heton, an Elementary Interaction Between Discrete Baroclinic Geostrophic Vortices, and Its Implications Concerning Eddy Heat-Flow. *Proc. Roy. Soc. London A* 397, 1–20.
- [4] Lamb, H., Hydrodynamics, pp. 225–229, 6th ed., Cambridge Univ. Press. 1932

Three-dimensional structure, instability and interactions of vortices in a linearly stratified fluid

M. Beckers¹, R. Verzicco², H.J.H. Clercx¹ and G.J.F. van Heijst¹

¹ Fluid Dynamics Laboratory, Dept. of Applied Physics, Eindhoven University of Technology, P.O. Box 513, 5600 MB, Eindhoven, The Netherlands. (marcel@tnv.phys.tue.nl)

² Università di Roma "La Sapienza" Dipartimento di Meccanica e Aeronautica, Italy.

This presentation describes three aspects of vortices in a linearly stratified fluid: the 3D structure and cyclostrophic balance of axisymmetric vortices (monopoles), the azimuthal instability of these vortices (*i.e.* the formation of tripoles) and the interactions between two monopolar vortices. These aspects have been investigated by using laboratory experiments, analytical modelling and 3D numerical simulations.

Decaying turbulence in a stratified fluid has some features in common with the evolution of 2D turbulence and the process of 'self-organization'. In both cases initially randomly distributed motion eventually results in the formation of vortices that, by mutual interactions (between vortices with equally signed vorticity) grow in size and decrease in number. Oppositely signed vortices can, when their separation distance becomes small enough, form pairs (dipoles) which start to translate through the fluid, providing a mechanism for the transport of matter. In the past, laboratory experiments have shown various demonstrations of self-organization in a stratified fluid, *e.g.*, the formation of a dipole, resulting from a turbulent jet in a stratified fluid (Flór & van Heijst 1994), the formation of a regular street of vortices behind an object (usually a sphere) towed through a stratification (Spedding *et al.* 1996), or the decay of rake generated turbulence and the subsequent formation of specific vortex patterns in a stratified fluid bounded by lateral no-slip walls (Maassen *et al.* 1999).

3D structure and cyclostrophic balance

In a stratified fluid vortices have essentially a 3D structure, in contrast to purely 2D flows, and, furthermore, there is an interaction between the vorticity field and the density distribution. The study of vortices in a stratified fluid has yielded four interesting features: (1) A single monopolar vortex, submerged in a stratified fluid, will always be surrounded by a ring of oppositely signed (vertical) vorticity, because the vortex lines form closed loops inside the fluid. This suggests that the vortex lines which are directed upwards inside the core of the vortex, need be directed downwards somewhere else in the fluid. (2) The vortex has a limited, but finite vertical thickness, and therefore its momentum will also diffuse in the vertical direction. This causes a much more rapid decay of the velocity field of each vortex, than in case of 2D flows with only lateral diffusion. (3) The centrifugal force in the vortex needs to be balanced, and, because the vortex exists within the fluid (not at the free surface), a radial pressure gradient can only be provided when the iso-density planes inside the vortex are deformed. It was found that they are deflected towards each other in the core of the vortex, resulting in a local stratification maximum. (4) The fluid we consider is density-stratified by using salt. The Schmidt number Sc , *i.e.* the ratio between the diffusivities of momentum and salt, is much larger than one, and this means that any perturbation of the linear density gradient will diffuse on a much larger time scale than momentum. This causes a buoyancy driven circulation inside the vortex during its decay. It has been found that this circulation can cause a stretching of the vortex, and this results in a weaker decay of the flow than due to pure diffusion. In other words, during the decay

of the vortex the potential energy, stored in the density perturbation, is released and converted into kinetic energy. This stretching effect was found to become relatively stronger for higher Froude number flows (*i.e.* a weaker stratification), and for thinner vortices.

Azimuthal instability and tripole formation

The inherently shielded character of the monopolar vortex in a stratified fluid can give rise to azimuthal instability of the flow and the formation of a tripole, or even a triangular vortex. The parameter that determines whether instability takes place is the steepness (or radial gradient) of the vorticity profile. It was found that, for a 2D, axisymmetric, shielded vortex, lateral diffusion causes an evolution of any initial, shielded vorticity profile towards a specific self-similar vorticity profile, called the isolated Gaussian profile, that is (more or less) stable to azimuthal perturbations. Profiles with initially much steeper (and therefore unstable) vorticity gradients thus evolve, due to viscosity, to a stable profile. Investigations of monopolar vortices in a stratified fluid have shown that the stretching effect, that arises during the decay of the vortex, can in fact enhance this viscous stabilization of the vorticity profile. Accordingly, it was found that the tripole resulting from a monopole with a low Froude number (*i.e.* in a relatively strong stratification) is more developed than the tripole resulting from a high Froude number vortex. Furthermore, it was found that the destabilization and tripole formation in a (non-rotating!) stratified fluid is predominantly a barotropic process.

Interactions between shielded monopoles

The third aspect that we have investigated is the interaction between two shielded monopoles, both with equally signed and oppositely signed vorticity distributions. We have previously found, see Schmidt *et al.* (1998), that during the interaction between two oppositely signed monopoles, the shieldings provide an essential mechanism in bringing the two cores closer together, such that a compact dipole is formed. When the shieldings are peeled off from the monopoles they form a second, but weaker dipole, moving in the opposite direction. In the interaction between two equally signed shielded monopoles, the shielding particularly frustrates the interaction, and, in contrast to the interaction between non-shielded monopoles, no merging between the vortices was found to take place, because the shieldings and the cores together formed two dipoles that move in opposite directions. Three-dimensional numerical simulations have been performed and compared with the experimental results, and, furthermore, the 3D structure of a dipole in a stratified fluid could be investigated in more detail.

Flór, J.B. & van Heijst, G.J.F. 1994. An experimental study of dipolar vortex structures in a stratified fluid. *J. Fluid Mech.* **279**, 101–133.

Maassen, S.R., Clercx, H.J.H. & van Heijst, G.J.F. 1999. Decaying quasi-2D turbulence in a stratified fluid with circular boundaries. *Europhys. Lett.* to appear.

Schmidt, M.R., Beckers, M., Nielsen, A.H., Juul Rasmussen, J. & van Heijst, G.J.F. 1998. On the interaction between two oppositely signed, shielded, monopolar vortices. *Phys. Fluids* **10**, 3099–3110.

Spedding, G.R., Browand, F.K. & Fincham, A.M. 1996. Turbulence, similarity scaling and vortex geometry in the wake of a sphere in a stably-stratified fluid. *J. Fluid Mech.* **314**, 53–103.

Internal density structure of stratified vortices

Marion BONNIER ^{a,b}, ¹Olivier EIFF ^b, Philippe BONNETON ^c

^a Institut de Mécanique des Fluides, allée du professeur Camille Soula, 31400 Toulouse

^b Centre National de Recherches Météorologiques, 42, av. G. Coriolis, 31057 Toulouse

^c D.G.O., Université Bordeaux 1, av. des Facultés 33405 Talence

Recent experiments, Bonnier et al. (1999), have revealed the internal density structure of pancake-like vortices generated by towing a sphere in a linear saline stratification. It was shown that the core of the vortices is marked by an intensification of the stratification with respect to the background. This intensification, moreover, was shown to be in qualitative agreement with a simple analytical model based on a Gaussian velocity field.

New data on the temporal evolution of the density deviation with respect to the background stratification in the core of the vortex structures exhibit a transitory regime. In the early stages of evolution, the vortex is deformed by strong advection in the flow and does not exhibit a Gaussian shape. Later, the vortices reach a quasi-steady state exhibiting Gaussian horizontal and vertical density deviation profiles in quantitative agreement with the model. These experiments also reveal that in the core of the vortices, secondary downward motions are superimposed to the primary cyclostrophic movement.

The vortical structures emerging in the far-wake of a sphere, in both the laminar and turbulent regimes, exhibit the same characteristics although their mechanisms of generation are different. This suggests that these density characteristics are universal features of stratified vortices independant of their origin. Indeed, a similar density structure was measured by Beckers et al. (1999) in the case of a monopole. Further evidence for single-layer vortical structures is given by the vertical density profiles measured in the cores of the head of a dipolar vortex shown in figure 1.

To extend these single-layer results to multi-layer vortical structures, we have also examined the vortices generated in the wake of a vertical cylinder. Fincham et al. (1996) provided a description in terms of the velocity and vorticity fields of the multi-layer arrangement behind a rake of vertical bars. A vertical cylinder, because of its two-dimensional geometry, generates columnar vortices that break up into individual pancake-like vortices organised in several horizontal layers. Fluorescent-dye visualizations of such vortices in horizontal or vertical planes of examination exhibit strong qualitative resemblance with the single-layer case previously described. Vertical density profiles measured in the wake of the cylinder show the decorrelation of the different layers but revealing the same density structures as in the single-layer case. Thus, these density profiles provide new insight on the underlying structures constituting multi-layer flows, as first suggested by Fincham et al. (1996) and shown in the sketch of figure 2.

¹Corresponding author : e-mail bonnier@cnrm.meteo.fr, fax 33 5 61 07 95 66

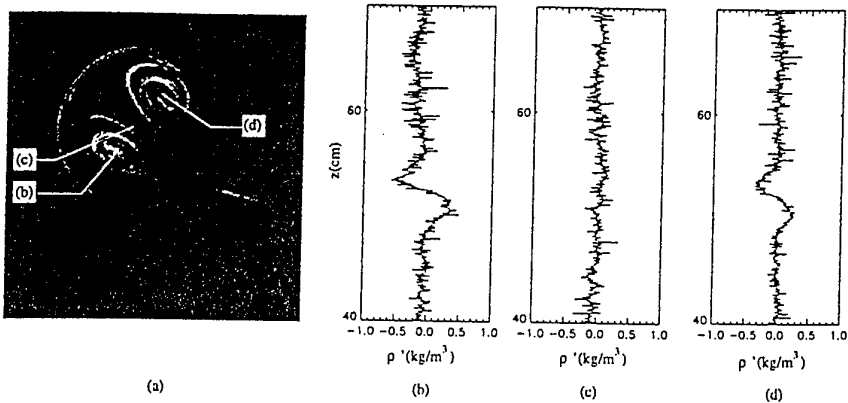


Figure 1: (a) Horizontal plan view of a dipolar vortex generated by a turbulent jet and visualised with fluorescent dye. (b) and (d) Vertical density deviation profiles, $\rho'(z)$, performed in the core of the vortex head. (c) Vertical density deviation profile, $\rho'(z)$, measured in between the two vortices.

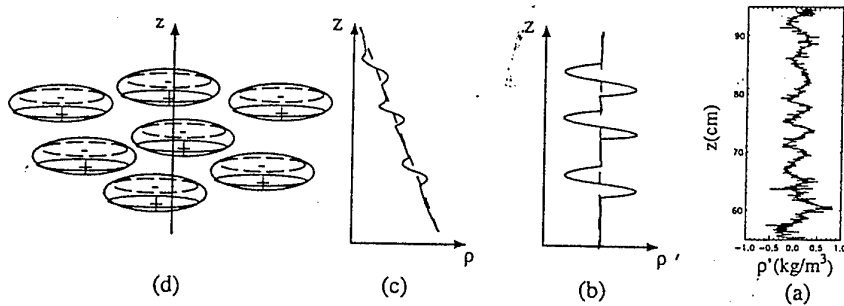


Figure 2: (a) Schematic of a multi-layer arrangement as a pile of several single-layer structures presenting a deficit and an excedent in ρ , in their upper and lower part, respectively. (b) Schematic of a corresponding density profile $\rho(z)$. (c) Schematic of the corresponding density deviation $\rho'(z)$. (d) Exemple of a density deviation profile of a multi-layer situation measured in the wake of a vertical cylinder.

References

Beckers, M., Verzicco, R., Clercx, H.J.H., Van Heijst, G.J.F., 1999. The vertical structure of pancake-like vortices in a stratified fluid : experiments, theory and numerical simulations. Submitted to *J. Fluid Mech.*.

Bonnier, M., Eiff, O., Bonneton, P., 1999. On the density structure of far-wake vortices in a stratified fluid. To appear in *Dyn. Atmos. Oceans*.

Fincham, A., Maxworthy, T., Spedding, G.R., 1996. Energy dissipation and vortex structure in freely decaying stratified grid turbulence. *Dyn. Atmos. Oceans*, 23, 155-169.

Jun 5 1999 15:35

detl

Page 1

Small scale atmospheric vortices

D. Etling
Institute for Meteorology and Climatology
University Hannover, Germany

Large scale atmospheric vortices like cyclones are familiar to everybody due to their influence on daily weather. But there are a variety of intense small scale vortices like dust devils, water spouts or Tornadoes which occur only occasionally and hence are difficult to observe. These vortices form under various atmospheric conditions, depending on background wind shear, stratification and ambient rotation, but the exact mechanism of their formation is still not totally clear in some cases.

We will present some examples of small scale atmospheric vortices and discuss their formation in the light of vortex dynamics.

-- =

Prof. Dr. D. Etling
Institut fur Meteorologie und Klimatologie
Universitat Hannover
Herrenhauser Str. 2

30419 Hannover

Tel.: ++49 0511 762 2618
e-mail: etling@muk.uni-hannover.de

Three-dimensional instability of anticyclonic barotropic vortices
in a rotating fluid

Ya.D.Afanasyev and W.R.Peltier

Department of Physics, University of Toronto, Toronto, Ontario, Canada M
5S 1A7

Ambient rotation can be a crucial factor in determining the stability
properties of small and meso-scale vortices in the oceans and atmosphere

Although there a small number of recent articles have appeared that have

focused on the behaviour of barotropic vortices in a rotating fluid,
this geophysically important problem seems yet to be fully understood.

New results from a sequence of especially designed laboratory
experiments that focus on the instability of swirling anticyclonic flow
will be presented. The flow is created by a cylinder rotating in a fluid

which is itself initially in a state of solid-body rotation. The
experiments demonstrate that secondary motions appear in an annular regi
on

surrounding the cylinder and are governed by the process of
three-dimensional centrifugal instability. These motions have spiral
structure in the vertical characterized by a well defined wave number.
The width of the unstable annular region as well as the vertical
wavelength of the motions is determined by the main nondimensional
parameter of the flow - the Rossby number. The evolution of the
secondary motions gives rise to the appearance of tertiary motions -
which are Kelvin-Helmholtz like vortices that develop at the periphery
of the annulus, thus creating a complex three-dimensional structure in t
he

unstable flow. If the rotating cylinder is withdrawn vertically
from the fluid, the instability rapidly destroys the core of the
vortex in a way that is consistent with the behaviour of unstable vortic
es

observed in previous laboratory experiments by Kloosterziel and
van Heijst (J.Fluid Mech., 223, 1992). The results of the experiments
will be compared with the results of recent numerical stability analyses

by Potylitsin and Peltier (J.Fluid Mech. 1998), and with the
theoretical results for homogeneous fluid previously obtained by
Smyth and Peltier (J.Fluid Mech., 265, 1994).

Zigzag instability of a vertical columnar vortex pair in a strongly stratified fluid

Paul Billant^{1,2} and Jean-Marc Chomaz¹

¹*LadHyX, CNRS-UMR 7646, Ecole Polytechnique, F-91128 Palaiseau Cedex, France*

²*Météo-France CNRM Toulouse, 42 avenue Coriolis, F-31057 Toulouse, France*

A striking and prominent feature of strongly stratified turbulence observed in experiments and numerical simulations is the emergence of coherent horizontal pancake vortices organized in decoupled horizontal layers. To understand the mechanism responsible for the emergence of such decoupled layers and the thickness selection, we study the dynamics of a prototype flow initially uniform along the vertical: a columnar vertical vortex pair in a strongly stratified fluid. Most interestingly, we found experimentally that an instability, which we name zigzag instability, is at the origin of the vertical decoupling. We shall present experimental, theoretical and numerical investigations on this new instability.

A 60 cm long columnar vertical vortex pair is created by computer-controlled flaps, i.e. two rotating vertical plates. When the horizontal Froude number F_h ($F_h = U/RN$, where U is the dipole traveling velocity, R the dipole radius and N the Brunt–Väisälä frequency) is below 0.2, the vortex pair is subjected to the zigzag instability which is distinct from the Crow and elliptic three-dimensional instabilities known to occur on vortex pairs in a homogeneous fluid[1]. This instability consists of a vertically modulated rotation and a translation of the columnar vortex pair perpendicularly to the traveling direction with almost no change of the dipole's cross-sectional structure. Ultimately the vortex pair is sliced into thin horizontal layers of independent pancake dipoles (figure 1). This is to be contrasted with the elliptic instability which develops for $F_h \geq 0.2$ and bends each vortex core in the opposite direction to the vortex periphery[1].

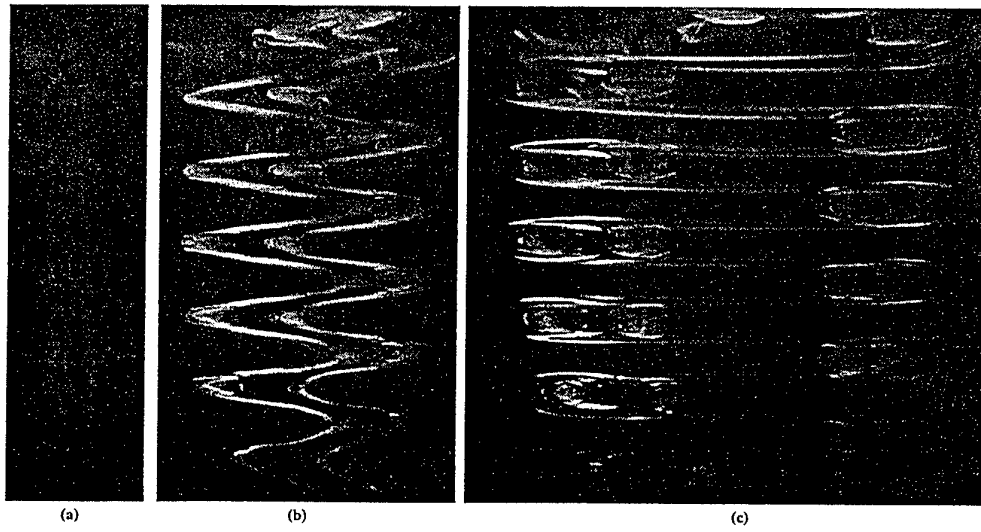


Figure 1: Front views showing the development of the zigzag instability for $F_h = 0.17$ and $Re = 233$ at $t = 7$ s (a), 75 s (b) and 176 s (c).

A multiple-scale perturbation analysis for small horizontal Froude number and long-wavelength links this zigzag instability to the breaking of translational and Galilean invariances. The dispersion relation as well as the spatial eigenmode of the zigzag instability are determined. The main prediction is that the growth rate of the zigzag instability should be self-similar with respect to the variable $F_h k_z$, where k_z is the non-dimensional vertical wavenumber. This implies that the maximum growth rate should be independent of F_h while the most amplified wavelength λ should scale as $\lambda \propto U/N$.

Physically, the zigzag instability survives in the limit of strong stratification and the thickness of the ensuing layers are predicted to become thinner and thinner as the stratification increases.

A numerical stability analysis fully confirms these theoretical predictions. The analytical zigzag eigenmode and the dispersion relation are in excellent agreement with the numerical results (figure 2). As observed experimentally, for $F_h \leq 0.2$, the instability is of the zigzag type while for $F_h \geq 0.2$ it is of the elliptic type. The numerically calculated wavelength is also in good agreement with the experimental measurements.

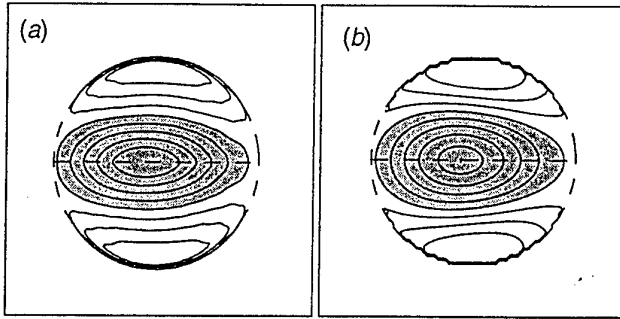


Figure 2: Comparison between the numerical (a) and analytical (b) vertical vorticity of the zigzag eigenmode in the horizontal plane for $F_h = 0.033$, $k_z = 8.25$, $Re = 10000$.

These results demonstrate that an active mechanism, an instability, can be responsible for the emergence of layered pancake-shaped vortices. This instability determines the maximum vertical length of coherence by breaking-up tall vortices into smaller ones. In view of the ubiquitous observations of decoupled layers in stratified flows, we conjecture that this type of instability is generic and not specific of the vortex pair case. Such a decoupling instability could occur as soon as a stratified flow contains several interacting tall vertical vortices and leads to a horizontal layering with a vertical scale of order U/N .

On the basis of an invariance of the non-linear equations of motion when $F_h \ll 1$, we further show that the scaling law $\lambda \propto U/N$ is not specific to the linear instability of a vortex pair but very general: the buoyancy lengthscale U/N is the natural characteristic vertical scale of strongly stratified flows. For such a fine scale, the vertical motion cannot be neglected and the horizontal motion does not follow the 2D Euler equations[2, 3]. Applied to strongly stratified turbulence, this instability mechanism transfers energy from large vertical scales directly to the small scale U/N at which approximate equipartition between potential and kinetic energies is achieved. As a result, the vertical spectrum of horizontal kinetic energy in strongly stratified flows should be of the form $E(k_z) \propto N^2 k_z^{-3}$ as indeed observed in the upper atmosphere[4].

References

- [1] Leweke, T. & Williamson, C.H.K. Cooperative elliptic instability of a vortex pair. *J. Fluid Mech.* 360, 85–119 (1998).
- [2] Riley, J.J., Metcalfe, R.W. & Weissman, M.A. Direct numerical simulations of homogeneous turbulence in density stratified fluids. In *Proc. AIP Conf. Nonlinear Properties of Internal Waves* (ed. B. J. West), 79–112 (1981)
- [3] Lilly, D.K. Stratified turbulence and the mesoscale variability of the atmosphere. *J. Atmos. Sci.* 40, 749–761 (1983).
- [4] Smith, S.A., Fritts, D.C. & VanZandt, T.E. Evidence for a saturated spectrum of atmospheric gravity waves. *J. Atmos. Sci.* 44, 1404–1410 (1987).

Experiments on wave-vortex interactions in a rotating stratified fluid

J.-B. Flór

Laboratoire des Ecoulements Géophysique et Industriels,
UJF-CNRS-INPG, B.P. 53X, 38041 Grenoble Cedex, France.

In order to investigate the interactions between waves and vortices in geophysical flows, laboratory experiments are conducted in a stratified rotating fluid. A stationary geostrophic vortex lens is perturbed by inertia-gravity waves, which are generated by a vertically oscillating ring with a diameter of approximately 10 times that of the vortex. The wave energy thus converges to the centre which reduces the effect of energy dissipation by viscosity. By placing the vortex at some eccentric position with respect to the oscillating ring centre, the location of wave-vortex interaction was determined precisely. The waves are guided by the intensification in stratification near the vortex lens, break due the local increase in velocity in the PV barrier of the vortex, and make the PV barrier locally unstable. As a result, mixing occurs in the PV-barrier. High resolution velocity measurements of the horizontal flow field are made by using PIV, and the transfer of passive tracers across the PV-barrier is measured quantitatively by using laser induced fluorescein methods.

Formation of a polar vortex by oscillatory forcing in a rotating fluid

by **Johan van de Konijnenberg, Volker Naulin, Bjarne Stenum and Jens Juul Rasmussen**

Risoe National Laboratory, Optics and Fluid Dynamics Laboratory Building 128
PO Box 49 4000 Roskilde Denmark

Introduction

It is well known from experiments (see e.g. Carnevale, Kloosterziel & Van Heijst 1990) and numerical simulations (e.g. Sutyrin, Hesthaven, Lynov & Rasmussen 1994) that vortices on a β -plane have a tendency to move to regions where they become weaker; i.e. cyclones move to the North, anticyclones to the South. Departing from a distribution of cyclones and anticyclones, one would therefore expect the development of a surplus of cyclonic vortices in the North, and anticyclones in the South. On the other hand, any replacement of fluid between different latitudes leads to the opposite conclusion: the formation of cyclones in the south, and anticyclones in the North. Although a closer look at these arguments makes it clear that no paradox really exists, the subject has triggered discussion, experiments and numerical simulations.

A closely related issue is the coupling between nonlinear Rossby waves and a polar circulation. This interaction was studied experimentally by Colin de Verdière (1979). His set-up consisted of a rotating tank with a flat bottom and a free surface; the parabolic curvature of the surface leads to a γ -plane. The flow was forced by an array of 144 holes at the perimeter of the tank, fed by a distribution system so the position of the active sources and sinks could be made to run along the perimeter. The experiments showed that if the sources and sinks were adjusted to a wave propagating in the westward direction (the direction of the phase velocity of Rossby waves), an anticyclonic vortex was formed in the centre of the tank.

Experimental set-up

In our group we built a set-up that reminds of the one used by Colin de Verdière. We use a tank with demineralized water, covered with a flat rigid lid (the tank is filled completely to the lid, so there is no free surface), and equipped with a conical false bottom in order to obtain a topographic β -plane. The flow is forced by an oscillating source/sink-pair, achieved by connecting two holes in the bottom of the tank with a pipe in which a piston is moved back and forth by a small motor. Moreover, we have the possibility of adding an oscillation to the background angular velocity. A disturbance from solid-body rotation can then be obtained by adding a local topography. The flow is visualized with small tracer particles with a density close to that of the water. For this purpose, the set-up is illuminated with a horizontal light sheet, which can be adapted in height. The flow is surveyed by a video camera in the rotating system. We use the DigImage system to view and extract particle traces from the video signal.

Numerical simulations

The experiments are compared with a numerical solution of the two-dimensional vorticity equation, including terms representing the source/sink pair, the β -effect and Ekman suction. For this purpose we use a finite-difference method in the vorticity-streamfunction formulation. In this method the flow is assumed to be strictly incompressible, so although the dynamical consequences of vortex stretching and squeezing (induced by the topography, source/sink terms and Ekman suction) are taken into account, the contraction or dilatation itself is neglected. The numerical scheme utilizes a third-order stiffly stable time-stepping algorithm as described by Karniadakis et al. (1991). The circular domain is discretized in polar co-ordinates. The use of a staggered grid in the radial direction avoids the need for a special treatment of the co-ordinate singularity in the centre. Gridpoints are spaced non-equidistantly in the radial direction, the highest concentration being near the wall, where the no-slip boundary conditions leads to steep vorticity gradients. The no-slip boundary condition was implemented by adjusting the vorticity at the sidewall, so that the normal derivative of the stream function vanishes. The advective term is calculated using the discretized form given

by Arakawa (1966). This discretization retains the most important symmetries of the advection term, that is, conservation of energy and enstrophy.

Results

Up to now we have only obtained preliminary results. The particle trajectories indicate that oscillatory pumping leads indeed to the formation of an anticyclonic central vortex, but the effect appears to be independent of the presence of a beta-plane; the effect is also observed if the topography is removed. An oscillating background rotation also leads to a net anticyclonic motion. However, this effect, too, remains present in the absence of the topography. It is probably caused by an asymmetry between spin-up and spin-down. In short, we find anticyclonic vortices in most experiments, but they are not caused by the mechanism we were really looking for. In the numerical simulations, coupling between oscillatory pumping and the appearance of a circumpolar vortex on the given topographic plane is more easily established. However, so far we have run without Ekman damping, and one has to anticipate the possibility that for the parameters corresponding to the laboratory experiment, disturbances formed at opposite sides of the tank will be subject to a certain decay before they meet. At the meeting we will present further and more conclusive results.

Literature

A. Arakawa, Computational design for long term numerical integration of the equations of fluid motion: Two-dimensional incompressible flow. Part 1, *J. Comp. Phys.* 1, 119, (1966).

G.F. Carnevale, R.C. Kloosterziel & G.J.F. van Heijst, Propagation of barotropic vortices over topography in a rotating tank, *J. Fluid Mech.* 233, 119 (1991).

A. Colin de Verdière, Mean flow generation by topographic Rossby waves, *J. Fluid Mech.* 94, 39 (1979).

G.E. Karniadakis, M. Israeli & S.A. Orszag, High-order splitting methods for the incompressible Navier-Stokes equations, *J. Comp. Phys.* 97, 414 (1991).

G.G. Sutyrin, J.S. Hesthaven, J.P. Lynov & J. Juul Rasmussen, Dynamical properties of vortical structures on the beta-plane, *J. Fluid Mech.* 268, 103 (1994).

Vortex structures in stratified rotating fluids

By

Adam Fincham

Laboratoire des Ecoulements Géophysiques et Industriels (LEGI)
Equip Coriolis
Université Joseph Fourier-CNRS-INPG
Grenoble France

A stable linear density gradient supports a horizontal baroclinic torque that promotes "layering" and a tendency for horizontal alignment of the vorticity vector. The internal Froude number $Fr=U/ND$ gives a measure of the relative importance of the buoyancy forces, for $Fr<1$ there is very little vertical motion and the flow is quasi 2D in nature. Uniform background rotation promotes a vertical alignment of the vorticity vector when the Rossby number $Ro=U/fD$ is small. Rotation tends to increase vertical coherence of structures while stratification confines structures to weakly correlated layers. Both of these effects lead to the development of long lived coherent vortex structures similar to those found in the ocean and atmosphere. By exploiting the inherent anisotropy associated with low Froude number flows a stack of horizontal slices is sufficient to fully reconstruct the 3D vorticity field. Large vortices created in the 13 meter diameter rotating platform Coriolis gain their Reynolds numbers from their size and have very long turn-over times. These long time scales permit the effectively instantaneous acquisition of relatively large numbers (50) of horizontal image slices. Full 3D vorticity fields are obtained in time using an accurate Correlation Imaging Velocimetry (CIV) technique. The vortex dynamics is captured and parameterized as a function of the Reynolds, Rossby and Froude numbers. The coherent nature of these flows (which typically consist of quasi-2D multipolar vortices with vertical structure) can be explained in terms of the three-dimensional compactness of the vorticity field where vortex filaments meander between adjacent poles forming closed loops. The relatively well known stratified vortex dipole is revealed to have a complex vortex topology arising from its self induced propagation which strips vertical vorticity from its upper and lower bounds leaving a wake consisting of 4 horizontal tubes of vertical vorticity and giving the enstrophy field a somewhat streamlined appearance. The enstrophy field in low Froude number flows is typically governed by the horizontal vorticity components and in the vortex cores where the vertical coherence is greatest the absolute enstrophy is weakest resulting in pockets of low viscous dissipation. At low Reynolds number the Karman vortex like wake of a single vertical flat plate in a linearly stratified fluid quickly develops a stably vertical zig-zag instability that is coupled in phase for many diameters downstream. Rotation can be seen to inhibit the development of the vertical wavelength, initially columnising the vortices but leading to their early decay as the zig-zag phase relation is broken. The dynamics and interactions of the vortices created under these relatively controlled conditions are related to the more general decaying stratified turbulent case, which consists of a densely packed sea of pancake like structures that grow by vortex pairing type interactions in the horizontal plane, but interact vertically through viscous mechanisms.

The rotating turbulent pipe as a tool to understand the manipulation of wall turbulent structures : flow physics and turbulence modeling

By P. Orlandi

Università di Roma "La Sapienza" Dipartimento di Meccanica
e Aeronautica, via Eudossiana n° 18, 00184 Roma, Italy.

The study of turbulent flows through a pipe rotating about its axis is of fundamental interest for all the practical applications it offers. Some are of engineering interest, such as the study of combustors, rotating machinery or applications connected to aeroacoustics. The effects of solid body rotation on turbulence in a pipe presents similarities with three-dimensional boundary layers of practical importance, such as on swept wings of airplanes.

When a fluid enters a pipe rotating about its axis, tangential shear forces acting between the pipe wall and the fluid cause the fluid to rotate with the pipe, resulting in a flow pattern rather different from that observed in a stationary pipe. Rotation was found to have a very marked influence on the suppression of the turbulent motion because of centrifugal forces. The experimental results indicate that the pipe rotation deforms the mean axial velocity profile towards a shape similar to that observed in laminar flow, i.e. a parabolic profile (the Poisseuille profile), with larger mean axial velocities near the centerline of the pipe and smaller mean velocities near the wall compared to pipe flow without wall rotation.

The rotating pipe, even if necessitates of some attention on the numerics, on the other hand, avoids assumptions on the spanwise dimension in a rotating channel. In fact in the case of a rotating channel along the axis the spanwise dimension should account not only of the increase of the spacing and size of the wall structures with the rotation rate, but also of the large scale longitudinal structures at the center of the channel. The pipe has the further advantage to allows comparisons with experiments in a laboratory.

Orlandi & Fatica (1997) recently performed simulations for a rotating pipe for values of the rotation number N up to 2, and showed that the changes in turbulence statistics in the rotating case are due to the tilting of the near-wall streamwise vortical structures in the direction of rotation. The present study is an extension of the previous one by increasing N in the range between 2 and 10 and to perform visualization of the vorticity field. The other main objective of the present work lies in the evaluation of the Reynolds stress budgets. The aim of the work is to create a data-base that can help the developer of one-point turbulence closure to find new models that take into account the modification of wall structures.

The rotating pipe can be considered as the basic flows to give ideas to those who are developing engineering turbulence models for flows where a control acts to modify the vortical structures in order to achieve the established goal.

REFERENCES

ORLANDI, P. & FATICA, M. 1997 Direct simulation of turbulent flow in a pipe rotating about its axis. *J. of Fluid Mech.* 343, 43-72

"Control and Dynamics of a Vortex Confined in a Lid-driven Cylinder"

by

Jens N. Sorensen and Bo H. Jorgensen
Department of Energy Engineering, Bldg. 404
Technical University of Denmark

ABSTRACT:

The cylindrical lid-driven cavity is a cylindrical vessel in which an enclosed fluid is brought into motion by rotating one of the end walls. The problem is uniquely defined by specifying the Reynolds number, Re , and the height to radius ratio, H/R .

This problem has now for many years been studied extensively, both experimentally and numerically, and in spite of the simple geometry, several interesting phenomena have been revealed. Experiments as well as computations have shown that the rotation forms a concentrated vortex

on the axis of the vessel which, as function of Re and H/R , may exhibit up to three distinct breakdown bubbles. In some of the early studies it was found that well into the unsteady domain the flow maintains axi-symmetric behaviour.

Axi-symmetric computations have revealed that various phenomena known from non-linear dynamical systems, such as hysteresis, period-doubling and onset of chaotic behaviour, may appear as function of Reynolds number and aspect ratio.

Recent experiments indicate that non-axisymmetric behaviour appears at a Reynolds number in the range from 3000 to 3500 or even in the steady domain.

In the present study we focus on two specific problems.

First, how can we explain the transition to three-dimensional flow and at what conditions does it appear?

Next, is it possible to control the dynamical behaviour of the breakdown bubbles, either it be enhanced or damped out?

The latter question we clarify by imposing a thin rotating rod along the center axis. Numerical "experiments" show that even small rotational velocities of the rod results in dramatic changes of the flow structures

The controlling mechanism, which we attribute to the generation of secondary vorticity, will be explained in the presentation.

Abstract submitted to EUROMECH 396: Vortical Structures in Rotating and Stratified Fluids,
Cortona 22-25 June 1999

Vortical Structures in Rotating Plane Couette Flow

N. TILLMARK & P.H. ALFREDSSON

Department of Mechanics, KTH, S-100 44 Stockholm, Sweden

1 Introduction

System rotation substantially influences the flow behavior both in laminar and turbulent shear flows due to the effect of the Coriolis force, which may give rise to streamwise oriented vortices. In the case of rotating plane Couette flow (see figure 1) linear stability analysis show that the critical Reynolds number is as low as 20 (the Reynolds number is defined as $Re = hU_w/\nu$ and the Rotation number as $Ro = 2\Omega h/U_w$). Numerical simulations have been carried out by different groups (Bech & Andersson, 1997, Komminaho, Lundbladh, & Johansson, 1996) which show that streamwise oriented vortices form in the flow also for high Reynolds numbers. In plane Couette flow, as compared to for instance plane channel flow, the sign of the mean vorticity is the same across the whole width of the channel. In this case the effect of rotation is either stabilizing or destabilizing across the the full width of the channel. This leads to the possibility to obtain relaminarization for a flow which is initially turbulent, but for which rotation is applied (Komminaho et al., 1996, Tillmark & Alfredsson, 1996).

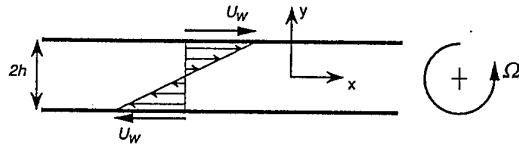


Figure 1: Laminar rotating plane Couette flow

2 Experimental set-up

The present study make use of the plane Couette flow apparatus previously used by Tillmark & Alfredsson (1992) to study transition in plane Couette flow. In the study the channel is mounted on a rotating table. The apparatus uses a endless belt of a transparent material which, in the test channel, slides against two glass walls. In this way optical access through the moving wall is possible, both for flow visualization and LDV measurements. With this arrangement both walls are moving, but in opposite directions, and the mean flow in the channel is hence zero.

Flow visualization is made through the use of reflective platelets mixed with the fluid and the flow pattern is recorded with a digital video camera mounted on the rotating table. The LDV measurements are made by mounting the full LDV equipment (DANTEC FlowLite) on the rotating table. The length of the test channel is 1500 mm, the height 300 mm and the width is 20 mm in the present study. For further information of the design of the channel the reader is referred to Tillmark & Alfredsson (1992).

3 Results

The present work deals with the case where the applied rotation is destabilizing, both for low (laminar) and high (turbulent) Reynolds numbers. For both cases flow visualization clearly shows how streamwise oriented vortices are established in the flow, with a spanwise size of the order of the channel width. In the laminar case the flow visualization (see fig. 2(a), where $Re=200$ and $Ro=0.01$) shows light and dark bands (the size of the picture is approximately 500×300 mm 2). These bands are not stationary but drift slowly in the spanwise direction, sometimes also merging with each other. LDV-measurements show (see

figure 3(a)) how the streamwise velocity at $y/h = -0.5$ actually changes sign with a periodic pattern (note that the mean streamwise velocity should be negative at this position). The peak-to-peak amplitude is roughly 10 mm/s which can be compared with the wall velocity of 14 mm/s. Similar measurements of the spanwise velocity component (not shown) show variations of this component of the order of ± 3 mm/s. This pattern is due to the slow drift of the vortices across the measurement volume. It is hence clear that the vortices drastically change the velocity distribution in the channel.

Also for Reynolds numbers for which the flow is fully turbulent the streamwise vortices are present and still dominate the flow field. From the flow visualizations (figure 2(b)) it seems that the turbulence is 'contained within each streamwise vortex and the width of the dark bands is much smaller than in the laminar case. A time signal obtained by LDV is shown in figure 3(b). Here the flow shows regions where the velocity fluctuates around zero (which one expects for a fully turbulent flow) and short duration periods of negative velocities. An interpretation of this is that the negative regions are the periods when the border of two vortices pass the measurement volume and the flow is directed from the moving wall (hence giving rise to high (negative) velocity fluid moving towards the center of the channel).

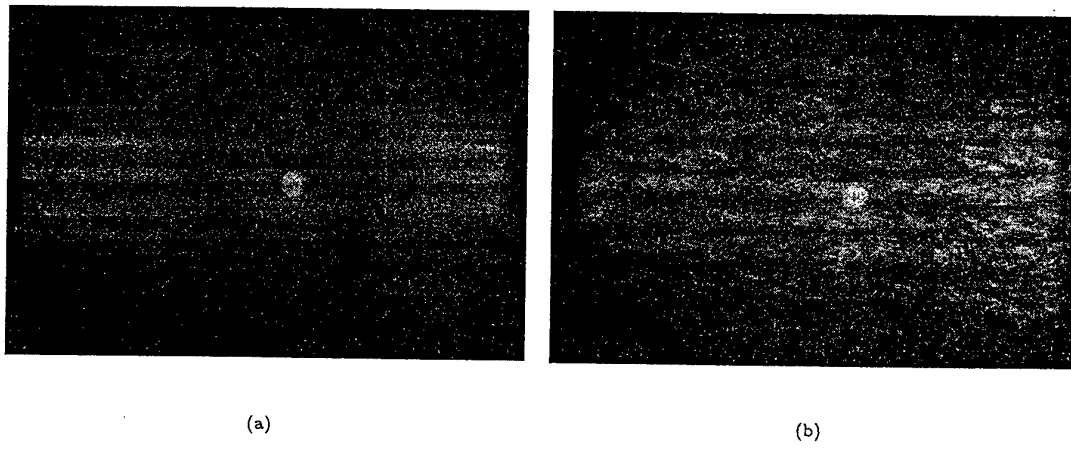


Figure 2: a) Laminar flow at $Re = 200, Ro = +0.01$ b) Turbulent flow at $Re = 700, Ro = +0.10$

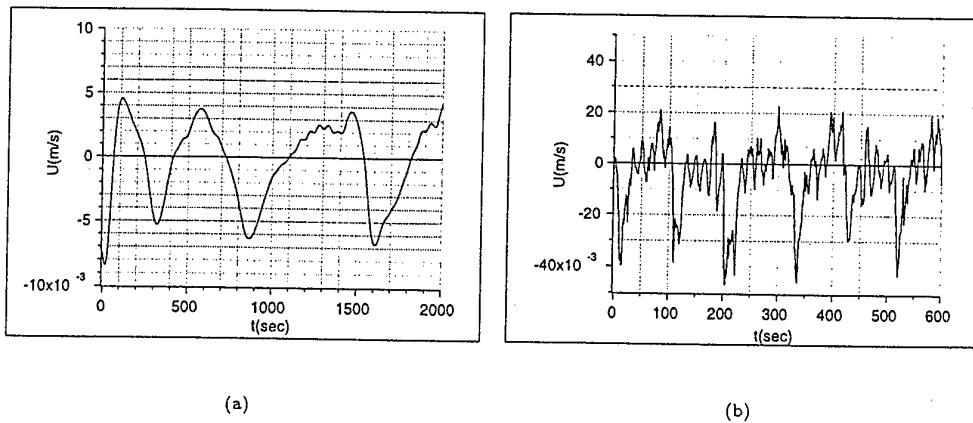


Figure 3: a) Streamwise velocity $U(t)$ at $y = -1/2h, U_w = 0.014$ m/s $Re = 140, Ro = 0.16$ b) Streamwise velocity $U(t)$ at $y = -1/2h, U_w = 0.073$ m/s $Re = 730, Ro = 0.10$

4 Discussion

The flow visualization results of the rotating plane Couette flow show that streamwise vortices is a prominent feature of the flow, both in the laminar and turbulent flow regimes. In order to get a clearer interpretation of the flow visualizations simultaneous video recordings and LDV-measurements (both of the u and w components) were made in the laminar case. In figure 4 a tentative sketch of the velocity flow field and the corresponding flow visualizations are shown. The light regions are seen to correspond to regions of high absolute values of the spanwise velocity component, whereas the dark regions seems to be regions where the flow is oriented either towards or away from the wall, i.e. regions in between vortex pairs. In the presentation we will further discuss the dynamics of the vortical structures both in the laminar and turbulent cases.

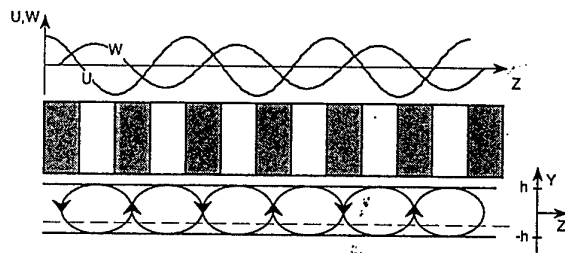


Figure 4: A tentative sketch. Top: velocity distribution at $y = -0.5h$, center: dark and light bands, bottom: vortex distribution

References

Bech, K.H. & Andersson, H.I. 1997 Turbulent plane Couette flow subjected to strong system rotation. *J. Fluid Mech.* **347**, 289-314.
 Komminaho, J., Lundbladh, A. & Johansson, A. 1996 Very large structures in plane turbulent Couette flow. *J. Fluid Mech.* **320**, pp. 259-285.
 Tillmark, N. & Alfredsson, P.H. 1992 Experiments on transition in plane Couette flow. *J. Fluid Mech.* **235**, 89-102.
 Tillmark, N. & Alfredsson, P.H. 1996 Experiments on rotating plane Couette flow. In *Advances in Turbulence VI* (ed. Gavrilakis, S., Machiels, L. and Monkewitz, P.A.), 391-394. Kluwer.

On Isolated Solutions for Flows in the Ekman-Couette Layer

N.P. Hoffmann and F.H. Busse

Institute of Physics, University of Bayreuth, D-95440 Bayreuth

Isolated solutions have been found describing solitary vortex motions in a fluid layer between two parallel plates moving relative to each other in a system that rotates about an axis normal to the plates. The solutions are called isolated since they do not seem to be connected by bifurcations to any other known solutions of the problem. The solitary vortex solutions are unstable with respect to three-dimensional disturbances, but attempts to find three-dimensional steady states have not yet been successful.

The Ekman-Couette Layer is obtained when two rigid parallel plates move relative to each other with the constant velocity \mathbf{U} in a system rotating with the angular velocity vector $\boldsymbol{\Omega}$ normal to the plates. This configuration is realized experimentally in a local sense when two parallel disks are rotating with different angular velocities about their common axis. Even if the angular velocity of one of the disks vanishes the theory of the Ekman-Couette layer still appears to be applicable as the comparison of computational results with the experimental measurements suggests [1,2].

There are three different types of instability. For low values of the dimensionless rotation parameter the instability in the form of Ekman-Couette rolls occurs first. These rolls are point symmetric with respect to their axis on the midplane of the layer and are stationary with respect to the reference system of vanishing averaged mass flux. The other two instabilities are the Ekman layer instabilities of types I and II which occur in the Ekman boundary layers attached to the rigid plates and are asymmetric with respect to the midplane of the layer. There are thus two modes in the form of waves traveling along the respective boundaries for each of the instabilities of type I and type II. The secondary states of motion that evolve from these instabilities have been studied in a recent paper [2] where also bifurcations to tertiary states of fluid flow have been analyzed.

Serendipitously still another state of fluid flow has been discovered in the course of this work which will be described in the following. This new solution of the basic equations of motion does not seem to bifurcate from any other known solution. It exists at low Reynolds numbers where the basic state is still stable with respect to infinitesimal disturbances. This new solution is isolated also in other respects in that it describes a solitary type vortex. The unusual properties of

these new solutions alone justify the detailed study undertaken. On the other hand it is still unclear whether there is already experimental evidence for localized vortices in flows related to the one considered in the present work. Several experimenters have observed so called spots/rollers [3] and what was called solitary waves [1] in rotating disk experiments. While a conclusive theoretical explanation for these observed phenomena has not yet been given the solitary vortex solutions detected in the present work seem to be a promising starting point for further investigation.

Other promising aspects in the context of the present investigation can be found in making use of the analogy between shear flows in rotating coordinate systems and stratified flows. This analogy which has been known for a long time [4] states that as long as the solution of a shear flow problem in a rotating coordinate system stays homogeneous with respect to translation in one direction of space there exists an analogous flow situation in a stratified fluid of Prandtl number equal to unity. Applying the analogy to the present problem shows that solitary vortex solutions also exist in vertical fluid layers that are vertically stratified and have differentially heated and sheared walls. Although experiments [5] and direct numerical simulations [6] hint at the existence of localized solutions in vertical slot convection problems, to our knowledge no basic understanding of these phenomena seems to have been developed by now. Also for these types of flow the solitary vortex type solutions investigated in the present work might be a promising starting point.

- [1] Schouweiler, L., LeGal, P., Chauve, M.P., Takeda, Y., Experimental study of the stability of the flow between a rotating and a stationary disk. In Advances in Turbulence VI (ed. S. Gavrilakis, L. Machiels & P.A. Monkewitz), 385-388, Kluwer, 1996.
- [2] Hoffmann, N., Busse, F.H., Chen, W.-L., Transitions to complex flows in the Ekman-Couette layer. J. Fluid Mech. **366**, 311-331, 1998.
- [3] Sankow, P.L., Smirnov, E.M., Bifurcation and transition to turbulence in the gap between rotating and stationary parallel disks, Fluid Dyn. **19**, 695, 1985.
- [4] Veronis, G., The analogy Between Rotating And Stratified Fluids. Ann. Rev. Fluid Mech. **2**, 37, 1970.
- [5] Elder, J.W., Laminar free convection in a vertical slot. J. Fluid Mech. **23**, 77, 1965.
- [6] Wakitani, S., Formation of cells in natural convection in a vertical slot at large Prandtl number. J. Fluid Mech. **314**, 299, 1996.

Structure and stability of multipolar vortices

Stéphane Le Dizès

Institut de Recherche sur les Phénomènes Hors Equilibre,
12, avenue Général Leclerc, F-13003 Marseille, France.

The emergence of multipolar vortices in rotating fluids is a well-known feature which was evidenced both experimentally and numerically (see for instance Hopfinger & van Heijst, 1993 and references therein) These vortical structures are usually formed of a central vortex surrounded by several vortices of opposite sign. They are known to appear spontaneously by a 2D inviscid instability from monopolar vortices which have not a monotonous vorticity profile. But they were also obtained in numerical simulations by nonlinearly perturbing stable vortices (Rossi *et al.*, 1997).

In the first part of my talk, an analytical description of multipolar vortices is provided. These structures are described as a sum of an axisymmetric stationary vortex of angular velocity $\Omega_0(r)$ and a 2D neutral non-axisymmetric perturbation rotating around the vortex axis with an angular frequency ω . The azimuthal wavenumber m of the perturbation defines the fold symmetry of the multipolar vortex. The perturbation is found to have the following structure: it is linear everywhere except in the neighborhood of the critical radial coordinate r_c where the perturbation corotates with the vortex, i.e. where $\Omega_0(r_c) = \omega/m$. At r_c , the linear approximation exhibits a singularity (if the vorticity gradient is non-zero) which is resolved in a **nonlinear critical layer** (Benney & Bergeron, 1969). In this region, the streamlines in the corotating frame have a well-known cat's eye shape which is associated with satellite vortices. An illustration is displayed on figure 1 which shows the "tripole" solution obtained from a Lamb vortex. Multipolar vortices are shown to exist for both stable and unstable continuous vorticity profiles. Characteristics properties such as the angular frequency and the amplitude threshold for the perturbation are given for various vortices. The effects of steep-edge gradients is also analysed by considering a family of vorticity profiles ranging from Gaussian to top-hat.

In the second part of my talk, the 3D stability of multipolar vortices is discussed. I explore the possibility for the central vortex to be destabilised by a resonance mechanism similar to the one involved in the elliptic instability (Bayly, 1986). A simple criterion for instability is given as well as an estimate

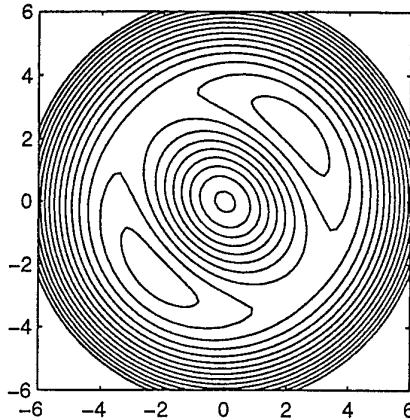


Figure 1: Streamlines in the corotating frame of the tripole solution ($m = 2$) obtained from a Lamb vortex (Gaussian vorticity profile). The amplitude of the perturbation, defined as the ratio of the strain rate by the vorticity in the vortex center is here $\varepsilon = 0.035$. The critical radius is at $r_c \approx 3.4$.

for the maximum growth rate (Le Dizès & Eloy, 1999).

References

- [1] E. J. Hopfinger and G. J. F. van Heijst, *Annu. Rev. Fluid Mech.* **25**, 241 (1993).
- [2] L. F. Rossi, J. F. Lingevitch, and A. J. Bernoff, *Phys. Fluids* **9**, 2329 (1997).
- [3] D. J. Benney and R. F. Bergeron, *Stud. Appl. Math.* **48**, 181 (1969).
- [4] B. J. Bayly, *Phys. Rev. Lett.* **57**, 2160 (1986).
- [5] S. Le Dizès and C. Eloy, *Phys. Fluids* **11**, 500 (1999).

Vortex structures in breaking mountain waves

Olivier EIFF

Centre National de Recherches Météorologiques

42, av. G. Coriolis, 31057 Toulouse Cedex France

Email: eiff@cnrm.meteo.fr, tel.: (33) 5.61.07.93.87, fax.: (33) 5.61.07.95.66

Recent three-dimensional numerical simulations of internal wave breaking have shown that the instabilities leading to wave breakdown are essentially three dimensional [e.g., Winters & Riley (1992) and Andreassen et al. (1998) in the case of wave breaking in critical layers and Afanasyev and Peltier (1998) in the case of flow over two-dimensional topography]. In these simulations it was found that convective instability leads to formation of streamwise vortices.

Using laboratory experiments at low Reynolds numbers ($Re \sim 10^2, 10^3$), Eiff and Bonneton (1998) and Eiff and Bonneton (1999) examined the transient evolution leading to wave breakdown as well as the emerging large-scale coherent vortices. The results revealed that the first breakdown of the overturning wave results in a quasi two-dimensional transverse vortex over the central portion of the uniform section of the obstacles. Measurements of the velocity and density profiles suggest that this vortex formation is essentially due to a shear-driven instability, in analogy with the numerical simulations of Winters and Riley (1992).

Figure 1 shows the particle trajectories (pathlines) obtained in the vertical center plane of the flow at high Reynolds number ($Re = 8000$). As in the lower Reynolds number cases, the wave has overturned into an *S*-shape and the top portion of the *S*-shaped wave has rolled up into a clockwise rotating transverse vortex. This roll-up occurs lower and further downstream from the obstacle crest than in the lower Reynolds number experiments.

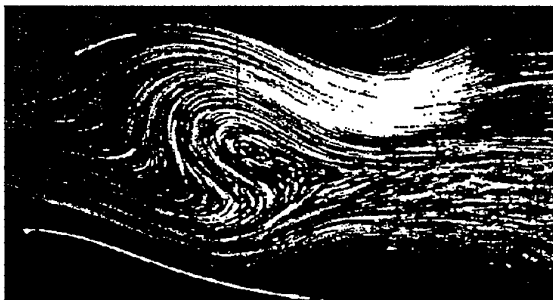


Figure 1: Pathlines in the vertical center plane over a quasi two-dimensional obstacle in the large tank. $Re = 8000$, $Nt = 21$. The obstacle measures 1.14m (length) by 2.5m (width) by 0.13m (height). The flow is from left to right.

The pathlines in the vertical symmetry plane reveal that the transverse vortex moves upstream along the inclined wave before undergoing further transition. However, this transition was optically obscured due to random variations of the index of refraction induced by mixing of the salt-stratified fluid between the plane of investigation and the glass side-wall. Recent particle image velocimetry measurements as well as numerical simulations [Reneson (1998)] show that three-dimensional vortices first appear near the edges of the uniform section of the quasi two-dimensional obstacles, which can account for the observed mixing at high Reynolds numbers.

The low Reynolds number experiments have shown that the transverse vortex does not remain stable. After a few buoyancy periods, significant three-dimensional perturbations are evident and the vortex breaks down into toroidal vortices as shown by Eiff & Bonneton (1998). Sectional streamlines through one of these vortices would result in a counter-rotating vortex

pair and sectional streamlines between adjacent vortices in an upward and streamwise flow without critical points. In the lower Reynolds number experiments, simultaneous examination of vertical and horizontal planes confirmed the topologies for the two positions of the vertical planes relative to the tori. The pathlines shown in figures 2(a) and (b) confirm the low Reynolds number topologies at high Reynolds numbers in the vertical center plane, i.e., a counter-rotating vortex pair in figure 2(a) and an upward/streamwise flow without critical points in figure 2(b). As in the lower Reynolds number experiments, the observation of two different topologies in a fixed vertical plane implies that the structures have advected laterally.

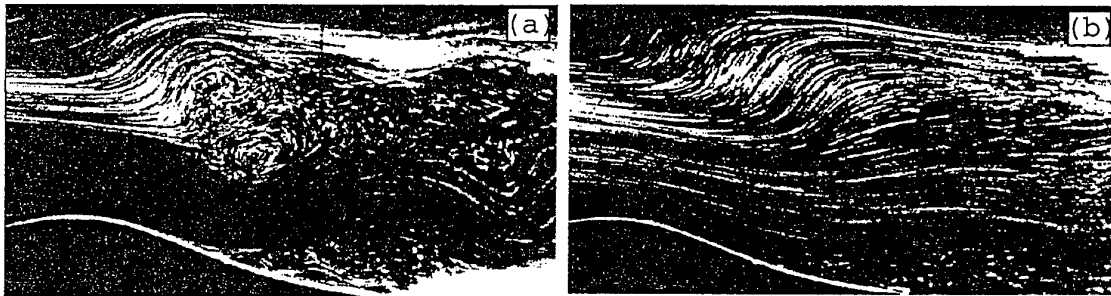


Figure 2: Pathlines in the vertical center plane over a quasi two-dimensional obstacle in the large tank. $Re = 8000$. (a) Counter-rotating vortex pair observed at $Nt = 118$; (b) Upward flow with no critical points observed at $Nt = 145$.

New particle imaging velocimetry results show that even at low Reynolds numbers the observed toroidal structures are not stable. The structures are seen to be occasionally convected downstream, even though the trapped lee-wave is generally seen to confine the vortex motion to be quasi-stationary [Gheusi et al (1999)]. In the higher Reynolds number situation, smaller scale turbulence appears to be advected downstream [e.g., figure 2(a)].

REFERENCES

- Y.D. Afanasyev & W.R. Peltier 1998 The three-dimensionalization of stratified flow over two-dimensional topography. *J. Atmos. Sci.* **55**(1), 19-39.
- O. Andreassen, P.O. Hvidsten, D.C. Fritts & S. Arendt (1998) Vorticity dynamics in a breaking internal gravity wave. Part 1. Initial instability evolution. *J. Fluid Mech.* **367**, 27-46.
- O.S. Eiff & P. Bonneton (1998) Structural features of breaking waves in stratified flow over mountains. Submitted to *Developments in Geophysical Turbulence*, Boulder, Colorado.
- O.S. Eiff & P. Bonneton (1999) Lee-wave breaking over obstacles in stratified flow. Submitted to *Phys. Fluids*.
- F. Gheusi, J. Stein & O.S. Eiff (1999) A three-dimensional numerical study of gravity wave breaking over two-dimensional topography. Under revision *J. Fluid Mech.*.
- M. Rennesson (1998) Simulations numériques d'ondes de gravité déferlantes observées en grande veine hydraulique sur un obstacle tridimensionnel. Rapport de Stage, CNRM, Météo-France.
- K.B. Winters & J.J. Riley (1992) Instability of internal waves near a critical level. *Dyn. Atmos. Oceans* **16**, 249-278.

Meddies Collide with Seamounts

P. L. Richardson, A. S. Bower,
Department of Physical Oceanography
Woods Hole Oceanographic Institution
Woods Hole, Massachusetts USA

and W. Zenk
Institut fur Meereskunde
an der Universitat Kiel
Kiel, Germany

Recent subsurface float measurements in 27 Mediterranean Water Eddies (Meddies) in the Atlantic are grouped together to reveal new information

about the pathways of these energetic eddies and how they are often modified and possibly destroyed by collisions with seamounts. Twenty Meddies were tracked in the Iberian Basin west of Portugal, seven in the

Canary Basin. During February 1994 14 Meddies were simultaneously observed, 11 of them in the Iberian Basin. Most (69%) of the newly formed Meddies in the Iberian Basin translated southwestward into the vicinity of the Horseshoe Seamounts and probably collided with them. Some Meddies (31%) passed around the northern side of the seamounts and translated southwestward at a typical velocity of 2.0 cm/sec into the Canary Basin. Some Meddies observed there were estimated to be up to ~5 years old. Four Meddies in the Canary Basin collided with the Great Meteor Seamounts and three Meddies were inferred

to have been destroyed by the collision. Overall an estimated 90% of Meddies collided with major seamounts. The mean time from Meddy formation to a collision with a major seamount was estimated to be around

1.7 years. Combined with the estimated Meddy formation rate of 17 Meddies per year from previous work, this suggests that around 29 Meddies co-exist in the North Atlantic. Therefore during February 1994 we observed about half of the population of Meddies.

INTERACTION OF DYPOL VORTICES IN THE MODEL ROTATING FLOW WITH A RIGID BOUNDARY AND FUTHER DYNAMICS

Zhvania B.I.,¹ Zhvania R.A.,¹ Lominadze J.G.,¹ Nanobashvili J.I.,¹ Tsakadze Z.J.,¹
Chagelishvili G.D.^{1,2 a)} and Yan'kov V.V.³

¹ *Abastumani Astrophysical Observatory, Tbilisi, Georgia;*

² *Space Research Institute, Moscow, Russia;*

³ *Kurchatov Institute Russian Research Centre, Moscow, Russia*

a) e-mail: georgech@mx.iki.rssi.ru

The aim of this report is to present results of study of the interaction of dipole vortices (generated in the rotating system) with rigid boundary/wall and the evolution of structures arising near the boundary. Dipoles are produced in the rotating experimental device shown schematically in Fig.1. It is used a cylindrical vessel 86 cm in diameter; the bowl bottom is parabolic, and its curvature radius at the vertex is 92 cm. The containing a shallow water rotated at a constant rate with period of 1.93 s. Corresponded to this period fluid depth is constant. This time is large enough to photograph events as well as observe them visually (or by videocamera). We can vary the constant depth over a fairly wide range of 1-5 cm; in particular, this makes it possible to change the Rossby radius by a factor of more than two. In addition, we can vary the vessel rotational speed over a wide range and thereby govern the β -effect and the fluid-depth gradient (its magnitude and direction).

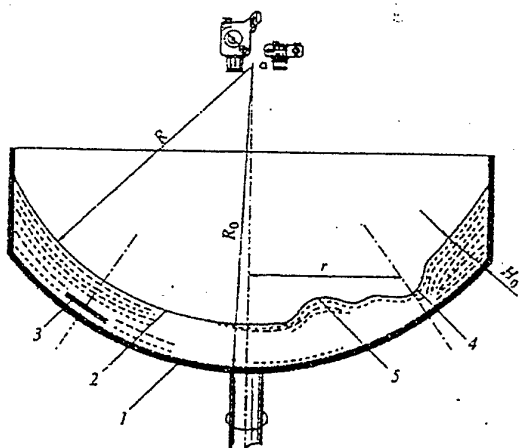


Fig.1 Schematic of the experimental device: (1) vessel with a parabolic bottom; (2) fluid surface; (3) disk, generating the vortex; (4) cyclone; and (5) anticyclone.

Through rotation, two-dimensional vortices are realized in the system. The main attention is given:

- to the role of the near-wall friction in the vorticity generation at the collision of dipoles with the wall;
- to the subsequent dynamics of the occurring vortex system.

The generation of satellite vortices (for each vortex of the dipole vortex system) is a natural result of the collision. The generated vortex satellite changes the distance between the "mother" vortex and the wall and intensifies interaction among the vortex structures. Since a decrease in the viscosity paradoxically results in the generation of more powerful vortices, the viscosity can never be neglected.

One example of the interaction is presented on Figs.2. It is presented a situation where the cyclone collides with the wall somewhat earlier than the anticyclone. The time interval between sequential figures is 2 s (i.e. approximately the rotation period of the system). In Fig. 2a, the

cyclone is in the late collision stage (the satellite, generated by this cyclone is beyond the frame and can be seen only in Fig. 2b), and the anticyclone is in the initial stage of collision. In the left lower part of the anticyclone, a vortex layer is seen to arise (the compact vortex satellite is no longer rolled). In Fig 2b, the initial vortices are already seen to become separated, and the weak satellite of the cyclone has grown and made half revolution around the mother cyclone; in the lower left part of the anticyclone, the compact cyclone-satellite has already been formed from the generated vortex layer. In Fig. 2c, the satellite of the anticyclone is somewhat enhanced and is driven by the current of the cyclone so that it has turned further around the mother vortex, while the satellite of the cyclone has weakened approaching the wall. The anticyclone satellite turns further (Fig. 2d); in its structure, one can see flow lines that are common to the neighboring (principal) cyclone; nevertheless, the satellite is "held" by the mother anticyclone. Further turning, the anticyclone satellite collides with the wall (Fig. 2e), separates from the mother vortex, is held by the cyclone (Fig. 2f) and comes to an end (Fig. 2g).

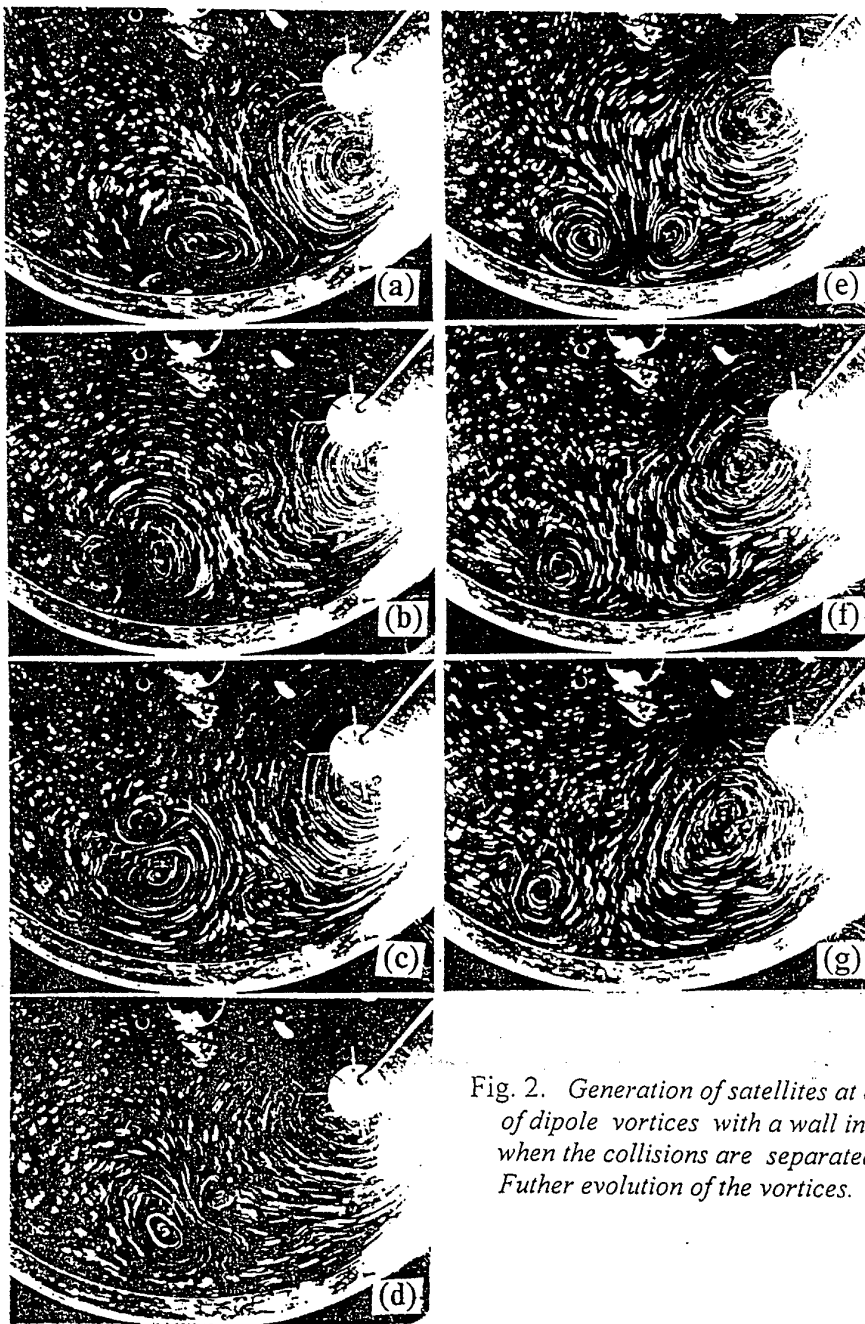


Fig. 2. *Generation of satellites at collisions of dipole vortices with a wall in the case when the collisions are separated in time; Futher evolution of the vortices.*

MEDDY COLLISION WITH TOPOGRAPHY

Claudia Cenedese

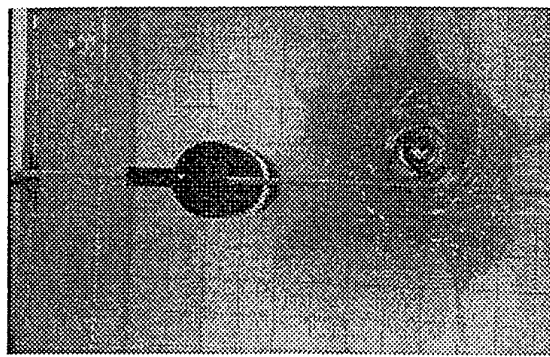
Woods Hole Oceanographic Institution

360 Woods Hole Rd., Woods Hole 02543 MA

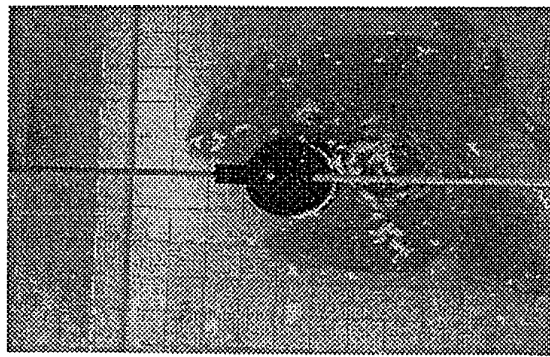
Intense subsurface eddies of warm, salty Mediterranean water (Meddies) are generated near the Strait of Gibraltar and translate westward into the Atlantic. Because their core fluid is protected from external mixing within a swirling vortex, Meddies can survive for several years while transporting anomalous watermass properties over thousand of kilometres. Meddies are thought to play an important role in the maintenance of large scale temperature and salinity distributions in the mid depth North Atlantic, especially the Mediterranean salt tongue, but how important is not clear. For example Arahñ *et al.* (1994) suggested that Meddies may be responsible for more than 50% of the westward salt flux at the level of the Med water. A recent study (Richardson *et al.*, submitted) gave good information on the number of eddies that forms per year, their sizes and their life histories giving insights on the role of Meddies in the salinity distribution in the mid depth North Atlantic. One of the most interesting results from this study, analysing a total of 27 Meddies, was that most Meddies (~90%) collided with major seamounts after a mean life of 1.7 years and that the collision resulted in a major disruption of the Meddies. The large number of Meddy collision with seamounts and the observed dispersal of float during and after collisions suggest that much of the warm salty Mediterranean outflow water advected by these Meddies is dispersed into the surrounding region. A decrease in temperature measured by floats looping in Meddies and especially the cold spikes observed during collision is interpreted to be the entrainment of colder background water into cores of Meddies where it is rapidly mixed with warmer Meddy water. The effect of Meddies on the salt tongue could be very different depending on whether Meddies remain clear of seamounts and slowly decay over long periods of time ~5 years as they slowly translate through the ocean, or crash into seamounts and are rapidly destroyed over periods of a few weeks to a few months. In the first case Meddies presumably leave a dilute trail of salty water in their wake. In the second case a much stronger concentration of warm salty water would be injected locally in the vicinity of seamounts.

In order to examine the physical processes that govern what happens when Meddies collides with sea floor topography, a series of idealised laboratory experiments have been performed. Previous studies by Lucas and Rockwell (1988), Orlandi (1993) and Verzicco *et al.* (1995) investigated vortex dipoles interacting with a circular cylinder. Experiments were carried out to extend these earlier studies and to focus in particular on monopole vortex interaction with an obstacle in order to simulate the Meddies' drift and collision with large topographic features. The dependence of the collision behaviour on different features such as horizontal (vertical) dimension of the obstacle compared with the vortex horizontal (vertical) scale, stratification, symmetry of the initial encounter of the incident vortex with the obstacle and shape of the obstacle, will be presented.

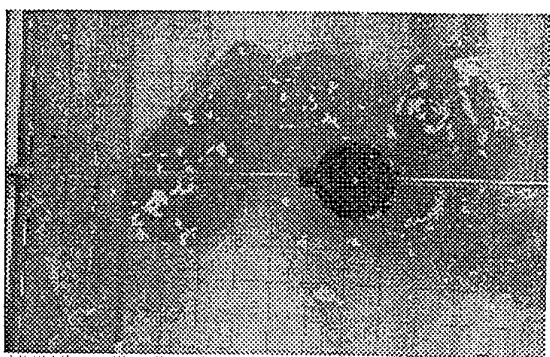
The experimental apparatus consisted in a rotating tank in which the vortex interaction with an obstacle was investigated both by moving the obstacle to the vortex and by allowing the vortex to self-propagate over a sloping bottom and impinge on the obstacle. In the first case a cylinder was slowly moved into a vortex where this approximates the situation of a Meddy swept by a mean flow into a seamount. As a result of the collision (figure 1) fluid was stripped from the outer edge of the vortex and injected into the region to the left of the obstacle. The core of the vortex continued to rotate rapidly and remain coherent throughout the collision. Experiments were conducted in a homogeneous background fluid investigating both barotropic and baroclinic vortices. Only barotropic cyclonic vortices were generated; special care is needed to investigate barotropic anticyclones since they tend to be centrifugally unstable (see Kloosterziel & van Heijst, 1991) and to become non-axisymmetric in few rotation periods.



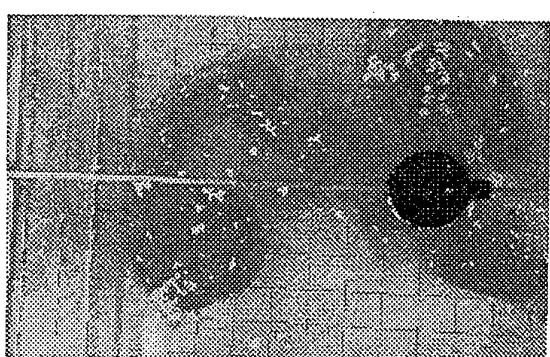
(a)



(b)



(c)



(d)

Figure 1. A sequence of plan view photographs showing a cylindrical obstacle having a radius of 4.5 cm, (darker circle) slowly colliding with a cyclonic barotropic vortex of radius approximately 13 cm (lighter grey fluid) embedded in a homogeneous background. As a result of the collision dyed fluid was stripped from the outer edge of the vortex and injected into the region to the left of the obstacle. The core of the vortex continued to rotate rapidly and remain coherent throughout the collision. Note that the dyed fluid near the left side of figures (c) and (d) is impinging on the tank wall.

References

Arhan M., Colin de Verdier A. & Memery L. 1994 The eastern boundary of the subtropical North Atlantic. *J. Phys. Oceanogr.* 24, 1295-1316.

Kloosterziel & van Heijst 1991 An experimental study of unstable barotropic vortices in a rotating fluid. *J. Fluid Mech.* 223, 1-24.

Lucas, J.H. & Rockwell D. 1988 Interaction of impulsively generated vortex pairs with bodies. *J. Fluid Mech.*, 197, 571-594.

Orlandi, P. 1993 Vortex dipoles impinging on circular cylinders. *Phys. Fluids*, 5, 2196-2206.

Richardson P.L., Bower A.S. & Zenk W. A census of Meddies tracked by floats. *Progress in Oceanography*, submitted.

Verzicco R., Flor J.B., van Heijst G.J.F. & Orlandi P. 1995 Numerical ad experimental study of the interaction between a vortex dipole and a circular cylinder. *Expt. In Fluids*, 18, 153-163.

STABILITY OF MEDDIES IN STRATIFIED GEOSTROPHIC FLOWS.

A.Tychensky (SHOM/CMO, Toulouse, France)
X.Carton (SHOM/CMO, Brest, France)

The Semaphore experiment at sea collected data over a 6-month period (june-november 1993) in the Azores-Madeira region. This data exhibited four intrathermocline eddies of Mediterranean water, called meddies (Swallow, 1969). These meddies were formed from the instability of the Mediterranean water undercurrents on the Portuguese shelf and then drifted southwestward to finally encounter the Azores current. Two of these meddies strongly interacted with the Azores front, creating large-amplitude meanders. Later, measurements of these meddies' trajectories showed that their propagation as well as their morphology were strongly affected by these interactions.

Therefore, the stability properties of these meddies is of considerable interest. These properties are connected with the three-dimensional distribution of potential vorticity inside these eddies. The analysis of SEMAPHORE hydrological data revealed that meddies are strongly baroclinic, with a multipolar structure, essentially along their vertical axis, but sometimes also horizontally. Morel and McWilliams (1997) have already mentionned the importance of the multipolar vertical distribution of potential vorticity for meddy propagation.

Armed with this potential vorticity distribution, we investigate here, in an idealized framework, the barotropic and baroclinic instabilities of intermediate-depths circular vortices with a non-monopolar potential vorticity distribution. We use a five-layer quasi-geostrophic numerical model, in which the vortex, idealizing the meddy, is initialized in the three central layers.

Much effort has been devoted lately to understand the stability of geostrophic vortices. Firstly, two-dimensional vortices were considered (Gent and McWilliams, 1986; Carton and McWilliams, 1989; Orlandi and van Heijst, 1991; Carton and Legras, 1994). When linearly unstable on an elliptical mode of deformation, these vortices can break into two horizontal dipoles (for strong barotropic instability). But, for weaker instability, they can stabilize nonlinearly as long-lived tripoles. Morel and Carton (1994) and Kloosterziel and carnevale (1994) showed that more complex vortex compounds, such as quadrupoles, can also form and persist, for triangular initial deformations.

These studies were extended to two-layer quasi-geostrophic flows (Flierl, 1988; Helfrich and Send, 1988). Very unstable vortices then usually break into vertical dipoles (hetons), But purely baroclinic, shielded Gaussian vortices can form counter-rotating, pulsating ellipses, when unstable on an elliptical mode (Carton and McWilliams, 1996). Recently, Correard and Carton (1998) showed that such unstable vortices, perturbed elliptically, can form long-lived steady tripoles. This stabilization is a nonlinear process, which occurs mostly for zero or negligible beta-effect. They applied their results to the observations of the oceanic swoddies (Pingree and Lecann, 1992).

Here, we extend these results to more stratified quasi-geostrophic vortices. Various horizontal and vertical potential vorticity distributions, both piecewise-constant and continuous, are considered. First, their linear stability is computed for normal-mode perturbations. Then, their nonlinear evolution with an asymmetric ($m=1$) and an elliptical ($m=2$) initial perturbation is studied by means of a pseudo-spectral and of a contour surgery code (D. Dritschel).

For vortices with a piecewise-constant potential vorticity distribution, linear stability calculations show that the elliptical mode is the most unstable. Then, numerical experiments show that the elliptical deformation can amplify nonlinearly and result in dipolar breaking (or heton

formation). For weaker instabilities, it can stabilize at finite amplitude and form steadily rotating, symmetric baroclinic tripolar meddies, on the f-plane. In the range of oceanic parameters, these tripoles are essentially observed in a regime of barotropic instability, due to the horizontal shear, weakened by the effects of stratification when the vortex radius is increased. The long-term evolution of these piecewise-constant tripoles on the f-plane is stable, in spectral code simulations with little hyperviscosity. On the contrary, these tripoles systematically exhibit asymmetric instability in inviscid evolutions in a Contour-Advective Semi-Lagrangian code; Dritschel and Ambaum, 1997). This is not explained as of now, especially since their linear instability diagram does not evidence mode 1 instabilities.

For vortices with a shielded Gaussian (or cubic exponential) profile of potential vorticity, the linear instability is essentially baroclinic, when the characteristic parameters of meddies in the Canary Basin are chosen ($R = 15 - 25 \text{ km}$, $R_d = 30 \text{ km}$). Such vortices, initially perturbed elliptically, break into two baroclinic dipoles if the instability and the initial perturbation are intense. For moderate instabilities, these vortices can form baroclinic tripoles. The stationnarity of these tripoles and their stability to initial disturbances is finally investigated.

Axisymmetric Gravity Currents in a Rotating System - some novel insights provided by numerical solutions

M. Ungarish, Dept. Computer Science, Technion, Haifa 32000, Israel

We consider axisymmetric gravity currents in a system rotating around a vertical axis which are produced when a dense fluid intrudes horizontally over a solid bottom under a less dense ambient fluid. This process is interested on its own, but it is also expected to throw light on the formation of the important quasi-steady-state structures called lenses, rings, bottom vortices or eddies. The previous studied are based on the shallow-water approximate equations supplemented by a semi-empirical correlation for the velocity of the nose (Ungarish & Huppert JFM vol. 362, 1998). In the present lecture an investigation based on the numerical solution of the full Navier-Stokes equations is described. It is shown that the capturing of the interface between the fluids and the vigorous motion in the "head" region pose challenges. Some results are presented and compared to predictions of the shallow-water model and with recent experiments (performed on the large Coriolis table at Grenoble in cooperation with H. Huppert, M. Hallworth and J. Mang). It is shown that the numerical results indicate a strong vortical motion in the meridional plane and a complex "multiple-front" structure of the interface; these effects, which could not be modeled by the shallow-water approximation, may have strong influence on the shape and stability of the resulting lenses, and are therefore presented as challenging topics of future research.

Ekman damping over a flat bottom
L. Zavala Sansón and G.J.F. van Heijst
Eindhoven University of Technology
Eindhoven, The Netherlands

Abstract

In the presence of background rotation, conventional two-dimensional (2D) models of geostrophic flow in a rotating system usually include Ekman friction -associated with the no-slip condition at the bottom- by adding a linear term in the vorticity evolution equation. This term is proportional to $E^{1/2}$ (where E is the Ekman number), and arises from the linear Ekman theory, which yields an expression for the vertical velocity produced by the thin Ekman layer at the flat bottom. In this paper, a 2D model with Ekman damping is proposed using again the linear Ekman theory, but now including non-linear Ekman terms in the vorticity equation. These terms represent non-linear advection of relative vorticity as well as stretching effects. It is shown that this modified 2D model gives a better description of the spin-down of experimental barotropic vortices than conventional models. Therefore, it is proposed that these corrections should be considered when the evolution of quasi-2D flows, during times comparable to the Ekman period (affected by bottom friction), is studied.

Instabilities of a stretched vortex

F. Bottausci¹, P. Petitjeans, J. E. Wesfreid
A. Maurel*, S. Manneville*

Laboratoire de Physique et Mécanique des Milieux Hétérogènes,

*Laboratoire Onde et Acoustique

Ecole Supérieure de Physique et de Chimie Industrielles

10, rue Vauquelin, 75005 Paris, France

freddy@pmmh.espc.fr

We present a controlled experiment on vortex stretching. Initial vorticity is obtained from a laminar-boundary-layer water flow in a long channel with rectangular cross-section. The stretching is produced by suction through two slots located on each lateral wall of the channel (Fig. 1). The suction flow through these slots is parallel to the initial vorticity. A stable vortex can be generated. Visualizations obtained by means of laser-induced fluorescence allow the characterization of the spiral nature of the cross-section of the vortex.

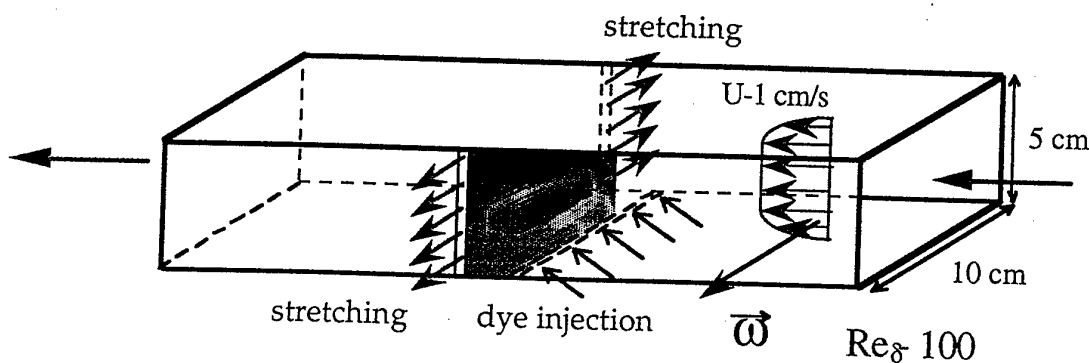


Fig. 1: Experimental set-up

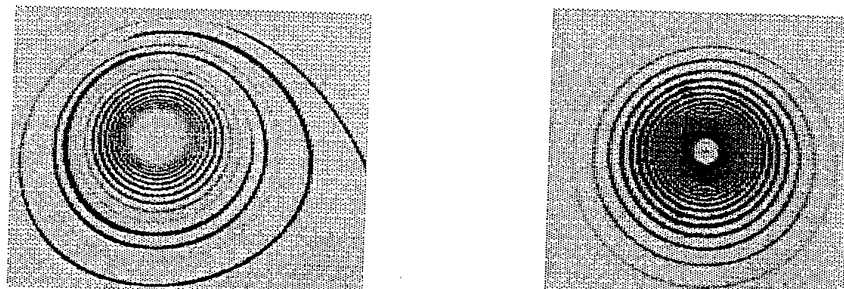


Fig. 2: Visualization of a cross section of the vortex

From velocity-profile measurements, deviations from Burgers' vortex profiles are pointed out. These deviations are due to the confinement of the flow. Indeed, the stretching being localized, the axial velocity U_z depends on r (the radial distance) leading to the existence of an azimuthal component of the vorticity.

When the flow rate at the outlet of the main channel is increased, vortex instabilities can be observed such as waves propagating along the axis of the vortex (Fig. 3).

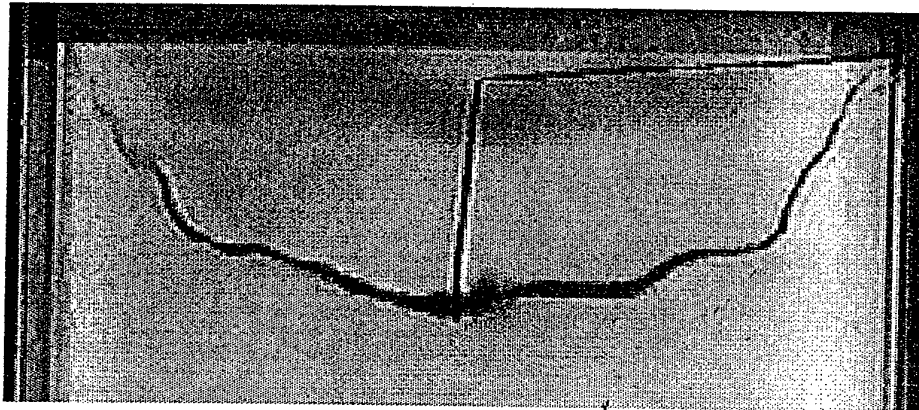


Fig. 3: Visualization of waves along the axis of the vortex

Later, the vortex can "explode" in a turbulent spot: when the main flow is too strong, the stretching is not enough to keep the coherence of the vortex. The vortex detaches from one of its ends, and breaks. The pressure is smaller in the core of the vortex than outside. Then, when the vortex detaches from a slot, and is not stretched any more, a flow penetrates into the vortex by this side, and propagates the breakdown. This mechanism can be observed in this experiment and will be described in the presentation.

This experiment gives access to fundamental mechanisms which play a role in vortex instabilities and turbulence where vorticity filaments are important. Hence, this flow, which is not turbulent, is able to mimic the behavior of what happens in turbulent flow, without the complex background of a fully developed turbulent flow.

Experiments on vortices on a *Beta*-plane

J.-B. Flór¹ & I. Eames²

¹Laboratoire des Ecoulements Géophysique et Industriels,
UJF-CNRS-INPG, B.P. 53X, 38041 Grenoble Cedex, France.

²School of Mathematics, Bristol University Bristol BS8 1TW, UK

Propagating vortices have a significant impact on mixing processes in the ocean, in coastal regions, the surf zone as well as large-scale processes in the atmosphere. We study the dynamics of isolated and non-isolated cyclonic vortices on a topographic β -plane experimentally. The novel aspect of this study is the measurement of both the displacement of material surfaces representing the

initial potential vorticity field, combined with measurements of the vorticity and velocity field. These results assist in providing a clear physical interpretation of how secondary vorticity, generated by the displacement

of ambient potential vorticity, interacts with the original monopolar or dipolar vortex and can induce monopolar vortices to propagate on a topographic

β -planes. The evolution of the vorticity and potential vorticity fields were followed for a range of initial vortex characteristics, and the mechanisms that determine the direction of propagation are discussed.

Experiments on vortex stretching

P. Petitjeans¹, F. Bottausci, J. E. Wesfreid
A. Maurel*, S. Manneville*

Laboratoire de Physique et Mécanique des Milieux Hétérogènes,

* Laboratoire Onde et Acoustique

Ecole Supérieure de Physique et de Chimie Industrielles

10, rue Vauquelin, 75005 Paris, France

phil@pmmh.espci.fr

A new experiment is devoted to the study of stretched vortices in order to understand the structure and the dynamics of such a structure in a laminar or turbulent flow. The vortex is produced in a water tank (80 x 80 cm, height = 40 cm) between two corotative disks (Fig. 1). The diameter of the disks is 5 cm or 10 cm (and can be modified), and the distance between each other can vary between zero to 50 cm. The disks rotate both at the same speed between zero and 20 rotations/s. At the center of each disk, a small hole (0.5 cm diameter) allows the suction of the water. The suction can be controlled between zero and 100 cm³/s independently on each disks.

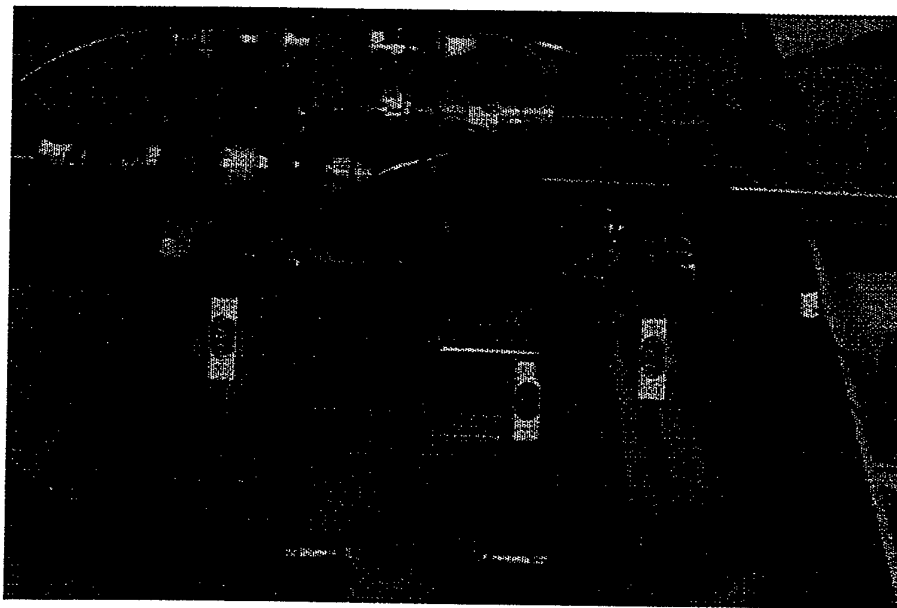


Fig. 1: Experimental set-up

Depending on these parameters, a quite stable vortex can be observed with a precessing motion. For another range of parameters, the vortex can be unstable and show a loss of its coherence and an "explosion" before another one is generated (Fig. 2).

The first objective of this work is to study the structure and the dynamics of a controlled stretched vortex. Different optical and acoustic techniques are used to access the characteristics of the vortex.

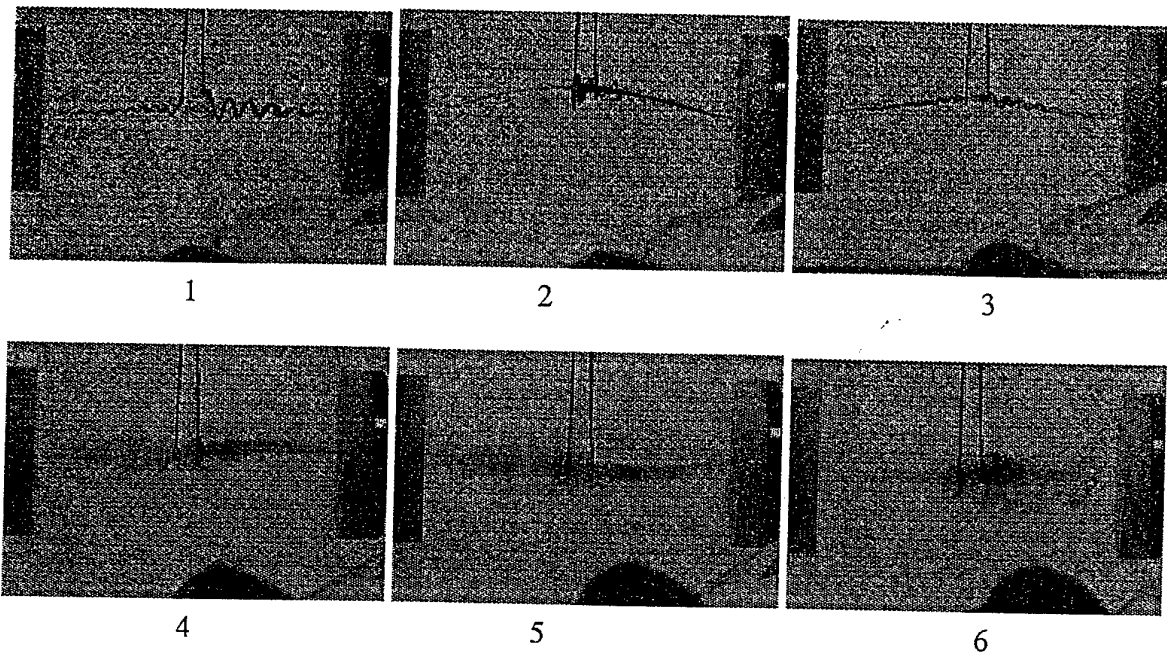


Fig. 2: Example of sequence of visualization of the dynamics of a stretched vortex

From visualizations, one can observe that the main energy dissipation occurs with the radial gradient of the axial velocity, i. e. in the term $\eta \frac{\partial U_z}{\partial r}$, where U_z is the axial velocity and r the radial distance. Indeed, the shear is very strong in this direction. Lots of "recirculation bulbs" (also called "vortex breakdown" in the literature) are observed in this flow. These "bulbs" are needed to help in the energy dissipation.

This experiment is also devoted to the study of the interaction between two vortices as a function of the angle between their axis. Reconnection depending on the characteristics of the two vortices will be studied very soon. The first results will be presented as well as the dynamics of one vortex.

Irregular scattering of acoustic rays by vortices

Vincent Pagneux¹ & Agnès Maurel²

¹Laboratoire d'Acoustique de l'Université du Maine
Av. O. Messiaen, 72 017 Le Mans Cedex 9, France

²Laboratoire Ondes et Acoustique
Ecole Supérieure de Physique et Chimie Industrielle de la Ville de Paris,
10, rue Vauquelin, 75005 Paris, France

¹vincent.pagneux@univ-lemans.fr

We present a study of the scattering of sound by several viscous vortex in two dimensions. We are treating propagation of sound whose wavelength is very short compared with any distance in which flow makes significant change. (The flow is composed of several vortices) It is known that classical scattering (as opposed to wave scattering) is capable of displaying irregular (chaotic) characteristic [1]. This property has already been studied for many types of scatterers and our aim is to characterize the irregular scattering of sound rays by vortices.

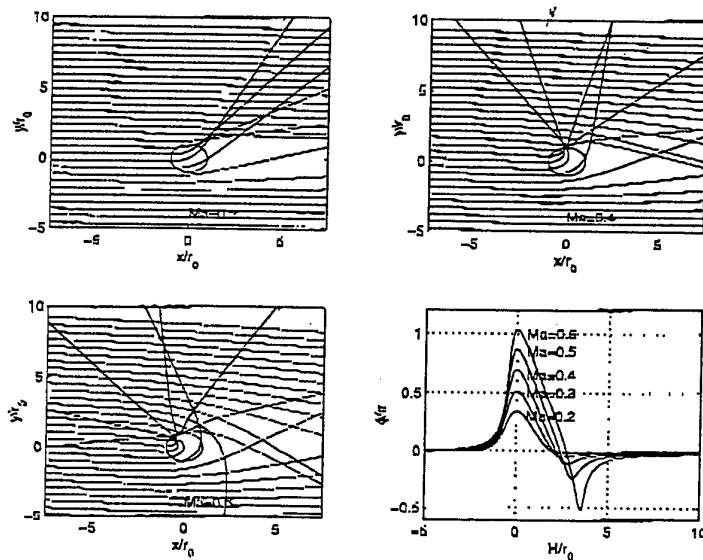


Figure 1

In figure 1, scattering of acoustic rays by one vortex is displayed for Mach numbers between 0.2 and 0.6, with the same method as used in [2]. It can be noticed that the maximum deflection of the rays is a function of the Mach number M , and that for $M > 0.5$ it can be higher than π . In order to observe irregular scattering we take a scattering region composed of 3 vortices whose velocity field is shown in figure 2. A series of sound rays is launched from the right of the 3 vortices with different impact parameters; when the angle ϕ of the rays is plotted as function of the impact parameter H (figure 2a), the scattering function ϕ vs H is composed of smooth regions that correspond to regular scattering but also composed of

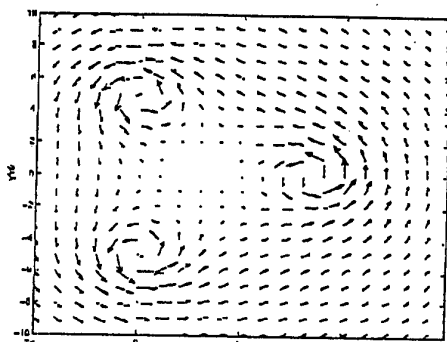


Figure 2

poorly resolved regions. These latter correspond to irregular scattering of rays since further magnifications show the same kind of poorly resolved regions. The chaotic scattering is characterized by the structure of the chaotic invariant set of periodic orbits between the vortices.

This work is devoted to a particular aspect of wave-vortex interaction which present an interesting alternative to usual system where chaotic scattering has been observed; here two important characteristics have to be taken into account, (1) the vectorial aspect of the scatterer and (2) the potential exchange of energy between the wave and the vortices (ie scatterers). Further studies are planned to compare this geometrical acoustics modeling to actual numerical simulation of the wave-vortex interaction.

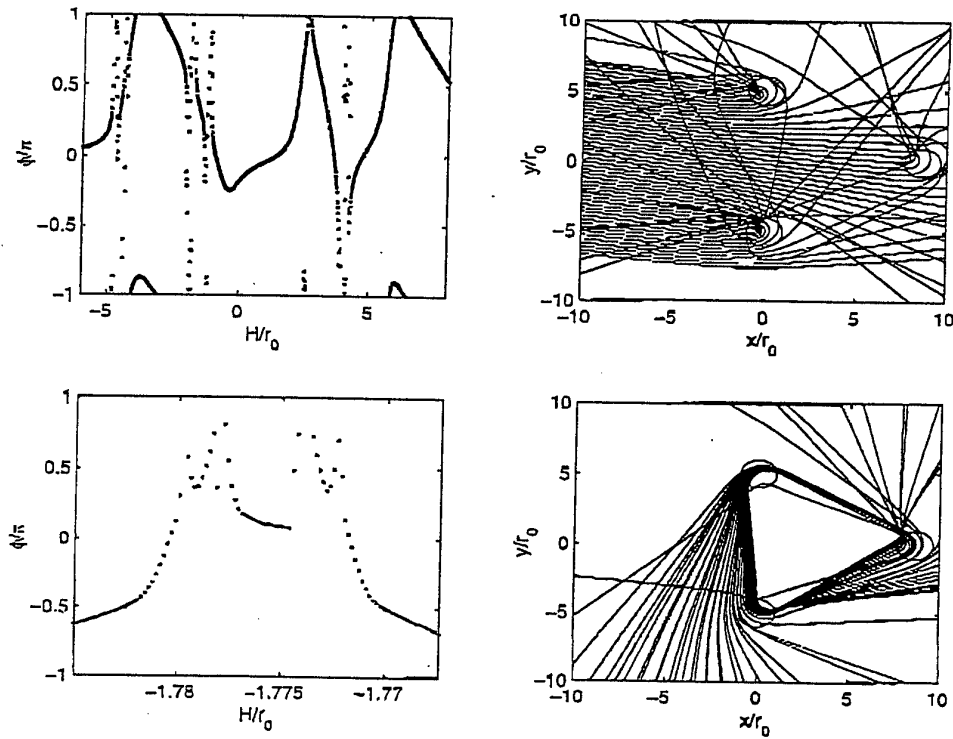


Figure 3

- [1] E. Ott, *Chaos in dynamical system*, Cambridge University Press, 1993
- [2] T.M. Georges, Acoustic ray paths through a model vortex with a viscous core, *J. Acoust. Soc. Am.*, 51: 206-209, 1971

The Internal Structure of the Leading-Edge Vortex Core.

M.B.H. van Noordenburg * H.W.M. Hoeijmakers †

1 Introduction

For the flow around a highly swept delta wing boundary layer separation occurs along the sharp leading-edge of the wing, beginning at small angles of attack. The viscous shear layers, formed due to the separation, roll up into coherent regions of concentrated vorticity of relatively small cross-section rendering a pair of counter rotating vortices above the delta wing. These vortices generate a so-called 'vortex-induced' lift force which enables flight at higher angles of attack in a controllable manner. Increasing the angle of attack yields an increase of the 'vortex-induced' lift force. Experimental observations indicate that above a critical angle of attack the internal structure of the vortex core changes abruptly. The cross-sectional size of the vortex increases substantially and the compact and coherent structure of the vortex is lost resulting in a disorganized and (possibly) turbulent flow field. This phenomenon is termed vortex breakdown or vortex burst.

In order to obtain a better understanding of the physical mechanism(s) responsible for the abrupt change in the internal structure a combined theoretical and numerical study of leading-edge vortex flow is currently carried out. The characteristic features of the leading-edge vortex are investigated by considering an isolated vortex core, i.e. in isolation from its natural surroundings by representing the external influence onto the vortex core through simplified boundary conditions. Experimental observations [1] indicate that the leading-edge vortex is rather slender and grows linearly in downstream direction thereby forming a conical flow region. The flow field inside the vortex core appears to be fairly axisymmetric and steady. As a consequence the time-independent and axisymmetric form of the governing Navier-Stokes equations have been adopted in the present investigation.

2 Inviscid Flow Solutions

Measurements of the flow inside the leading-edge vortex at different downstream locations furthermore indicate that the flow field possesses a conical similarity. Based on these observations Hoeijmakers [2] used the incompressible and axisymmetric form of the Euler equations to model the flow inside the leading-edge vortex core. At the outer edge of the vortex core the pressure, axial and azimuthal velocity component are assumed to be constant in accordance with observations. He derived two closed-form conical similarity solutions satisfying identical boundary conditions. One flow solution represents a jet-like swirling flow solution, whereas the second flow solution represents a completely different wake-like swirling flow solution. In figure (1) the jet-like swirling flow solution is compared with experimental observations. Except for a region near the axis of the vortex core the analytical solution is in excellent agreement with the experimental observations. In accordance with the slenderness of the core the radial component of the velocity is an order of magnitude smaller than the two other velocity components. Considering the vorticity distribution inside the vortex of both flow solutions in detail reveals that the main difference is present in the azimuthal component of the vorticity which changes direction. A switch in the direction of the azimuthal component of the vorticity has recently been indicated to be a key factor in the vortex breakdown process suggesting that the breakdown phenomenon might be related to multiple solutions of the governing equations.

At the axis of the vortex core the analytical flow solution possesses a logarithmic singularity for the axial and azimuthal velocity component. Clearly the effects of compressibility and viscosity cannot be neglected in this region. By adding compressibility effects to the flow solutions the logarithmic singularities present at the axis of vortex core are removed, but now at the axis of the vortex core vacuum conditions are reached. Two families of conical similarity compressible flow solutions satisfying identical boundary conditions are obtained numerically. Again one family representing jet-like flow solutions, whereas the second represents wake-like flows. Similar to the incompressible flow case the axial and azimuthal velocity components are an order of magnitude larger than

*PhD. student, Department of Mechanical Engineering, University of Twente, P.O. Box 217, 7500 AE, Enschede, The Netherlands, Phone: + 31-53-489 3550/4428, Fax: +31-53-489 3695, Email: M.B.H.vanoordenburg@wb.utwente.nl,

†Professor, Department of Mechanical Engineering, University of Twente

the radial component. Like for the incompressible flow case the main difference in the vorticity distribution inside the core is present in the azimuthal vorticity component which changes direction.

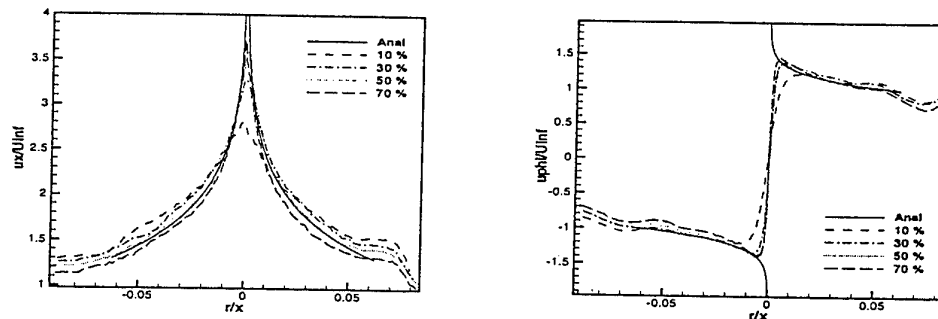


Figure 1: Experimental obtained axial (left-hand side) and azimuthal velocity distributions inside leading-edge vortex core compared to analytical conical similarity solution.

3 Viscous Flow Solutions

Including viscosity effects eliminates the possibility of obtaining a *conical* similarity flow solution. Following the work of Mayer & Powell [3] by assuming that the location of the outer edge of the vortex core is given by a parabolic-like equation the flow solution inside the vortex core can be described by a different similarity solution satisfying constant boundary conditions along the outer edge. Adding viscosity effects to the inviscid and incompressible flow solutions removes the logarithmic singularities at the axis of the vortex core. In the outer part of the vortex core the flow solution is nearly identical to the inviscid flow solution. Remarkably however only a jet-like flow solution has been obtained suggesting that the inclusion of viscosity effects renders the wake-like solution unphysical. Using slightly varying boundary conditions in downstream direction however yields two different flow solutions satisfying identical boundary conditions. One flow solution representing a slight modification of the earlier obtained jet-like solution whereas the second flow solution represents a completely different wake-like solution. For the outer part of the domain this flow solution resembles the viscous jet-like solution, near the axis of the core however a recirculation zone is present. Near the axis of the vortex core the azimuthal vorticity component changes direction in accordance with the inviscid wake-like solutions.

Adding compressibility effects to the viscous flow solution renders similar results, i.e. only a jet-like flow solution is obtained using constant boundary conditions whereas two flow solutions are obtained for slightly varying boundary conditions. In contrast to the inviscid flow case vacuum conditions are not reached at the axis of the vortex core.

4 Conclusion

The existence of multiple similarity flow solutions to describe the flow in a leading-edge vortex core indicates that the breakdown phenomenon might be connected to the non-uniqueness of the solution of the governing equations. Especially the switch in the direction of the azimuthal vorticity component between both flow solutions is remarkable. Recently a numerical compressible Euler solver [4] was used to verify that indeed two different flow solutions exist for specific flow conditions. It appears however that specific flow conditions are required for the second flow solution to be present.

References

- [1] VERHAAGEN, N.G. & VAN RANSBEECK, P. 1990 Experimental and Numerical Investigation of the Flow in the Core of a Leading-edge Vortex. *AIAA paper 90-0384*
- [2] HOEIJMERS, H. W. M. 1992 Aspects of Modelling and Numerical Simulation of Leading-Edge Vortex Flow. In *IUTAM symposium: Fluid Dynamics of High Angle of Attack* (ed. R. Kawamura & Y. Aihara). pp. 199–210. Springer-Verlag.
- [3] MAYER, E. W. & POWELL, K. G. 1992 Similarity Solutions for Viscous Vortex Cores *J. Fluid Mech.* **238**, 487–507.
- [4] VAN NOORDENBURG, M.B.H. & HOEIJMERS, H.W.M. 1998 Compressible Inviscid Flow Solutions for Isolated Leading-Edge Vortex Cores. *AIAA paper 98-2528*

Numerical experiment of wave propagation through vortex

¹Sébastien Manneville, ¹Mickaël Tanter, ¹Laurent Sandrin, ¹Agnès Maurel,
²Vincent Pagneux,

¹Laboratoire Ondes et Acoustique
Ecole Supérieure de Physique et Chimie Industrielle de la Ville de Paris,
10, rue Vauquelin, 75005 Paris, France

²Laboratoire d'Acoustique de l'Université du Maine
Av. O. Messiaen, 72 017, Le Mans Cedex 9, France

¹sebastien.manneville@espci.fr

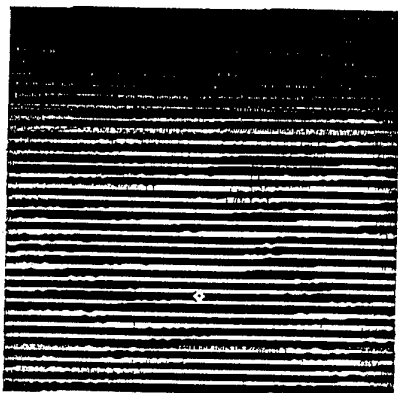
We study the propagation of a wave through a viscous vortex in two-dimension at low Mach number. Our aim is to clearly identify the different regimes of scattering when varying the ratio $a = \lambda/r_0$, where λ is the wavelength and r_0 the vortex core radius, corresponding to the characteristic length of the flow.

The method relies on a finite differences numerical scheme that solves for the linearized Euler equation at low Mach number. The results of the numerical calculations are exploited in order to clearly identify the scattered part of the pressure field (ie to separate the scattered and incident wave). Typical incident fields are plane or cylindrical waves.

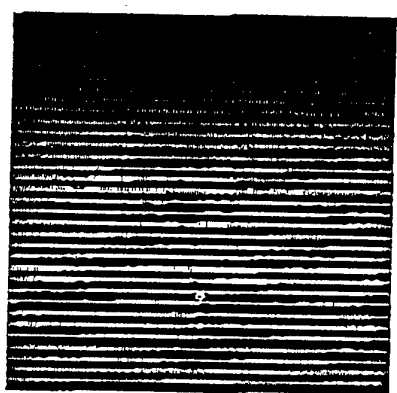
Figure 1(a) and (d) shows an example of the total pressure field obtained for respectively Mach number $Ma = 10^{-4}$ and 10^{-1} with an incident plane wave for $\lambda \sim r_0$. Figure 1(b),(c) and (e),(f) shows the corresponding amplitude and phase of the scattered field.

It can be seen that increasing the Mach number produces a strong asymmetry of the scattered pattern accompanied by the formation of a phase defect (spiral wave is generated from the vortex core and recovers a cylindrical shape far from the vortex).

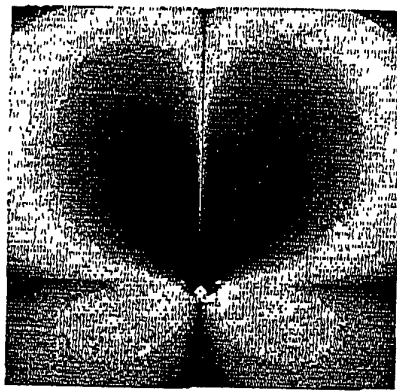
On the other hand, special care is taken to identify the validity range of various usual asymptotic, such as geometrical acoustic. For instance, we want to clarify the robustness of this approach when a goes from small values to 1, for small Mach numbers.



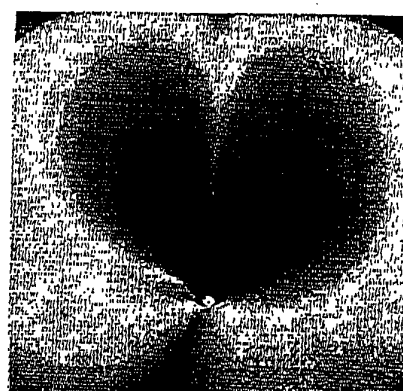
(a)



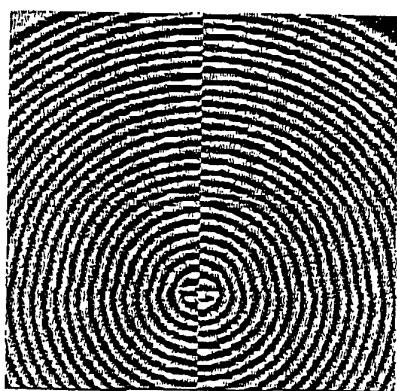
(d)



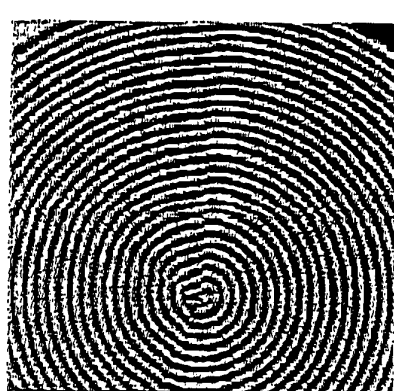
(b)



(e)



(c)



(f)

Either 2 short talks (15 min) or one talk of 30 min?

Title(s):

Maximum entropy or maximum viscous
mixing?

and

Quantifying the vorticity mixing leading to
2D coherent structures

Authors:

H. Capel and R. A. Pasmanter

Address:

KNMI, P.O.Box 201, 3730 AE De Bilt, The Netherlands.

email:

pasmanter@knmi.nl

fax:

[+31] 30 2202570

In many laboratory experiments and numerical simulations of 2D hydrodynamics at high Reynolds numbers one observes the evolution of an initial vorticity field into a quasi-stationary coherent structure. These structures are characterized by a functional relation between the vorticity ω and the streamfunction ψ . It will be shown how to extract from this $\omega - \psi$ relation a collection of "yardsticks", one for each moment of the vorticity distribution. This makes it possible to quantify the changes undergone by the vorticity distribution during the formation of the coherent structures. If the coherent structure happens to coincide with the prediction of the statistical mechanical theory of Lynden-Bell, Miller, Robert and Sommeria, then all the above-mentioned yardsticks are equal. Moreover, we will show that the predictions of this theory can be obtained by maximizing a measure of viscous mixing. This leads to a criterium for the applicability of the theory to flows with high, but finite, Reynolds.

VORTEX-WAVE LINEAR CONVERSION IN THE STRATIFIED DIFFERENTIALLY ROTATING FLUIDS

G.D. Chagelishvili,^{1,2 a)} R.G. Chanishvili,¹ J.G. Lominadze¹ and A.G. Tevzadze^{1,3}

¹ Department of Theoretical Astrophysics, Abastumani Astrophysical Observatory, Tbilisi, Georgia;

² Department of Cosmogeophysics, Space Research Institute, Moscow, Russia;

³ Centre for Astrophysics, KU Leuven, Heverlee, Belgium

a) e-mail: georgech@mx.iki.rssi.ru

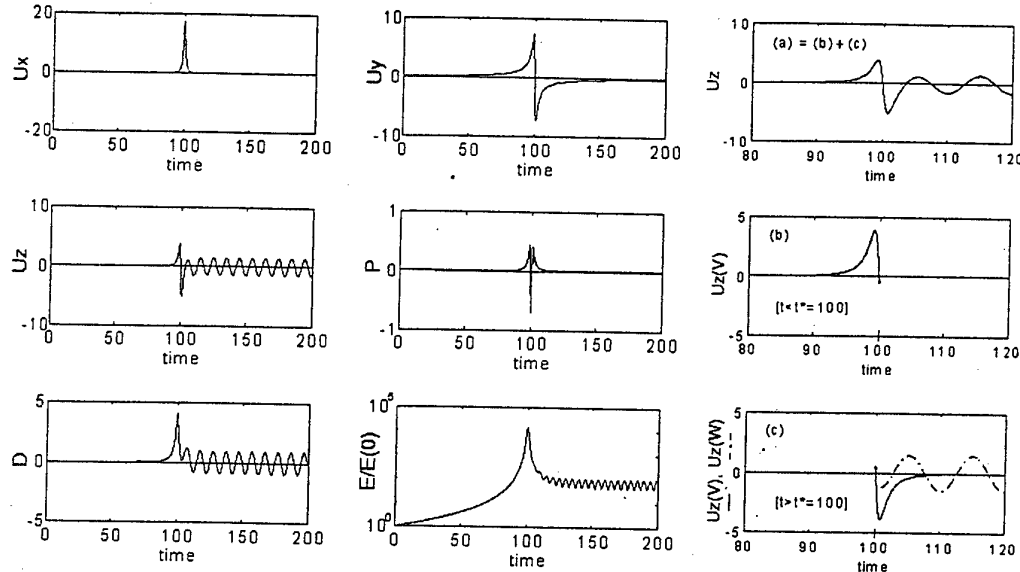
Phenomena of vortex transient growth followed by conversion to density-spiral waves in a unbounded, stratified, differentially rotating fluid are presented. It is assumed that: the angular momentum of the rotation increase outward ($\partial[\Omega(r)r^2]/\partial r > 0$); stratification is stable (buoyancy frequency is real); and the gravity force is perpendicular to the flow rotation plane. The transient/nonexponential growth of vortices in flows with constant shear rates is well-acknowledged in papers cultivating so-called nonmodal approach. As for the vortex-wave *linear* conversion phenomenon, it has to do with the fundamentals of the theory of oscillations and has been found recently in paper [1] for the simplest HD shear flow. Then [2,3], analogous phenomenon has been described for MHD and plasma shear flows. Here both phenomena are presented in the differentially rotating fluid that is stable from the point of view of the canonical/modal linear approach. For the purpose the linear dynamics of a small-scale non-axisymmetric vortices is studied in the flow in the framework of the nonmodal analysis. By this means temporal evolution of spatial Fourier harmonics (SFH) of vortices is traced in a local pseudo Cartesian co-ordinate system spaced at some distance r_0 from the rotational axis Z . Axes X and Y are aligned in radial and azimuthal directions, respectively.

Considered flow enables two different modes of disturbances in the Boussinesq approximation — wave mode that corresponds to the density-spiral oscillations and vortex mode that corresponds to the aperiodic vortical motion. The numerical calculations are carried out for initially input purely vortex mode disturbances, especially — for vortex SFH's. The *linear* dynamics of vortex SFH's, involving conversion to the wave SFH's proceeds as follows. The mean flow velocity shear (*i.e.* differential character of rotation: $A \equiv [r\partial\Omega(r)/\partial r]_{r=r_0} \neq 0$) results the temporal variation of each SFH wave-number projected along the radial direction ($k_x(t) = k_x(0) - k_y A t$); $k_y, k_z = \text{const}$). Initially, the vortex SFH's with negative ratio of radial and azimuthal wave-numbers ($k_x(0)/k_y < 0$) gain the shear flow energy and may amplify by the several orders of magnitude; reaching the point of maximal amplification at $k_x(t)=0$, each of them abruptly gives rise to the corresponding SFH of density-spiral waves. Further evolution of the vortex and generated wave SFH's proceed independently. The intensities of the vortex SFH amplification and the vortex-wave conversion depend heavily on the wave-numbers: vortex SFH amplification rate is as large as the parameter $k_x(0)/k_y$ is large and the parameter k_z/k_y is small; amplification rate is considerably reduced for SFH's with wave-numbers satisfying the condition $|k_z/k_y| \gg 1$; the vortex-wave conversion phenomenon may be at work for SFH with $k_z \sim k_y$; it becomes noticeable at shear parameters $R \equiv A/\Omega(r_0) = 0.4$ and even at $R=0.5$ is dominated in the flow dynamics.

The linear dynamics of the SFH is presented in the figure at: $R=1.5$; $k_z = k_y$; $k_x(0)/k_y = -150$; $k_z H = 10$ (H — stratification scale height). The graphs for velocity components (V_x, V_y, V_z), pressure (P), density (D) and normalized energy ($E(t)/E(0)$) of the SFH are presented in the first two columns. In the third column are separated the dynamics of V_z and its aperiodic/vortical ($V_z^{(v)}$) and oscillating ($V_z^{(w)}$) parts ($V_z = V_z^{(v)} + V_z^{(w)}$) in the vicinity of the vortex-wave conversion point in time ($t=t^*=100$): The upper graph of the third column describes the general dynamics of V_z in both side of t^* . The middle graph — the dynamics of $V_z^{(v)}$ at $t < t^*$ ($V_z^{(w)} = 0$ at $t < t^*$). The lower graph — the dynamics of $V_z^{(v)}$ and $V_z^{(w)}$ at $t > t^*$.

It turns out that the transient growth of the vortex is followed by the new phenomenon — it produces wave. As it is seen from the figures, evolving in the flow, the initially input vortex SFH

gaining mean flow energy and amplifying remains aperiodic nature till $k_x(t)/k_y < 0$. It may be said that the vortex SFH abruptly gives rise to the corresponding SFH of density-spiral wave at the point in time at which $k_x(t^*) = 0$. The abrupt character of the phenomenon is clearly seen from the graphs of $V_z^{(V)}$ and $V_z^{(W)}$.



The vortex-wave linear conversion should be universally present in flows with moderate and high shear rates. It is likely that the phenomenon is realised in terrestrial flows and grant significant novelties — vortices are able to generate different wave modes depending on the scales of the flow-perturbation system. It should also be inherent to many astrophysical flows, where high shear rates are of a common occurrence due to the involved extra high energetical processes.

From our study it follows that perturbations, that draw the mean flow energy in a most efficient way are vortices, rather than waves in differentially rotating flows with angular momentum increasing outward ($\partial[\Omega(r)r^2]/\partial r > 0$). These vortex mode perturbations fit naturally into the recently developed model of the bypass transition to turbulence of planar smooth shear flows [4-9]. It is reasonably safe to hope that the perturbations of this type are able to explain the subcritical transition in the rotating fluids also.

- [1] Chagelishvili G.D., Tevzadze A.G., Bodo G. and Moiseev S.S., Phys.Rev.Lett. 1997, **79**, 3178.
- [2] Tevzadze A.G., Phys. Plasmas. 1998, **5**, 1557.
- [3] Rogava A.D., Chagelishvili G.D. and Mahajan S.M., Phys. Rev. E, 1998, **57**, 7103.
- [4] Broberg L. and Brosa U., Z. Naturforschung Teil, 1988, **43a**, 697.
- [5] Chagelishvili G.D., Chanishvili R.G. and Lominadze J.G., Proceedings of the Joint Varenna-Abastumani International School and Workshop on Plasma Astrophysics (European Space Agency, SP-285), 1988, v.1, p.261.
- [6] Chagelishvili G.D., Chanishvili R.G. and Lominadze J.G., Proceedings from the U.S.-USSR Workshop on High-Energy Astrophysics (held in 18 June - 1 July, 1989), Eds. W.H.G. Lewin, G.W. Clark, R.A. Sunyaev, National Academy Press, Washington, D.C. 1991, p.55.
- [7] Gebhardt T. and Grossmann S., Phys. Rev. E, 1994, **50**, 3705.
- [8] Henningson D.S. and Reddy S.C., Phys. Fluids, 1994, **6**, 1396.
- [9] Baggett J.S., Driscoll T.A. and Trefethen L.N., Phys. Fluids, 1995, **7**, 833.

Tripolar vortices in plasmas and fluids

J. Vranješ

Institute of Physics, P.O. Box 57, Yu-11001 Belgrade, Yugoslavia

E-mail: vranjes@phy.bg.ac.yu

Recently, the investigation of tripolar vortices has attracted a lot of interests. Nice examples of such structures have been found in some experiments with rotating fluids [1] and observed by satellites in the Earth's seas [2]. Generally, a tripolar vortex is a coherent structure consisting of three parts, i.e., of a rotating core and two satellites of opposite vorticity, settled at certain position in the shear flow and carried with the flow, or in the centre of a rotating fluid system, as it is the case in the experiments mentioned above.

In our recent papers we have shown possibilities of appearance of tripolar vortices in various situations in plasmas. As the simplest case we investigated strongly nonlinear two dimensional perturbations in a two component plasma with sheared flow, propagating perpendicularly to the ambient constant magnetic field [3]. The linear development of such a system is well known from the literature. In the case when only the shear flow effects are present, it turns out that the instability is purely growing one, and it is in the regime $0 < kL < 1$, where k is the wavenumber and L is the characteristic length for the shear inhomogeneity. We proposed that these linearly unstable modes can saturate into stationary traveling solutions of the form of vortex chains and tripolar vortices, propagating perpendicularly to the external magnetic field, and analytical solutions of this type are found. The tripole obtained is found to be completely defined by the sheared flow.

In the problem of drift waves in a nonuniform streaming plasma placed in a sheared magnetic field [4], we have demonstrated that the magnetic shear stabilization criteria are severely restricted, and the velocity profile curvature $v_0''(x)$ is found to play a crucial role. In the strongly nonlinear regime, the system is described by the following set of the ion continuity, and parallel motion equations, respectively:

$$\left[\frac{\partial}{\partial t} + \frac{1}{B_0} \vec{e}_z \times \nabla_{\perp} (\Phi + B_0 \varphi) \cdot \nabla_{\perp} \right] \left[(1 - \rho^2 \nabla_{\perp}^2) (\Phi + B_0 \varphi) - B_0 (\varphi + \Psi) \right] + \frac{T_e}{e} \nabla_z \cdot \delta \vec{v}_z = 0,$$
$$\left[\frac{\partial}{\partial t} + \frac{1}{B_0} \vec{e}_z \times \nabla_{\perp} (\Phi + B_0 \varphi) \cdot \nabla_{\perp} \right] [\delta v_z - \Omega_i f(x)] = 0.$$

Here $v_0(x) = d\varphi/dx$, $v_{*e} = d\Psi/dx = -n_0' c_s^2 / n_0 \Omega_i$, Φ is the electrostatic potential, and $\rho = c_s / \Omega_i$, $c_s^2 = T_e / m_i$, $\Omega_i = e B_0 / m_i$. The basic state magnetic field is taken in the form $\tilde{B}_0 = \vec{e}_z B_0 + \vec{e}_y B_0 (d/dx) f(x)$, where $|(d/dx) f(x)| \ll 1$. For some specific profiles of the functions $\varphi(x)$, $\Psi(x)$, and $f(x)$, analytical solution for Φ in the form of a tripolar vortex, can be readily found. Typical contour plot of the solution is presented in Fig. 1.

We studied also the case of a dusty plasma [5], and similar equations are obtained. The presence of the dust component introduces only new scaling in the system, but the solutions are essentially of the same type.

Finally, we investigated nonlinear magnetic electron mode in a nonuniform, unmagnetized plasma, with a spatially dependent flow, and derived a set of two coupled equations, for the self-generated magnetic field and electron temperature perturbation. We studied electromagnetic perturbations with heavy ions making a neutralizing background, i.e. $\omega_{pi} \ll \partial/\partial t$, and $|k^{-1}| \ll L_n, L_T$, where k is a typical wavenumber, and L_n, L_T are the characteristic lengths of the concentration and temperature inhomogeneities, respectively. Electron momentum and energy equations, and the Maxwell equations are used:

$$\left(\frac{\partial}{\partial t} + \vec{v} \cdot \nabla \right) \vec{v} = -\frac{e}{m} \left(\vec{E} + \vec{v} \times \vec{B} \right) - \frac{1}{mn} \nabla(nT), \quad \left(\frac{\partial}{\partial t} + \vec{v} \cdot \nabla \right) (Tn^{1-\gamma}) = 0,$$

$$\nabla \times \vec{E} = -\frac{\partial \vec{B}}{\partial t}, \quad \nabla \times \vec{B} = -\mu_0 en\vec{v}.$$

In the basic state we have $\vec{v}_0 = v_0(x)\vec{e}_y$, and $T_0 = T_0(x)$. We neglect the density perturbations, $n \equiv n_0(x)$, and seek a z -independent solution of the above equations. Assuming weak time dependence, $\partial/\partial t \ll \omega_{pe}$, we find a tripolar solution similar to that given in Fig. 1.

To conclude, we present the scenario of formation of tripolar vortices in various plasma configurations. Analytical solutions obtained in our calculations are surprisingly similar to corresponding structures obtained in experiments with rotating fluids. As it is known there exists a strong similarity between nonlinear processes in plasmas and rotating fluids and results obtained in one of these media can be used to describe analogous processes in other.

References:

- [1] G. J. F. Van Heijst and R. C. Kloosterziel, Nature 338, 569 (1989); G. J. F. Van Heijst, R. C. Kloosterziel and C. W. M. Williams, J. Fluid Mech. 225, 301 (1991).
- [2] R. D. Pingree and B. Le Cann, J. Geophys. Res. 97, 14353 (1992).
- [3] J. Vranješ, Tripolar vortex in plasma flow, submitted to Planet. Space Sci. (1999).
- [4] J. Vranješ, D. Jovanović and P. K. Shukla, Phys. Plasmas 5, 4300 (1998).
- [5] J. Vranješ, G. Marić and P. K. Shukla, Tripolar vortices and vortex chains in dusty plasma, submitted to Phys. Lett. A (1999).

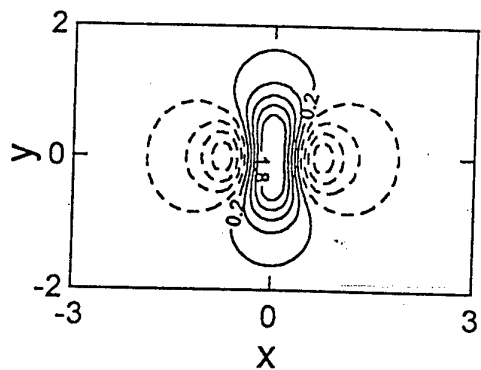


Fig. 1.

Printed by 21.00 font on 11/11/2011

"Transition from waves to turbulence in a stratified flow"

G.F. Carnevale

SCRIPPS INSTITUTION OF OCEANOGRAPHY, SCRIPPS, LA JOLLA, USA.

Much of the variability of the density and velocity of the oceans on scales greater than 10 m in the vertical is associated with internal wave activity. At scales below about 1m and down to a viscous or diffusive cutoff, the flow appears to be dominated by isotropic turbulence. Between these wave and turbulence ranges there is a transition range, sometimes called the 'buoyancy range,' in which waves and turbulence compete. The nature of the dynamics in this range is a controversial matter. It would be useful to be able to numerically model the flow in this range. An attempt to do this with an isotropic grid and a subgrid-scale model with its cutoff wavenumber in the inertial range is presented. The forcing is supplied only at large-scale in the form of a standing internal wave. If the amplitude of the forcing is low, the spectra of the resolved scales approximates that in the 'buoyancy range,' while for sufficiently high amplitude forcing, the spectra indicate a fully turbulent range. In between, the results are somewhat ambiguous, but perhaps can be understood in term of the intermittency in the buoyancy range.

Two-dimensional Dynamics of Concentrated Vortex Interactions

V. V. Meleshko,¹

Fluid Dynamics Laboratory, Faculty of Technical Physics, Eindhoven University of Technology, P.O.Box 513, 5600 MB Eindhoven, The Netherlands

The talk addresses the analysis of some typical two-dimensional flows of an incompressible inviscid fluid with concentrated vorticity: point vortices and circular vortex rings. The main issue consists in considering the behaviour of the surrounding fluid (the 'atmosphere' of vortex pair, in particular) under vortex interactions. The contour kinematics method for tracing the interface line was developed [2].

Special attention is paid to soliton-like behaviour of the vortex pair atmosphere under various types of interactions (exchange and direct scattering, mutual trapping or merging) of dipole-monopole or dipole-dipole interactions. Quantitative results on entrainment/detrainment processes are presented and their classification in terms of invariants of motion is provided. Comparisons with experimental results (figure) and with more complicated contour dynamics simulations of Chaplygin – Lamb dipoles interactions show a good correspondence. Although an extreme idealization, the model of point vortices appears to shed considerable light on what to expect in the laboratory experiments.

The fascinating old experimental phenomena [1] connected with vortex ring, namely, its attraction by a solid body (Thomson, 1869) and the impossibility of its cutting, since, "it would wriggle away from the knife" (Tait, 1876), is explained by means of studing two-dimensional interaction of a vortex pair and its atmosphere with a cylinder and a wedge.

The discussion of mixing of surrounding fluid by point vortices for von Kármán vortex street is based upon the principal invariants of the Lagrangian topology. The coherent structures formed by stable and unstable manifolds are identified. Construction of Poincaré mapping permits to distinguish other coherent structures connected with elliptic periodic points of different orders, which remain unmixed under periodic regimes.

The results obtained by contour kinematics method [2] for concentrated vorticity confirm von Kármán's (1911) words that "many peculiarities of real flow can be understood based on the notion of existence of separated vortices in the flow and the laws of motion of such vortices in an ideal fluid".

References

- [1] Love, A.E.H. (1887) "On Recent English Researches in Vortex-motion," *Math. Annalen* **30**, 326-344.
- [2] Meleshko, V.V., and van Heijst, G.J.F. (1994) "Interacting Two-dimensional Vortex Structures: Point Vortices, Contour Kinematics and Stirring Properties," *Chaos, Solitons & Fractals* **4**, 977-1010.

¹e-mail: slava@kiev.phys.tue.nl

Reversibility and nonmonotony of mixing quality

T. S. Krasnopol'skaya¹, V. V. Meleshko²

Department of Technical Physics
Eindhoven University of Technology,
P.O. Box 513, 5600 MB Eindhoven, The Netherlands

Communication addresses questions: how to organize steady or periodic mixing in a wedge cavity and where to put a blob (or blobs) in order to achieve the best result in the finite time. Time reversibility as an important issue (it concerns the reversibility of individual points and quality measures) was studied as well as dynamics of measures. The properties of distributive laminar mixing of highly viscous fluids are considered in an annular wedge cavity. Flow is induced by a motion of the top and bottom curved walls with prescribed periodic in time velocities and can serve as a prototype for the flow between two neighbouring paddles of a periodically rotating turbine. Study of mixing in the wedge cavity is special compared to other geometries because the annular wedge is the typical cross-section of a single screw extruder or a mixing element in any rotary device, which always is more realistic than for example a rectangular cavity. We present the analytical solution for the velocity field in the cavity, the algorithm for line tracking of any contour enclosing some dyed region, the technique for finding the periodic points in the flow, and the quantitative measures for estimation of quality of mixing.

The traditional approach, based upon the presentation of the dyed blob as a collection of N points uniformly distributed over the area S_b of the blob, can provide a reasonable treatment of mixing with good correspondence with the experiments, even in complex domains. For long time evolutions, however, this approach provides only a qualitative general picture of mixing. Fine details, especially the question whether an 'empty' space surrounded by a cluster of points really means the absence of the component to be mixed, remain unclear. Basically, the uniformly distributed multipoint approach can not provide a valid description of blob stretching and folding, if the thickness of filaments becomes less than $(S_b/N)^{1/2}$, or if the length of the contour line becomes more than $2(NS_b)^{1/2}$. Besides, being distributed uniformly at the initial moment, the points tend to spread out nonuniformly and, sometimes, collect into dense clusters. Any 'box-counting' calculations based upon the preservation of a Lebesgue measure of the set of N points (with an 'area' S_b/N associated with each point), can provide only qualitative estimates for quality of mixing.

Our analysis of distributive mixing is based upon a conservation of topological properties (connectedness and orientation) of the Lagrangian interface line between components deformed by an Eulerian velocity field. The key idea of our approach is the use of a non-uniform distribution of points at the initial contour to represent this interface, such that (i) the distance between neighbouring points remains between some chosen values (that is, points are added when the distance becomes too long and points are removed when it becomes too short) and (ii) the angle between any neighbouring straight lines

¹On leave from Ukrainian Research Institute of the Environment and Resources, Kiev, Ukraine.

²On leave from Institute of Hydromechanics, National Academy of Sciences, Kiev, Ukraine.

is greater than some prescribed value (to describe folding of the line). The principal advantage of this approach for line tracking is that

area preservation of the blob enclosed by the contour is guaranteed, even after complicated stretching and folding.

We will adopt Gibbs' approach and use the 'coarse-grained density' of the distribution as a basic measure for the three criteria of the mixed state: the mean square density (Welander 1955), the entropy (Gibbs 1902) and the intensity of segregation (Danckwerts 1952). All three criteria show the dynamics of mixing in their own scales and may be used descriptively but never causatively. By using these criteria we can for a given volume element size (the 'grain') estimate the time necessary for the mixed state to be uniform within some specified range. The three criteria are not independent, and they are statistical measures of the first order. For a more complete description of a mixture, we will also use the scale of segregation (Danckwerts 1952) which is a statistical measure of the second order. It represents an average of the size of the clumps of the mixed component.

Calculations with 30000 points *uniformly* distributed along the initial contour line have shown the accurate reversibility after ten periods. In spite of that the blob area was not conserved already after the two first periods.

The calculations based on our algorithm with *nonuniform* distribution of points conserved the blob area for twelve periods of forward and twelve periods of backward motions. In this case the computations of all coarse grained measures based on the value of the blob area are reliable. Nevertheless, for such computations not all points come back to their initial positions. After the reverse process some of the points are located along pieces of the unstable manifold for the backward motion (which coincides with the stable manifold for the forward motion). The contribution of these spurious lines to the blob area equals zero. Thus, we can conclude that computation of the measures shows a complete reversibility in spite of irreversibility of some individual points.

The periodic mixing is not always better than the stationary one – the specific location of the initial blob (nearby hyperbolic points) is of crucial importance. Therefore, optimization of mixing for a given energy input must be based not only upon the comparisons of the protocols themselves but upon consideration of the initial positions of the blobs. Moreover, among various hyperbolic periodic points, the point for which the unstable manifold covers more uniformly the whole cavity should be preferred as a blob's centre. Besides, initial splitting of the blob into several smaller blobs (if possible) can provide the best mixing under the same protocol and energy input. It is worth noting that all four measures which we constructed using the coarse grained concept give the same qualitative conclusions. Therefore, any of this criterion can be used for estimating the mixing quality. For dispersive laminar mixing the intensity I is generally accepted and it is logically using Q to judge on the related energy, as both are increasing quantities.

The data also show that the dyed material does not only spread over the cavity (the more material is located close to the moving wall the faster it spreads over new 'empty' boxes), but, opposite, due to existence of elliptical islands collects *back* and occupies less boxes. Thus, quality measures reveal fluctuations either increase or decrease with tendency to stabilize.

Either 2 short talks (15 min) or one talk of 30 min?

Title(s):

Maximum entropy or maximum viscous
mixing?

and

Quantifying the vorticity mixing leading to
2D coherent structures

Authors:

H. Capel and R. A. Pasmanter

Address:

KNMI, P.O.Box 201, 3730 AE De Bilt, The Netherlands.

email:

pasmanter@knmi.nl

fax:

[+31] 30 2202570

In many laboratory experiments and numerical simulations of 2D hydrodynamics at high Reynolds numbers one observes the evolution of an initial vorticity field into a quasi-stationary coherent structure. These structures are characterized by a functional relation between the vorticity ω and the streamfunction ψ . It will be shown how to extract from this $\omega - \psi$ relation a collection of 'yardsticks', one for each moment of the vorticity distribution. This makes it possible to quantify the changes undergone by the vorticity distribution during the formation of the coherent structures. If the coherent structure happens to coincide with the prediction of the statistical mechanical theory of Lynden-Bell, Miller, Robert and Sommeria, then all the above-mentioned yardsticks are equal. Moreover, we will show that the predictions of this theory can be obtained by maximizing a measure of viscous mixing. This leads to a criterium for the applicability of the theory to flows with high, but finite, Reynolds.

Mar 25 1999 18:58

e.pavia

Page 1

Some effects of thermodynamics on geostrophic rodons

E.G. Pavia, J.L. Ochoa and J. Sheinbaum
CICESE
A.P. 2732, Ensenada, B.C., 22800, Mexico

Rodons are typically vortices of homogeneous fluid. In this work we study their behavior when thermodynamical effects are included by the presence of a variable density. We find that in order to be unstable, a circular rodon must have a density increment at one point from the center to the edge. Unstable elliptical inhomogeneous rodons evolve toward less eccentric states, by shading mass to the surroundings, and homogenize, eliminating the thermodynamical effects.

Analysis of dispersion of passive tracers in a quasi two-dimensional convective flow

Stefania Espa, Giorgio Querzoli**

*Dept of Hydraulics Transportation and Roads

University "La Sapienza", Via Eudossiana 18, 00184, Rome, Italy

e-mail: stefy@cenedesel.ing.uniroma1.it

** Dipartimento di Ingegneria del Territorio

University of Cagliari, Cagliari, Italy

ABSTRACT

The dispersion of passive tracers in a quasi two-dimensional convective flow has been investigated. The convection has been generated by a line heat source placed 1 cm above the centre line of the lower surface of a transparent prismatic tank filled with pure water. The tank is 15.0 cm in width, 6.0 cm in height, 10.4 cm in depth. The horizontal surfaces of the tank (1.0 cm thick aluminium plates) are isothermal and the side walls (1.0 cm thick perspex) are adiabatic and made of perspex to have an optical access. The temperature of the plates is controlled by two heat-exchangers consisting in a series of counter-flow channels in which constant temperature water flows. The velocity measurements are based on tracking of non-buoyant seeding particles uniformly dispersed in the field (P.T.V.) on the measuring plane, placed at middle depth of the tank.

When convection starts, two counter rotating rolls occur. In a certain range of control parameters (Rayleigh number, Prandtl number, aspect ratio of the tank) the flow is stable, then it becomes unstable and the rolls start to oscillate in a plane orthogonal to the line heat source showing a natural swaying motion.

The aim of this study is the investigation of the basic mechanisms which drives both diffusion and advection phenomena occurring in the tank. A comprehensive description of the flow in terms of stability and instability by means of critical points identification has been performed. Considering a coordinate system which is assumed to translate without rotation with the origin following a fluid particle, it is possible to describe the fluid motion by the leading terms of a Taylor expansion of the Eulerian velocity field. In such a reference frame, the origin is a critical point and the coefficient of the linear terms are elements of the velocity tensor gradient. Complex eigenvalues of the velocity tensor gradient identify a vortical region characterised by a spiralling motion of particles around a common centre while real eigenvalues identify high strain regions.

The further identification of the centre of the two counter rotating rolls, has allowed to extract the flow phases and to obtain phase-averaged velocity fields by conditional phase sampling (plume on the left, plume on the right of the tank).

An integration of the instantaneous velocity fields during a complete oscillation (Figure 1), provides instantaneous streamlines: the analysis of the various kinds of local streamline patterns allows to investigate bifurcation processes and the possible onset of chaos around the separatrices of the flow basically due to the time dependence of the Eulerian velocity field. As a consequence, the analysis of

the dynamical system corresponding to the flow can effectively support the visualisation techniques in the understanding of the transport phenomena.

Since PTV is based on the recognition of particle trajectories, measurements are obtained in a Lagrangian reference frame. This fact gives the possibility to study the characteristics of mixing by conditionally averaging particle displacements. The role played by the topological structure identified in the field has been studied by evaluating the probability that a particle moving from a critical point could reach a selected interrogation area after a defined time interval. This kind of statistics describes the mixing within each of the two large rolls in which the field is divided. Using the same logical procedure the mixing process occurring between the left half-field and the right half-field of the convective cell has been described by computing the probability of transition of particles between the left and right side of the tank.

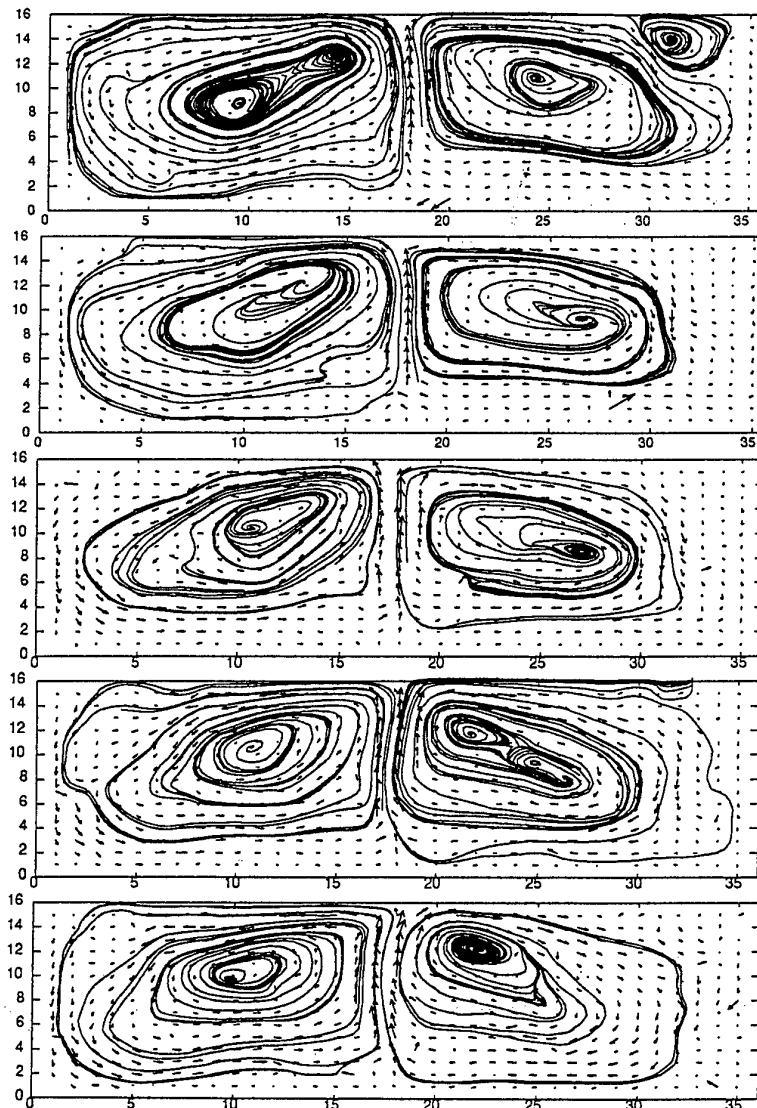


Fig. 1 Instantaneous velocity fields during a complete oscillation of the plume

Particle Tracking Velocimetry for the analysis of Penetrative Convection.

Giuseppe Mancini, Stefania Espa, Antonio Cenedese

Dept of Hydraulics Transportation and Roads

University "La Sapienza", Via Eudossiana 18, 00184, Rome, Italy

Penetrative convection rises when a source of turbulent kinetic energy is applied to a fluid with a density gradient. Let consider the case of a lake with a well defined thermal structure. It will possess a stable stratified hypolimnion, a sharp thermocline and an epilimnion which undergoes diurnal temperature fluctuations due to daytime heating and nighttime cooling. During night, heat losses begin to dominate the thermal exchange at the surface, the surface layer cools and convective motion mix the upper layer which develops by the entrainment of the underlying fluid.

An experimental set up has been realized to simulate this natural phenomenon in laboratory. The apparatus consists of a Perspex tank filled with pure water. At the top of the tank a shell and tube exchanger allows upper surface cooling while all the other surfaces can be considered adiabatic. A two layer stratification is produced by first filling the tank to the required depth with water at fixed temperature and then letting colder water flow slowly into the tank through a diffuser in the bottom. LIF visualization, temperature measures and velocity measures by means of PTV, have been used to study the deepening of the mixed layer and the entrainment phenomenon. Particle Tracking Velocimetry allows the Lagrangian reconstruction of the trajectories of pollen particles inside the fluid. Lagrangian position and velocity of each particle along the trajectories are used to infer Eulerian field of motion by interpolating on a regular grid. At the same time the temperature profile is registered by using a set of thermocouples displaced along the vertical.

The rate of mixed layer deepening together with the surface heat flux are obtained from the analysis of the evolution of temperature profile. Statistical interpretation of the velocity field allows to analyze plumes generation and entrainment mechanism. The measurements indicate that there is a transfer of energy from the vertical component to the horizontal components, thus rendering the turbulence strongly anisotropic. From the energy spectra analysis it is also apparent a preferential attenuation of low frequencies (large scale) as the interface is approached, implying that the density interface has significant influence on the large eddies. The high frequency ends of the spectra remain virtually unaffected implying that the net transfer of turbulent kinetic energy from the vertical to the horizontal components of velocity is confined to small frequencies or large eddy scales.

Laboratory experiments on fronts : the influence of the coast and of bottom topography.

P. Bouruet-Aubertot¹ & P.F. Linden²

1. D.A.M.T.P., University of Cambridge, Silver Street, Cambridge CB3 9EW, England

2. Department of Applied Mechanics and Engineering Sciences, U. of California San Diego, La Jolla, CA 92093-0411, USA

We investigate experimentally the instability and later evolution of a front in a two-layer stratification near a coast and over sloping topography. The front is produced through the adjustment of a buoyant fluid that is initially confined within a bottomless cylinder in a similar manner to that of Chia et al (1982). Two dimensionless parameters are relevant to describe the flow dynamics : a Froude number F , defined as the square of the ratio between the distance between the inner cylinder and the vertical boundary of the tank and the radius of deformation of the upper layer, and a depth ratio $\delta = h_0/H$, where h_0 is the initial upper layer depth and H that of the lower layer. The experiments are recorded onto a video tape recorder using a video camera. Detailed measurements of the velocity and vorticity fields at the surface are made using the image analysis program, DigImage.

A front establishes typically when the Froude number, F , is greater than 1. The adjustment process is dominated by large amplitude oscillations arising from inertial waves. Meanwhile, as rotation effects become significant, an anticyclonic circulation develops in the upper layer. A quasi-cyclostrophic equilibrium is reached after about two rotation periods. The front then rapidly becomes unstable toward wave perturbations (see fig.1.a). During the growth of the waves cyclonic vorticity is induced in the lower layer at the wave troughs where the fluid columns are stretched to replace the collapsing upper layer fluid (fig.1.a). This leads, for sufficiently large wave amplitude, to closed cyclonic motions of coastal waters (fig.1.b). Different behaviour is obtained depending on the distance between the front and the coast. When the front is still far from the coast eddy pairs (consisting of a coastal water cyclonic eddy surrounded by fresh water and an anticyclonic eddy of upper layer fluid) can form and detach (e.g. Griffiths & Linden 1981). By contrast when the wave crest reaches the coast before the formation of cyclonic eddies an asymmetry between cyclones and anticyclones is observed as previously mentioned by Chia et al (1982). The anticyclonic wave crest spreads in two directions (fig.1.b, right upper part). The part which is spread upstream has the coast on its right and therefore flows along the coast as a buoyancy driven boundary current. This branch contributes to the enhancement of the cyclonic eddy of coastal water induced behind the crest. The other branch, which spreads downstream, is characterized by strong off-shore currents which advect cyclonic eddies of coastal water across the front toward the centre (fig.1.c). The late evolution of the front is characterized by the interaction and decay of large-scale eddies (fig.1.d).

We provide a quantitative analysis of the instability. We first find, consistently with baroclinic instability, that the wavelength of the perturbation scales like the geometric mean of the radii of deformation of the two layers. Also the wavelength does not vary with the distance between the front and the coast which is consistent with the fact that the instability first develops far from the boundary. Similar results are obtained when introducing a bottom topography of conical shape such that the depth is linearly decreasing toward the coast. Growth rates of the instability are then inferred from the time evolution of the spatially averaged cyclonic and anticyclonic vorticities. An exponential growth is obtained until the instability saturates when cyclonic eddies start to detach. We find that the effect of the coast is crucial and leads to the enhancement of cyclonic eddies consisting of coastal waters : the smaller F is the higher the intensification is. This has significant impact on exchanges across the front. By contrast, when a conical topography cross-frontal exchanges are weakened as the cyclonic eddies remain confined to the sloping region.

References :

Chia, F., Griffiths, R.W. & Linden, P.F. 1982 Laboratory experiments on fronts. Part 2 the formation of cyclonic eddies at upwelling fronts. *Geophys. Astrophys. Fluid Dyn.* **19**, 189-206.
Griffiths, R.W., & P.F. Linden 1981. The stability of vortices in a rotating, stratified fluid. *J. Fluid Mech.*, **105**, 283-316.
Phillips, N.A. 1954. Energy transformations and meridional circulations associated with simple baroclinic waves in a two-level, quasi-geostrophic model. *Tellus*, **6**, 273-286.

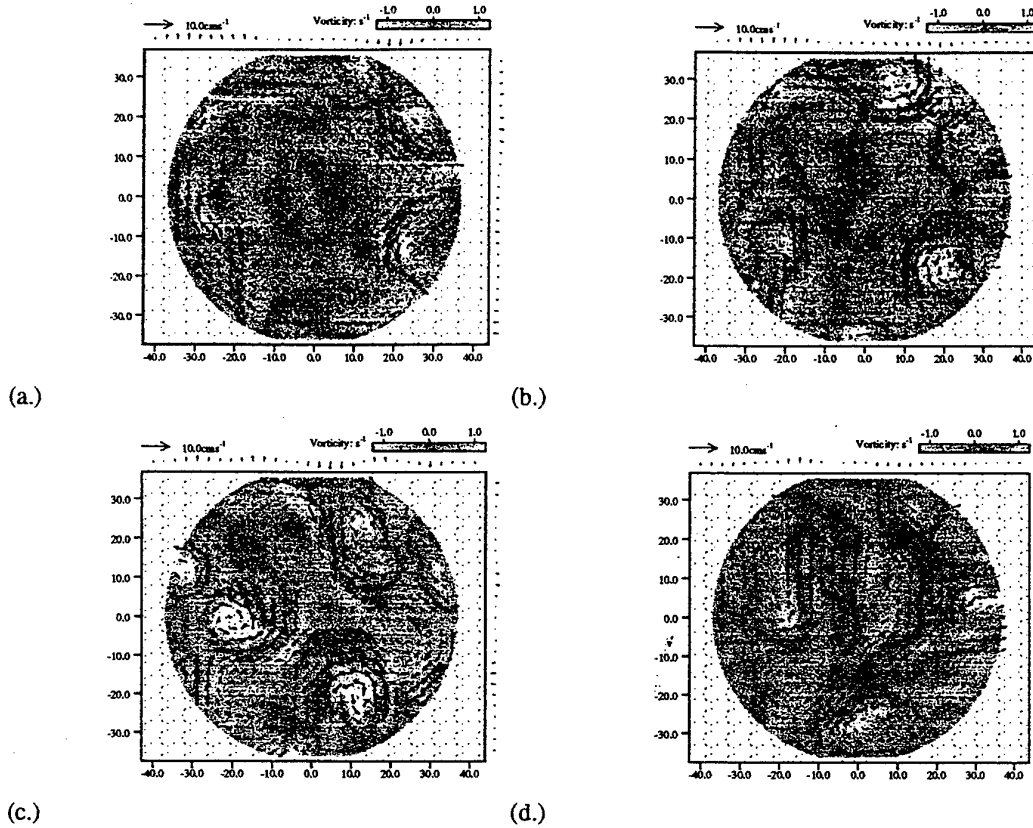


Figure 1 : Surface velocity and vorticity fields ($F=4$, $\delta=1$, $f=2.0$ rad/s). Velocity vectors are represented by arrows and vorticity by the colour scale, in which blue corresponds to anticyclonic vorticity while orange and yellow correspond to cyclonic vorticity.

- (a.) at time $t=2.5 T$ (rotation periods) after the adjustment of the front : a wave perturbation has grown leading to the development of cyclonic vorticity in the lower layer, situated at the wave troughs
- (b.) at time $t=4 T$: cyclonic eddies had formed ; two of which are advected by an off-shore current across the front
- (c.) at time $t=6 T$: some of the cyclonic eddies have been advected across the front toward the centre
- (d.) at time $t=12 T$: the later evolution is characterized by the interaction and decay of large-scale eddies.

Dipolar vortices in a strain flow

R.R. Trieling, J.M.A. van Wesenbeeck & G.J.F. van Heijst

Fluid Dynamics Laboratory, Department of Physics, Eindhoven University of Technology,
P.O. Box 513, 5600 MB Eindhoven, The Netherlands.

Dipolar vortices play an important part in large-scale geophysical flow systems. Due to their self-propelling motion, dipoles may transport scalar properties like heat and salt over great distances. A fundamental question concerns the stability of these vortex structures in a deforming ambient flow. For example, in the atmosphere dipolar vortices may lead to a phenomenon called 'atmospheric blocking', which means that the global west-east circulation is locally hindered or 'blocked' by two pressure cells of opposite circulation. Atmospheric blocking systems may persist for a relatively long time and consequently may have a large effect on local weather conditions. Therefore, it is essential to investigate the effects of a deforming background flow on the stability of these systems.

In the present study, the evolution characteristics of dipolar vortices in a strain flow were investigated both experimentally and theoretically, the strain flow being the simplest representation of a deforming background flow. Two different initial configurations were considered in which the vortex centres of the dipole were either compressed or separated by the ambient flow. In the former situation, Fig. 1(a), the strain flow is 'cooperative' in view of its progressive effect on the translational motion of the dipole, whereas in the latter case, Fig. 1(b), the strain flow is 'adverse' since it opposes the dipole's self-induced motion.

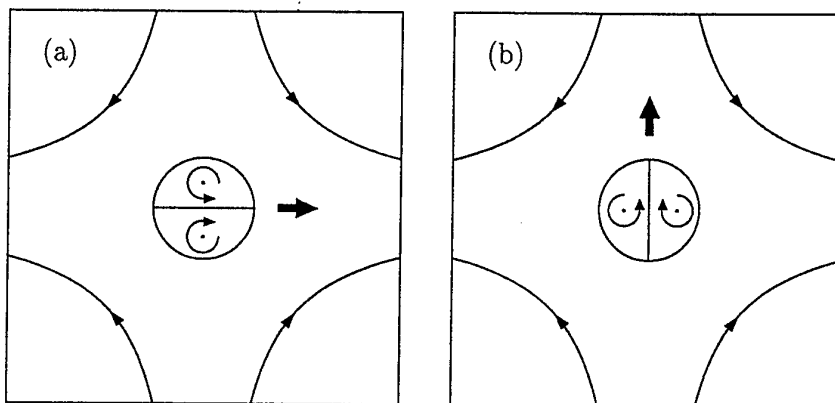


FIGURE 1: Schematic drawing of a dipolar vortex in (a) a cooperative and (b) an adverse strain flow.

The laboratory experiments were performed in a stratified fluid. The strain flow was generated by four rotating horizontal discs, whereas the dipolar vortex was created by a pulsed injection of a small amount of fluid. Dye-visualization studies and particle-tracking techniques were used to obtain qualitative and quantitative information about the horizontal flow field. Depending on the initial orientation of the dipole, either a head-tail structure or a pair of elliptic-like monopolar vortices was formed (see Fig. 2). A similar head-tail structure was found in a numerical study by Kida *et al.* (1991). The main kinematic characteristics of the observed vortex evolutions could be well captured by a simple point-vortex model in which the dipolar vortex was represented by two point vortices (of equal but opposite-signed strengths) surrounded by a contour of passive tracers (see Fig. 2). Full-numerical simulations based on the quasi-two-dimensional vorticity equation showed a close agreement with the laboratory observations.

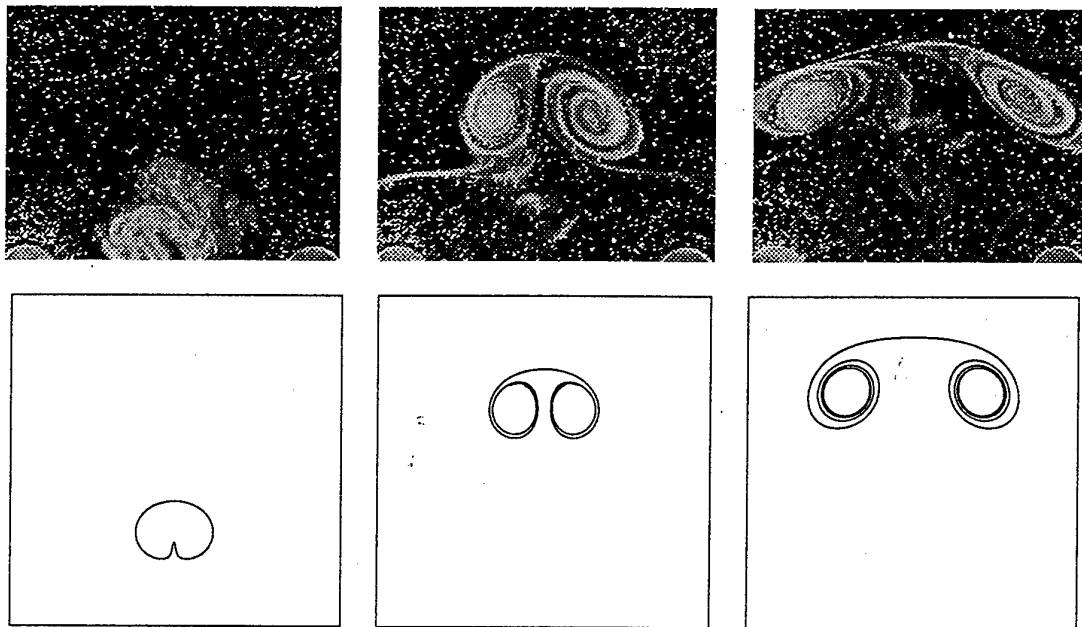


FIGURE 2: Upper panels: Observed evolution of a dye-visualized dipolar vortex in an adverse strain flow. Lower panels: Corresponding passive tracer distributions obtained by the point-vortex model. For details see Trieling *et al.* (1998)

References

S. Kida, M. Takaoka & F. Hussain – Formation of head-tail structure on a two-dimensional uniform straining flow. *Phys. Fluids A 3*, 2688–2697 (1991).

R.R. Trieling, J.M.A. van Wesenbeeck & G.J.F. van Heijst – Dipolar vortices in a strain flow. *Phys. Fluids 10*, 144–159 (1998).

LABORATORY EXPERIMENTS WITH COLLISION OF VORTICES IN ROTATING AND STILL FREE-SURFACE SHALLOW WATER.

Zhvania B.P.¹, Zhvania M.A.¹, Lominadze J.G.¹, Nanobashvili J.I.¹, Tsakadze S.J.¹, and Petviashvili V.I.²

¹ Abastumani Astrophysical Observatory, Tbilisi, Georgia;

² Kurchatov Institute Russian Research Centre, Moscow, Russia

Address:

Abastumani Astrophysical Observatory
#2a Kazbegi Ave, Tbilisi 380060, Georgia, Europe
e-mail: rezo@dapha.kheta.ge, jlomin@parliament.ge
Fax: +995/32/ 987000

Interaction of vortices in rotating and still water has been studied. The vortices in rotating water (Rossby vortices) were created in the device, represented schematically in Fig. 1 of abstract of this colloquium ("Interaction of Dipole Vortices with a Rigid Boundary and Further Dynamics" by Zhvania B.P. at all). Turbulent spots were created in it, which rapidly decayed into a number of vortices. Then we could follow the interaction of the structures. The interaction of vortices in a still water was studied in a rectangular vessel (200x100x14 cm). The vortices were created by a movement of flat plate. Varying the size of the plate, its initial location and speed, it is easy to obtain a rich collection of travelling dipole vortices and standing monopole ones.

Let us place emphasis on the main distinction of the vortices in a rotating water from those in a still one.

The stable vortices in a rotating water: The anticyclone is a convex vortex rotating against the global rotation of the fluid. The cyclone is a concave vortex rotating in the direction of the global rotation. Its lifetime roughly corresponds to the Eckman damping time. The dipole is a twinned anticyclon-cyclone (convex-concave) vortex.

The vortices in a motionless water: The monopole vortices of the opposite signs only differ from each other by their rotation direction. The both vortices are concave. During their lifetime they make, on the average, about 9 revolutions. Monopole vortices have no travelling velocity relative to the fluid. If the vortices in a pair are of nearly the same intensity, they travel in a straight path, otherwise - in a curved one.

Our observation show, that in spite of the difference in self-localization mechanisms of the vortices in rotating and motionless media, the qualitative laws of interaction for all of them have a great deal in common. When two vortices of the same sign collide, a partial or complete reconnection of the closed stream-lines takes place. When two vortices of different signs interact, a bound state, i.e. a dipole appears. During a noncentral interaction of dipoles in countermovement with considerable displacement (a collision of vortices of the same sign), a reconnection of the stream-lines takes place. An intermediate three-eddy structure is formed that recognizes itself into two dipoles going away from each other (Fig. 1). The pattern is similar to the numerical experiment carried out for solitary Rossby waves (Larichev V.D. and Reznick G.M., Oceanology 1983, 23(5), 725-733).

At non-central collision in countermovement with a small displacement the three-eddy structure remains till the damping takes place.

When two dipoles of the same intensity interact in a central countermovement collision, an exchange of the partners takes place. Then they move in opposite directions perpendicular to the initial ones (Fig. 2).

If the colliding dipoles differ in intensities, the vortices of the class of the less intensive pair are entertained by the currents of the "antivortices" of the more intensive one, roll round them and reconstitute their pair. Then the dipoles move farther apart in their initial directions. Central countermovement collision we observed only in still waters.

At an encounter of a monopole with a dipole the reconnection of the stream-lines of the vortices of the same sign occurs (the monopole absorbs the vortex of the same sign from the dipole) (Fig. 3).



Fig. 1. Non-centered countermovement collision (with considerable displacement) of two dipoles:

a. in rotating water. First, two dipoles and a cyclone were formed. The cyclone interacts with a dipole and takes its anticyclone, forming a new pair. Then we see a non-centered encounter of the dipoles. When the anticyclones of the dipoles are merging for a while forming a pair of a coupled anticyclone and then pairs are separated.

b. in still water

c. in numerical experiments of solitary Rossby wave interaction obtained by Iarichev and Reznik.



Fig. 3. A countermovement collision of a monopole with a dipole.

a. in rotation water

b. in still water



Fig. 2. Centered encounter of two dipoles having equal size and strength:

a. in still water

b. in a stratified fluid obtained in laboratory experiments by G.J.Van Heijst and J.B.Flor. (Nature, 1989, 340 (6230) 212-215).

Stability study of Charney-Hasegawa-Mima modons by variational principle

D. Jovanović

Institute of Physics, P.O. Box 57, Yu-11001 Belgrade, Yugoslavia, djovanov@phy.bg.ac.yu

Large-scale planetary flows in the Earth's atmosphere and oceans are described by the well known Charney-Hasegawa-Mima (CHM) equation

$$\left[\frac{\partial}{\partial t} + (\vec{e}_z \times \nabla) \cdot \nabla \right] (1 - \nabla^2) (\varphi - \beta x) = 0, \quad (1)$$

where β is the Coriolis parameter and φ is the stream function, which is proportional to the perturbation of the effective fluid depth. The same equation describes also certain nonlinear phenomena in plasma physics, such as the plasma density associated with the drift mode, and longitudinal magnetic field in the electron magneto-hydrodynamics (EMHD). While the study of geostrophic flows is of a great importance in metereology and oceanography, the strong drift mode turbulence is widely recognized to be the crucial factor for the transport in magnetically confined plasmas, which to a large extends determines the performance of the fusion device. Likewise, the plasma magnetization by relativistic ultrashort laser pulses, used for the ignition of inertially confined plasmas in laser-plasma fusion schemes, is described by EMHD.

The CHM equation possesses the following *modon* solution, which is a localized, two-dimensional, strongly nonlinear solution, stationary in the reference frame moving with the velocity u in the direction of the y axes

$$\varphi_0(x, y) = uR \cos \theta \begin{cases} \left(1 + \frac{\rho^2}{\kappa^2}\right) \frac{r}{R} - \frac{\rho^2}{\kappa^2} \frac{J_1(\kappa r)}{J_1(\kappa R)}, & r < R, \\ \frac{K_1(\rho r)}{K_1(\rho R)}, & r \geq R, \end{cases} \quad (2)$$

where $r = [x^2 + (y - ut)^2]^{1/2}$, $\theta = \arctan(y/x)$, $\rho = (1 - \beta/u)^{1/2}$, J_1 , K_1 are the Bessel function of the first and second kind, order 1, κ is determined from the nonlinear dispersion relation $-(1/\kappa)J_2(\kappa R)/J_1(\kappa R) = (\beta/u)K_2(Ru/\beta)/K_1(Ru/\beta)$, and R is the free parameter related to the size of the modon. Obviously, the modon is spatially localized if either $u/\beta < 0$ or $u/\beta > 1$.

Both from numerical [1] and laboratory experiments [2], and from atmospheric observations, modons are known to be very robust. They have some soliton-like properties, such as 'survival' after collisions with other modons under certain conditions. Attempts have already been made to describe the strong drift- (or Rossby-) turbulence as a gas of weakly interacting modons on the background of radiation. However, it has been shown [3] that the CHM equation is non-integrable, and that it does not posess soliton solutions in the strict sense. The analytic proof of the modon stability in the presence of small perturbations has still remained elusive, and thus it is not clear under which conditions they exhibit the soliton-like robustness. An extensive list of related literature can be seen in [4, 5].

In this paper we discuss the linear stability of modons in the presence of arbitrary perturbations. Linearizing Eq. (??) around the stationary solution (??) one obtains the following equation for the small perturbations $\delta\phi(x, y, t)$

$$\frac{\partial}{\partial t} \hat{p} \delta\phi = \hat{A} \hat{H} \hat{p} \delta\phi, \quad (3)$$

$$\hat{p} = 1 - \nabla^2, \quad \hat{A} = -[\vec{e}_z \times \nabla (\hat{p}\phi_0 - ux)] \cdot \nabla, \quad \hat{H} = G(r) - \hat{p}^{-1}, \quad G(r) = \begin{cases} 1/(\kappa^2 + 1), & r < R, \\ u/\beta, & r \geq R. \end{cases}$$

This equations has one quadratic conserved quantity $\partial L/\partial t = 0$, where $L = \int dx dy \hat{p} \delta\phi \hat{H} \hat{p} \delta\phi$.

Using the variational principle, we prove rigorously that the solutions of the eigenvalue equation $\hat{H}h_n(r, \lambda) e^{in\theta} = \lambda h_n(r, \lambda) e^{in\theta}$ constitute a complete basis, for any arbitrary value of the parameter u/β . The discrete spectrum of these eigenfunctions contains *only two negative eigenvalues* λ , which correspond to the lowest order solution in the zeroth and first cylindrical harmonic. For the zero-order solutions with $u/\beta > 1$ the entire continuous spectrum corresponds to positive values of λ . Solutions propagating in the opposite direction, $u/\beta < 0$, have a negative ($\lambda < 0$) continuous spectrum, but it is absent if the zero-order modon propagates fast enough, $|u/\beta| > \kappa^2/(\kappa^2 + 1)$.

Expanding the perurbation $\delta\phi$ as $\hat{p}\delta\phi = \sum_n e^{in\theta} \int d\lambda \varphi_n(\lambda) h_n(\lambda) + \sum_{m,n} e^{in\theta} \varphi_{m,n} h_{m,n}$, and using the orthonormality of the eigehfunctions h , we readily obtain

$$L = \sum_n \int d\lambda \lambda |\varphi_n(\lambda)|^2 + \sum_{m,n} \lambda_{m,n} |\varphi_{m,n}(\lambda)|^2 = \text{const.} \quad (4)$$

Obviously, an instability is possible only in the presence of eigenmodes with both signs of the eigenvalue λ . In other words, it is sufficient to study only the long-time behavior of the two modes with negative values of λ . Those are the lowest order monopole ($m = 1, n = 0$) and dipole ($m = 1, n = 1$), corresponding to the small asymmetry and tilt of the modon, respectively.

The full evolution equation (??) is solved approximately, assuming initially a small tilt and monopolar asymmetry. The perturbation is found to be exponentially growing in the case of modons propagating in the negative direction, $u/\beta < 0$. Such a behavior would eventually result in the flip-over and destruction, observed in the numerical experiment [5]. Modons with $u/\beta > 1$ appear to be stable. In most cases they just oscillate around their unperturbed paths, following a curved wave-like trajectory, with the simultaneous variations of their amplitude. Our analytical results fully agree with the classical numerical experiments [1, 5], providing exact stability criteria and quantitative expressions for the small amplitude modon oscillations.

References

- [1] Makino, Kamimura and Taniuti, J. Phys. Soc. Jpn. **50**, 980 (1981).
- [2] R. A. Antonova, B. P. Zhvaniya, D. K. Lominadze, Dzh. Nanobashvili and V. I. Petviashvili, JETP Lett. **37**, 651 (1983).
- [3] L. I. Piterbar and E. I. Shulman, Phys. Lett. **140**, 29 (1989).
- [4] J. Nykander, Phys. Fluids A4, 467, (1992).
- [5] D. Jovanović and W. Horton, Phys. Fluids **B5**, 9 (1993).

2. *Statistical convective down motion driven by random inputs of
localized buoyancy in the sea*

A model for the dynamics of dense water plumes in a sea initially at rest, suddenly perturbed on the sea surface by random buoyancy inputs localized on small space and time scales is presented. A general Lagrangian representation allows the time evolution for a single, mixing plume, able to carry down dense water mass, to be obtained. For long times scaling laws are also found, which depend on the surface air-sea interaction statistics involved. The effect of viscosity and stratification are finally discussed.

Dott.ssa Vanda Bouché Dipartimento di Fisica Università "La Sapienza"
Tel. 49914301